



BRNO UNIVERSITY OF TECHNOLOGY

VYSOKÉ UČENÍ TECHNICKÉ V BRNĚ

FACULTY OF ELECTRICAL ENGINEERING AND COMMUNICATION

FAKULTA ELEKTROTECHNIKY
A KOMUNIKAČNÍCH TECHNOLOGIÍ

DEPARTMENT OF POWER ELECTRICAL AND ELECTRONIC ENGINEERING

ÚSTAV VÝKONOVÉ ELEKTROTECHNIKY A ELEKTRONIKY

3,8 KW INDUCTION MACHINE

ASYNCHRONNÍ MOTOR S VÝKONEM 3,8 KW

BACHELOR'S THESIS

BAKALÁŘSKÁ PRÁCE

AUTHOR

AUTOR PRÁCE

Bogdan Adrian Stoican

SUPERVISOR

VEDOUCÍ PRÁCE

Ing. Martin Mach, Ph.D.

BRNO 2020

Bakalářská práce

bakalářský studijní program **Silnoproudá elektrotechnika a elektroenergetika**

Ústav výkonové elektrotechniky a elektroniky

Student: Bogdan Adrian Stoican

ID: 187792

Ročník: 3

Akademický rok: 2019/20

NÁZEV TÉMATU:

Asynchronní motor s výkonem 3,8 kW

POKYNY PRO VYPRACOVÁNÍ:

1. Pomocí vhodného softwaru (Excel, Matlab, ...) vytvořte jednoduchý program pro analytický návrh asynchronního motoru s výkonem 3,8 kW.
2. Návrh ověřte pomocí programu RMxprt.
3. Analyzujte vliv konstrukčních úprav na rozměry stroje.
4. Navržený stroj upravte tak, aby došlo ke zmenšení jeho rozměrů.

DOPORUČENÁ LITERATURA:

- [1] BOLDEA, I. a NASAR, S. A. The induction machine handbook. Boca Raton: CRC Press, 2002. ISBN 08-49-0004-5.
- [2] PYRHONEN, J.; JOKINEN t.; HRABOVCOVÁ V. Design of rotating eletrical machines. John Wiley and Sons, 2007. ISBN 978-0-470-69516-6.

Termín zadání: 3.2.2020

Termín odevzdání: 29.5.2020

Vedoucí práce: Ing. Martin Mach, Ph.D.

doc. Ing. Petr Toman, Ph.D.
předseda rady studijního programu

UPOZORNĚNÍ:

Autor bakalářské práce nesmí při vytváření bakalářské práce porušit autorská práva třetích osob, zejména nesmí zasahovat nedovoleným způsobem do cizích autorských práv osobnostních a musí si být plně vědom následků porušení ustanovení § 11 a následujících autorského zákona č. 121/2000 Sb., včetně možných trestněprávních důsledků vyplývajících z ustanovení části druhé, hlavy VI. díl 4 Trestního zákoníku č. 40/2009 Sb.

Abstrakt

Úkolem této semestrální práce je návrh asynchronního motoru. Pro výpočet technických parametrů asynchronního motoru je použita analytická metoda, která je implementována do vytvořeného počítačového programu. Výsledek je ověřen pomocí programu ANSYS RMxpert.

Technickým úkolem je umístit tento motor do určeného prostoru. Návrh sleduje stanovené technické parametry a výsledek respektuje požadovaný průměr statoru i optimalizaci jeho rozměrů. Pomocí programu ANSYS RMxpert jsou výsledky analyzovány s cílem najít technické řešení umožňující zmenšení rozměrů stroje.

V závěru práce je návrh motoru změněn dle výsledků, které umožňují optimalizaci technických parametrů návrhu stroje.

Klíčová slova

Asynchronní motor, návrh, počítačový program, analýza, RMxpert.

Abstract

This thesis deals with design of an induction motor. A computer program that implements the analytical method used for calculating the technical parameters of the motor is built and used in the first phase of design process of the induction machine. The design takes the defined technical requirements formulated for the engine into consideration: output power, speed and dimension of exterior diameter of the stator. Computer program calculated solution it is verified with the help of the ANSYS RMxpert simulation program. Next, the results are being analyzed using ANSYS RMxpert with the goal of studying the options for reducing dimensions of the machine. In the last section of the thesis the gained insights are applied for proposing an optimized design for the induction machine.

Keywords

Induction machine, design, computer program, analysis, RMxpert.

Rozšířený abstrakt

Tématem bakalářské práce je asynchronní motor s výkonem 3,8 kW. Dílčími cíli bakalářské práce je vytvoření jednoduchého programu pro analytický návrh asynchronního motoru s výkonem 3,8 kW, 1600 ot./min a průměrem statoru 156 mm, ověření návrhu pomocí programu RMXprt, analýza vlivu konstrukčních úprav na rozměry stroje a úprava navrženého stroje vedoucí ke zmenšení jeho rozměrů.

V první části je popsáno provedení výpočtu motoru pomocí počítačového programu. Tento program je vytvořen v programovacím jazyce Python 3 na bázi “open source” Anaconda. Jako uživatelské prostředí pro práci s programem je používán Jupyter notebook. Výhodou použití Jupyter notebook je, že uživatelské prostředí (webová stránka) vyhovuje velmi dobře požadavkům pro iterace potřebné pro výpočty parametrů v různých fázích návrhu. Další výhodou je dostupnost různých knihoven pro nakládání, analýzu a prezentaci dat a také jejich neplacené použití.

Analytický výpočet motoru je proveden na bázi zdroje [1]. Parametry motoru vyhovující zadání jsou postupně vypočítávány pro stator, rotor a vinutí statoru a rotoru. Rotorové vinutí je klec. Požadavek na stator o průměru 156 mm představuje významné omezení při výpočtu hlavních rozměrů stroje. Dále jsou vypočítány elektrické parametry stroje a elektrické, mechanické a magnetické ztráty. Tyto jsou spočítány pro chod motoru naprázdno a nakrátko. To umožňuje výpočet parametru náhradního schématu stroje, rozběhové charakteristiky a zatěžovacích charakteristik motoru. V posledním kroku je vypočítána oteplovací charakteristika a potřebná ventilace.

Pro dosažení dílčího cíle jsou v další části bakalářské práce vypočítané parametry asynchronního motoru analyzovány za pomoci ANSYS Electronics Desktop – RMXprt design and simulator program ke zjištění, zda parametry motoru vypočítané v první části bakalářské práce odpovídají simulaci v RMXprt.

V následující části bakalářské práce, též s pomocí RMXprt, je analyzován vliv konstrukčních úprav na rozměry stroje. Na základě metody použité pro výpočet parametrů stroje jsou určeny technické možnosti optimalizace rozměrů. Je provedena simulace a analýza optimalizace rozměrů.

V závěrečné části bakalářské práce je na základě zjištěných technických možností upraven návrh asynchronního motoru tak, aby došlo ke zmenšení jeho rozměrů. Toho je dosaženo nahrazením statorového plechu, změnou rozměru drážek statoru, zvýšením průřezu vodiče statorového vinutí a použitím měděné klece. Všechny tyto změny optimalizují elektrické vlastnosti stroje a následně umožňují zmenšení rozměrů.

Bibliografická citace:

STOICAN, Bogdan Adrian. Asynchronní motor s výkonem 3,8 kW [online]. Brno, 2020 [cit. 2020-06-07]. Dostupné z: <https://www.vutbr.cz/studenti/zav-prace/detail/117006>. Bakalářská práce. Vysoké učení technické v Brně, Fakulta elektrotechniky a komunikačních technologií, Ústav výkonové elektrotechniky a elektroniky. Vedoucí práce Ing. Martin Mach, Ph.D.

Prohlášení autora o původnosti díla

Jméno a příjmení studenta: Bogdan Adrian Stoican
VUT ID studenta: 187792
Typ práce: Bakalářská práce
Akademický rok: 2019/20
Téma závěrečné práce: Asynchronní motor s výkonem 3,8 kW

Prohlašuji, že svou závěrečnou práci jsem vypracoval samostatně pod vedením vedoucí/ho závěrečné práce a s použitím odborné literatury a dalších informačních zdrojů, které jsou všechny citovány v práci a uvedeny v seznamu literatury na konci práce.

Jako autor uvedené závěrečné práce dále prohlašuji, že v souvislosti s vytvořením této závěrečné práce jsem neporušil autorská práva třetích osob, zejména jsem nezasáhl nedovoleným způsobem do cizích autorských práv osobnostních a jsem si plně vědom následků porušení ustanovení § 11 a následujících autorského zákona č. 121/2000 Sb., včetně možných trestněprávních důsledků vyplývajících z ustanovení části druhé, hlavy VI. díl 4 Trestního zákoníku č. 40/2009 Sb.

V Brně dne: **7. června 2020**

.....
Podpis autora

Poděkování

Chtěl bych poděkovat Ing. Martinu Machovi, Ph. D. za cenné rady, věcné připomínky, vstřícnost při konzultacích, trpělivost, podporu a porozumění při zdolávání úrovně mé češtiny při zpracovávání mé bakalářské práce.

V Brně dne: **7. června 2020**

.....
podpis autora

Contents

1.INTRODUCTION	11
2.THEORY.....	11
2.1General considerations	11
2.2 Theoretical principle of induction machine	14
3.INDUCTION MACHINE DESIGN	16
3.1 Induction machine calculation computer program.....	16
3.2 Design requirements	18
3.2 Design considerations	18
3.3 Main dimensions selection.....	19
3.4 Stator parameters	23
3.5 Stator slot parameters.....	27
3.6 Air gap size	28
3.7 Rotor parameters.....	29
3.8 Rotor slot parameters	30
3.9 Magnetic circuit	32
3.10 Electrical resistance and reactance	34
3.11 Energy losses	38
3.12 Load characteristic of the induction machine	42
3.13 Starting characteristic of the induction machine.....	44
3.12 Thermal characteristic and cooling.....	49
4. RMxprt SIMULATION	53
5. STATOR STACK LENGHT REDUCTION.....	56
5.1 General considerations.....	56
5.2 Decreasing losses	57
5.2.1 Copper rotor bars	57
5.2.2 Stator slot fill increase	58
5.3 Reducing iron core losses	59
5.6 Design output.....	62
6. CONCLUSION	66

List of figures

Figure 2.1: Production of rotating magnetic field [4]	14
Figure 2.2: Torque characteristic of induction motor [3]	15
Figure 3.1: Jupyter notebook - engine calculation program	16
Figure 3.2: Jupyter notebook – calculated data export	17
Figure 3.3: k_E coefficient values [1]	21
Figure 3.4: Efficiency and power factor [1]	21
Figure 3.5: Induction flux and linear current density [1]	22
Figure 3.6: Slot length to pole pitch ratio [1]	23
Figure 3.7: Stator slot width [1]	24
Figure 3.8: Thermal load parameter [1]	26
Figure 3.9: Stator slot dimensions [1]	27
Figure 3.10: Air gap size [1]	29
Figure 3.11: k_i coefficient [1]	30
Figure 3.12: Rotor slot dimensions [1]	31
Figure 3.13: Stator slot parameters [1]	36
Figure 3.14: Coefficient $k\gamma'$ [1]	36
Figure 3.15: Rotor slot parameters [1]	37
Figure 3.16: Coefficient Δz [1]	38
Figure 3.17: β_0 coefficient [1]	39
Figure 3.18: κ_δ coefficient [1]	41
Figure 3.19: Load characteristics of the machine (based on [1])	44
Figure 3.20: $\varphi(\xi)$ function [1]	45
Figure 3.21: $\varphi'(\xi)$ function [1]	46
Figure 3.22: $\kappa_\delta(B_{f\delta})$ function [1]	47
Figure 3.23: Equivalent heat transfer coefficient [1]	50
Figure 3.24: Heat transfer coefficients [1]	51
Figure 3.25: Cooling fins height [1]	52
Figure 4.1: ANSYS RMxprt model	53
Figure 4.2: Output torque characteristics	55
Figure 4.3: Input current characteristics	55

Figure 5.1: Specific iron core losses at 50 Hz [6][11][12][13][14]	61
Figure 5.2: B-H characteristics for tested magnetic steels [6][11][12][13][14]	62
Figure 5.3: Output torque characteristics.....	65
Figure 5.4: Input current characteristics	65

List of tables

Table 3-1: Allowed K_D parameter values [1]	20
Table 3-2: Coefficient k_{wsl} values [1]	25
Table 3-3: Permitted number of stator bars [2].....	29
Table 4-1: Modeled machine parameters.....	54
Table 5-1: Copper rotor bars simulation.....	58
Table 5-2: Stator slot fill increase simulation	59
Table 5-3: Magnetic steel tests	60
Table 5-4: Designed model characteristics	64

1. INTRODUCTION

Throughout history, mankind's ability to produce, transform, transport and consume energy formed the foundation of society development and growth, of value creation and fostered innovation and discovery.

Scientific and technological development is in direct relationship with scale at which energy use and conversion is possible. In modern world, electricity and electrical machines, as engines, are the main source of mechanical power creation.

The main advantages of electrical machines are relative simplicity, readiness for use, versatility in terms of output torque and speed capabilities, low maintenance requirements, low noise and almost no emissions. These and other characteristics made electrical machines to be the foundation of modern industry and the main instrument for creating mechanical energy or, in reverse, for transformation of mechanical energy to electrical one.

Advantages brought by use of electrical machines are overpassing their disadvantages and constant need of deploying electrical machines for traditional or new use cases is creating a need for constant development and innovation.

Theoretical principles of electrical machines are well defined and applied for a long time. Today's accent is put on integration, versatility, performance and efficiency.

In actual terms this means deploying electrical machines fit for purpose but at the same time manufactured in a standardized way, having modular options for custom integration, being efficient not only as a specific technical item, but also as a complete system in which the motor works.

2. THEORY

2.1 General considerations

Induction machines are widely used in diverse application, engines deployed with output power varying from tens of watts to multi mega-watt ranges [5], engines being deployed widely in all industry domains for applications requiring constant power outputs.

In the past, a drawback that limited the use of induction machines to some applications was the fact that rotation speed was strictly tied to the load's current frequency and the number of poles. This was limiting its use to applications requiring full control of rotation speed with minimal energy losses. The evolution of power electronics made high-power pulse width modulated (PWM) power convertors (IGBT, MOSFET, GTO) available at a relative low cost. Past limitations of speed control capabilities are removed, making induction machine an efficient, cost-effective choice for traditional and new applications,

providing wide range of power outputs, good efficiency, low maintenance requirements and long lifespan.

In the recent decades, the evolution of the power systems is marked by the advance in power electronics field. For example, the wind turbine technologies evolution saw advance from the direct-connected induction generators (Type I), to the wound-rotor induction generator with external resistance control (Type II), to the doubly-fed induction generator (Type III) and, currently, to the variable speed turbine with full-rated power converter (Type IV) [18]. This evolution was enabled by the development and the advance of power electronics and, together with this, by the development of power convertors.

Constructively, induction machines are relatively simple, being composed of two main components: the stator and the rotor. Both stator and rotor are providing a dual-purpose role: being made of magnetic steel, they provide magnetic circuit for the motor and, at the same time, are hosting electrical circuits for the stator and rotor windings that are magnetizing the machine.

Power conversion takes place in the air gap separating the rotor and the stator.

This setup creates a compact and robust torque generation or energy conversion system.

Additionally, stator and rotor are hosting electrical insulators, electrical terminal box, ventilation and cooling elements, bearings. Power output shaft is connected directly to the rotor, on the shaft a ventilation fan and a brake mechanism can be also hosted.

The power supply of the induction machine is usually a three phase or a two-phase system, a higher number of phase systems being possible.

One disadvantage associated with the power supply form, especially for machines connected directly to the electrical network, is that the induction machine requires reactive power to function. A second concern regarding the power supply for induction motors is that they require a larger amount of current (inrush current) during the engine start-up. This is due to the need of magnetization of the magnetic circuit during the start-up process. Starting current can exceed several times the nominal current required for the motor nominal run and several technical options are used for limiting the amount of current required from the power network during the engine start [7].

The advantage of the induction machine is that it is self-starting [7]. This is an important characteristic which, besides other advantages, contributes to the wide use of these motors in industrial and domestic applications.

Transformation of energy is possible both ways: the induction machine transforms electrical energy to mechanical one and is also able to work in the generator mode and convert mechanical energy to electric.

Both the rotor and the stator magnetic circuits are composed of low hysteresis laminated steel sheets manufactured with slots that host electrical windings. The requirement of a magnetic and electric circuit for both the stator and the rotor

is an important design characteristic of the induction machine that affects motor characteristics [17].

Shape and size of the stator and the rotor slots influences electrical and mechanical characteristics of the engine. Slots can be open, semi-closed and closed, the selection of a specific type being done based on requirements. The selection of a type or a combination being done based on motor's starting and rated load requirements, constant voltage/frequency (V/f) or variable voltage/frequency supply operation and required torque characteristic [8].

The electrical winding of the stator is usually composed of copper wiring deployed in an m phase system. As mentioned earlier, when directly attached to the public power network, three-phase or two-phase winding systems are being used. Higher number phase system is possible, requirement being that power supply phases and stator winding type are to create a rotating magnetic field.

Depending on rated power/size of the engine, for stator winding copper round wires or bars are being used.

The rotor winding's design is based on two rotor types: squirrel cage or wound rotor. A squirrel cage rotor is built of soft magnetic steel sheets with electrical circuit winding based on die-cast aluminum, brass or copper bars that are hosted in rotor slot openings and that are electrically connected at the ends of the rotor slot forming a delta winding connection configuration.

For double cage rotors a combination of brass bars for upper/exterior cage and aluminum for lower/interior bars it is used. Given its intrinsic design, a "squirrel cage" rotor is, in general, supporting higher mechanical stresses and will better suit, when compared with a wound rotor, high speed applications [8].

A wound rotor is based on a regular three phase star connected winding which has terminal ends connected to three slip rings at one end of the rotor. This is deployed for applications requiring control of the torque characteristics of the machine [8].

Besides magnetic and electric materials, induction motor stators and rotors are composed of insulation materials that are meant to provide electrical isolation for prevention of phase to phase, coil to coil or eddy currents flows through bearings of the motor.

In general, induction machines generate higher losses than other motor types. Difference comes from rotor's ohmic and iron losses, that are triggered by the requirement for a rotor winding for magnetizing rotor's magnetic circuit [17]. In other motor types, rotor copper losses are inexistent, and, for synchronous speeds, rotor iron losses are very small, too.

2.2 Theoretical principle of induction machine

The principle of an induction machine is the creation of a rotating magnetic field in the air gap. For a three-phase power system, this is achieved by deploying overlapping stator windings in a regular circular pattern with a 120° electrical angle offset.

This is matching the connected electrical power phases, characterized by electric current oscillations with a 120° angle offset (equations that are detailed in this paragraph are sourced from [8]):

$$u_U = U_m e^{j\omega_0 t} \quad (2.1)$$

$$u_V = U_m e^{j(\omega_0 t + \frac{2\pi}{3})} \quad (2.2)$$

$$u_W = U_m e^{j(\omega_0 t + \frac{4\pi}{3})} \quad (2.3)$$

The resulting magnetic field is a vector sum of magnetic field vectors generated by each stator winding:

$$\phi = \phi_m e^{j\omega_s t} \quad (2.4)$$

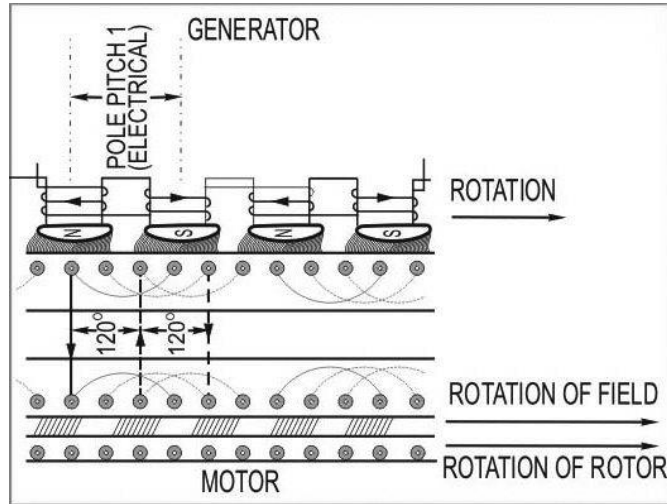


Figure 2.1: Production of rotating magnetic field [4]

The relationship between the magnetic field synchronous angular velocity ω_s and the phase current angular velocity ω_0 is:

$$\omega_s = \frac{\omega_0}{p} \quad (2.5)$$

where p is the stator's number of pole pairs.

The stator's rotating magnetic field induces magnetomotive force (MMF) in the rotor's winding. Stator's flux linkage creates torque and rotation of the rotor's magnetic field. The force acts on rotor's open surfaces (rotor's outer diameter and rotor's slots) resulting in transversal forces acting on rotor slots walls that creates torque which is mechanically transmitted to the rotor shaft [2]. This rotation is in the same direction as the rotation of the stator magnetic field.

Electromagnetic induction in a rotor winding is maximal when rotor is at a stand-still and zero when rotor's angular speed is equal with stator's magnetic field synchronous speed. Relationship between the mechanical angular moment ω and the magnetic field synchronous speed is defined by the slip value s :

$$s = \frac{\omega_s - \omega}{\omega_s} \quad (2.6)$$

Induction machine moment characteristic contains three areas defining work characteristic of the induction machine:

- motor, for slip $s \in [0; 1]$;
- generator, $s < 0$;
- brake, $s > 1$.

In terms of mechanical torque generation, the induction machine is characterized by the following properties:

- nominal torque, T_n , with its corresponding slip s_n ;
- maximum torque, T_{max} , with its corresponding slip s' ;
- locked rotor torque T_0 , for slip s equaling 1;
- Torque $T = 0$, for slip s having a 0 value.

Associated with this properties, two working regions are associated with the motor operation characteristic:

- an unstable operation region, for s taking values from 1 to s_{max} ;
- a stable operation region, for s taking values from s_{max} to 0.

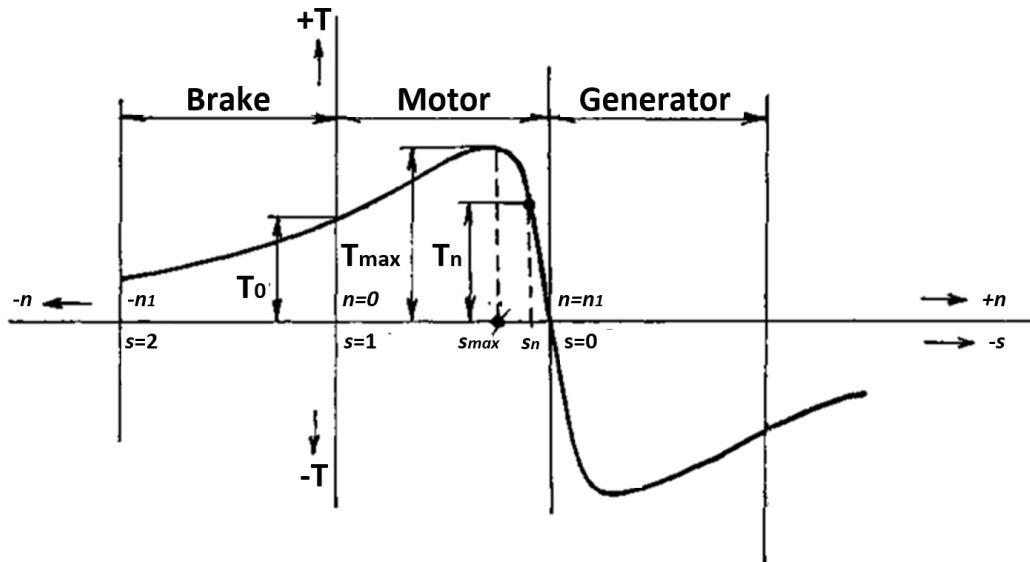


Figure 2.2: Torque characteristic of induction motor [3]

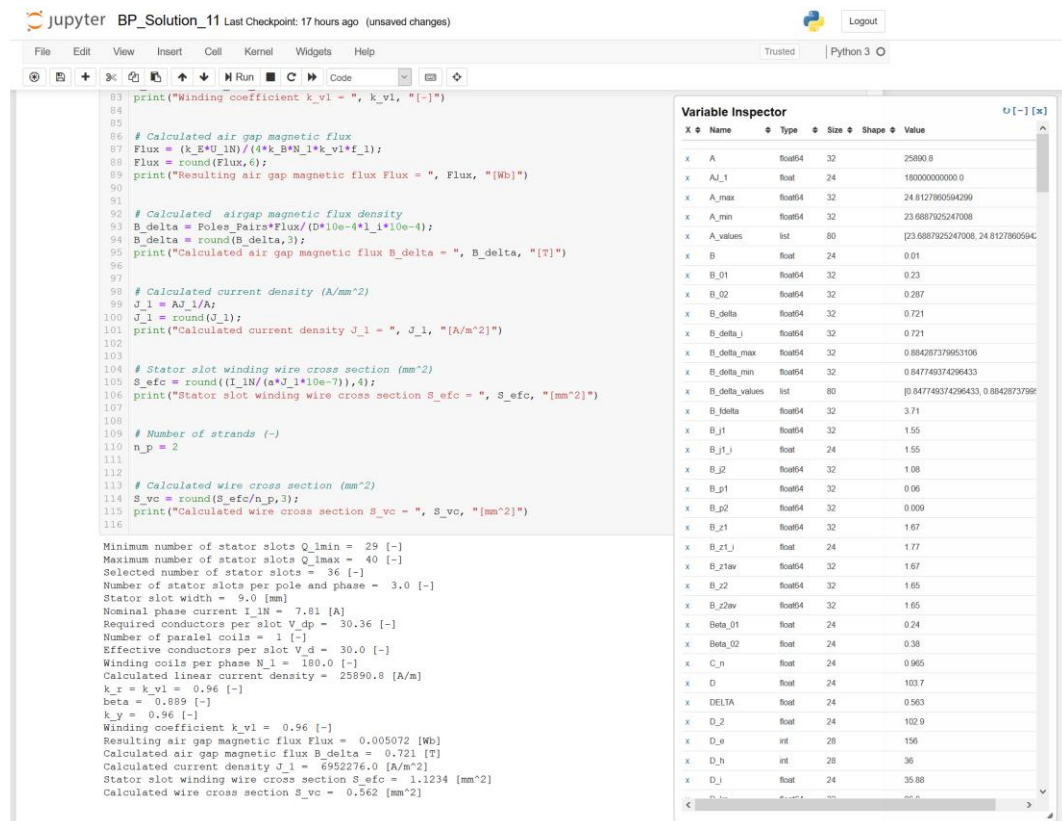
3. INDUCTION MACHINE DESIGN

3.1 Induction machine calculation computer program

Overall, this thesis' main goal is the design and the analysis of a small size induction machine. For machine parameters calculation a computer program was built. This program is implementing an analytical method defined in [1].

As a programming language, Python 3.0 has been used, based on the Anaconda (<https://www.anaconda.com/distribution/>) open source code distribution platform. As a programming client interface, Jupyter notebook is being used. Jupyter notebook runs, as a client interface layer, "on top" of the Anaconda platform. For programming support of data computing and manipulation *numpy*, *pandas* and *math* Python libraries are used.

Analytical calculation of an electrical engine is an iterative process. Jupyter notebooks enables grouping distinct code motor computation sections which can be executed sequentially for following algorithmic flow for defining induction machine parameters. Code sections can be separated by markdown sections which serve as code and algorithm documentation and can include section heading data, notes, formulas, images, etc.



The screenshot displays a Jupyter notebook interface with a code editor on the left and a Variable Inspector on the right. The code editor contains Python code for calculating induction machine parameters. The Variable Inspector shows a list of variables with their names, types, sizes, and values.

```
83 print("Winding coefficient k_v1 = ", k_v1, "[-]")
84
85
86 # Calculated air gap magnetic flux
87 Flux = (k_E*U_1N)/(4*k_B*N_1*k_v1*f_1);
88 Flux = round(Flux,6);
89 print("Resulting air gap magnetic flux Flux = ", Flux, "[Wb]")
90
91
92 # Calculated airgap magnetic flux density
93 B_delta = Poles Fairs*Flux/(D*10e-4*1_1*10e-4);
94 B_delta = round(B_delta,3);
95 print("Calculated air gap magnetic flux B_delta = ", B_delta, "[T]")
96
97
98 # Calculated current density (A/mm^2)
99 J_1 = A_J_1/A;
100 J_1 = round(J_1);
101 print("Calculated current density J_1 = ", J_1, "[A/m^2]")
102
103
104 # Stator slot winding wire cross section (mm^2)
105 S_efc = round((I_1N/(a*J_1*10e-7)),4);
106 print("Stator slot winding wire cross section S_efc = ", S_efc, "[mm^2]")
107
108
109 # Number of strands (-)
110 n_p = 2
111
112
113 # Calculated wire cross section (mm^2)
114 S_vc = round(S_efc/n_p,3);
115 print("Calculated wire cross section S_vc = ", S_vc, "[mm^2]")
116
117
118 Minimum number of stator slots Q_lmin = 29 [-]
119 Maximum number of stator slots Q_lmax = 40 [-]
120 Selected number of stator slots = 36 [-]
121 Number of stator slots per pole and phase = 3.0 [-]
122 Stator slot width = 9.0 [mm]
123 Nominal phase current I_1N = 7.81 [A]
124 Required conductors per slot V_dp = 30.36 [-]
125 Number of parallel coils = 1 [-]
126 Effective conductors per slot V_d = 30.0 [-]
127 Winding coils per phase M_1 = 180.0 [-]
128 Calculated linear current density = 25890.8 [A/m]
129 k_r = k_v1 = 0.96 [-]
130 beta = 0.889 [-]
131 k_v = 0.96 [-]
132 Winding coefficient k_v1 = 0.96 [-]
133 Resulting air gap magnetic flux Flux = 0.005072 [Wb]
134 Calculated air gap magnetic flux B_delta = 0.721 [T]
135 Calculated current density J_1 = 6952276.0 [A/m^2]
136 Stator slot winding wire cross section S_efc = 1.1234 [mm^2]
137 Calculated wire cross section S_vc = 0.562 [mm^2]
```

X	Name	Type	Size	Shape	Value
x	A	float64	32		25890.8
x	AJ_1	float	24		18000000000.0
x	A_max	float64	32		24.8127860594299
x	A_min	float64	32		23.6887925247008
x	A_values	list	80		[23.6887925247008, 24.8127860594299]
x	B	float	24		0.01
x	B_01	float64	32		0.23
x	B_02	float64	32		0.287
x	B_delta	float64	32		0.721
x	B_delta_1	float64	32		0.721
x	B_delta_max	float64	32		0.88426737965106
x	B_delta_min	float64	32		0.847749374296433
x	B_delta_values	list	80		[0.847749374296433, 0.88426737965106]
x	B_delta	float64	32		3.71
x	B_11	float64	32		1.55
x	B_11_1	float	24		1.55
x	B_12	float64	32		1.08
x	B_11	float64	32		0.06
x	B_12	float64	32		0.009
x	B_11	float64	32		1.67
x	B_11_1	float	24		1.77
x	B_11ev	float64	32		1.67
x	B_12	float64	32		1.65
x	B_12ev	float64	32		1.65
x	Beta_01	float	24		0.24
x	Beta_02	float	24		0.38
x	C_n	float	24		0.965
x	D	float	24		103.7
x	DELTA	float	24		0.563
x	D_2	float	24		102.9
x	D_e	int	28		156
x	D_h	int	28		36
x	D_j	float	24		35.88

Figure 3.1: Jupyter notebook - engine calculation program

Engine calculation output is displayed as well at the bottom of each code section, through print commands.

As the Jupyter notebook interface is accessed via a regular web browser, navigation from one section to another is very simple, the notebook allowing a quick review of the calculated values and a re-run of the programming code after an update of input values, for allowing testing of different design options. Notebook calculation can be done also for all code sections together, output data being presented in the same way as in a step by step run.

Jupyter allows platform extensions through configurable *nbextensions*. *Variable inspector* extension has been installed for enabling access to Jupyter notebook code variables overview anytime during engine calculation process.

By using the *Pandas* library file processing functions, during code execution Jupyter notebook can import settings or parameters from external file sources (Excel workbooks or in comma separated values text files) or can save content to an external file.

Jupyter notebook sections can be executed individually in a sequential (if needed repeated) order or globally for all notebook code sections. In the final section of the program code, an export to Excel of calculated data it is performed.

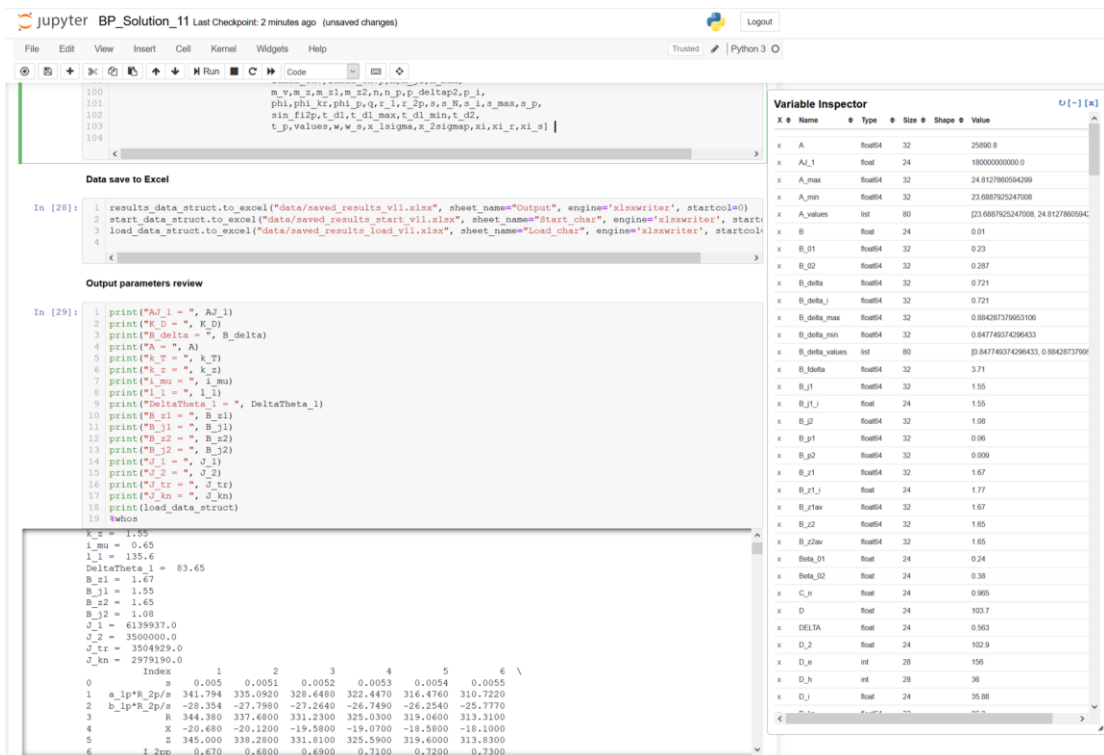


Figure 3.2: Jupyter notebook – calculated data export

All steps and outputs provided by this computer program for the design of the induction machine were used for calculating engine parameters detailed in next sections.

3.2 Design requirements

The design of an induction machine with the following characteristics:

- Output power $P_2 = 3.8$ [KW]
- Outer diameter of the stator $D_{se} = 156$ [mm]
- Rotation per minute $n = 1600$ [1/min]

The induction machine should fit into a water pipe to drive a pump, requiring a totally enclosed machine. Given this requirement, for the calculation of the motor's parameters IP44 internal protection standard will be considered.

The physical design of the machine will be constrained to required outer diameter of the stator and the given purpose.

Cooling of the induction machine will be dependent on motor mounting inside the pipe and on temperature of the fluid that will be circulated by the pump driven by the induction machine. As temperature of the liquid and heat transfer parameters of motor mounting inside the pipe are not known, for calculating motor parameters, considering standard cooling area and air as external medium.

3.2 Design considerations

Any design process has as its objective reaching the intended characteristics for the designed system or item. This is a complex subject as requirements are sourced from different domains. The design process should take in consideration and resolve requirements which arise from the entire life cycle of the designed. [2] defines this concept as eco-design.

For the case of this thesis, besides delivering required parameters, the design optimization goal objective is to minimize the size of the machine (minimizing stator stack length).

Having stated the design objectives, we can start the design process first by analyzing a few general elements regarding an induction machine of an intended output power.

Consulting product catalogs, insights can be gathered regarding usual size of the industry-produced engines of the same or similar output power is. ABB's Low voltage motors guide (2014) [16], lists 4 kW (2 or 4 poles) as 112M frame size (similarly also to other references).

In source [1], the corresponding stator exterior diameter D_{se} for this frame size is 191 mm. Source [1] also lists for output power $P_2 = 4$ [kW] (2 and 4 poles) a range of shaft height h ranging in between 90 and 110 mm. The corresponding stator exterior diameters for these h values are:

- $D_{se} = 149$ [mm] for $h = 90$ [mm]
- $D_{se} = 168$ [mm] for $h = 110$ [mm]

The required outer diameter size $D_{se} = 156$ [mm] belongs to the lower part of sizing ranges advised in [1]. The required stator outer diameter will raise constraints with regards to electrical and magnetic parameters of the motor.

A second observation is related to the optimal number of poles of the stator $2p$. Even if both pole number options $2p = 2$ [-] or $2p = 4$ [-] are advised as possible by the analytical method used, given the fact that a $2p = 2$ implies a lower electrical and magnetic load of the machine, a higher length of the stator core can be expected for a fixed output power and a specific moment density.

During the design process, both poles number options have been tested and, based on the design's objective, the option of $2p = 4$ [-] was selected to be used.

The last observation is linked to the required nominal speed $n = 1600$ [1/min]. Given the required nominal speed, an induction motor cannot be connected and function efficiently through a direct connection to the standard European 50 Hz frequency power grid. A pulse-width modulated (PWM) inverter is required to provide electrical energy to the induction machine. This will have an impact to the overall efficiency budget of the induction machine and PWM inverter system. Besides energy losses generated by intrinsic efficiency of the PWM inverter, the proximity effect losses increase will also affect IM fed by the PMW inverter. For a power grid-powered induction machine these losses would be negligible [7].

Advantages for powering an induction machine by means of a power inverter: harmonics filtering, power factor correction (PF) and limitation of starting current at zero speed.

Note: parameters and factors naming used in this thesis is based on [2]. When no correspondent available in [2], the naming is based on [1].

3.3 Main dimensions selection

First step for defining the induction machine design parameters is choosing its main dimensions, by selecting and calculating the stator's interior diameter D_s and the ideal stator slot length l_i .

In practice this is done based on information gathered from predefined tables and from previous experience. The method detailed in [1] is defining these parameters, by using a machine constant:

$$\frac{D_s^2 l_i \omega_s}{P_i} = \frac{2}{\pi \alpha_\delta k_B k_{ws1} A_s B_\delta} \quad (3.1)$$

which is, in fact, a different representation of Arnold's constant (Engelbert Arnold 1856-1911). The constant defines relationship between current and flux densities and the physical volume of the rotor stack, the synchronous speed and machine's internal power [2]. Values are gathered through previous observation and they can be used as the first step in calculating required machine parameters, by using tables presented by [1] for performing analytical calculation of the motor.

As detailed in the previous section, the selected value for number of poles:
 $2p = 4$ [-] (3.2)

K_D parameter characterizes the ratio between the outer diameter and the inner diameter of the stator. Using this, the inner diameter of the stator is calculated based on the selected number of poles:

$$K_D = \frac{D_s}{D_{se}} [-] \quad (3.3)$$

Table 3-1: Allowed K_D parameter values [1]

$2p$	2	4	6	8	10 to 12
K_D	0.52 to 0.57	0.62 to 0.68	0.70 to 0.72	0.74 to 0.75	0.75 to 0.77

As per Tab. 3-1, K_D value for $2p = 4$ ranges from 0.62 to 0.68.

Stator's exterior diameter has a fixed value. Selecting K_D value with the goal of maximizing the airgap length and, at the same time, maximizing the rotor slot cross section area for allowing a relatively small rotor bar current density, while providing acceptable rotor magnetic circuit parameters.

At the same time, the stator slot cross section area, the stator tooth width and the yoke height should be provided acceptable dimensions, as well, for enabling good parameters of the engine.

The selected value is $K_D = 0.665$ [-], resulting in the inner diameter of the stator D_s :
 $D_s = K_D D_{se} = 0.665 \cdot 156 = 103.7$ [mm] (3.4)

Based on this selection, calculation of the pole pitch can be done:

$$\tau_p = \frac{\pi D_s}{2p} = \frac{\pi \cdot 103.7}{4} = 81.4$$
 [mm] (3.5)

The next step is about defining the internal electromagnetic characteristics of the machine, by selecting initial estimates of the following parameters:

- machine related electrical coefficient k_E ;
- electrical efficiency η ;
- power factor $\cos \varphi_1$.

As per Figure 3-3, based on the outer diameter D_e and the number of poles, selecting value of coefficient $k_E = 0.96$ [-].

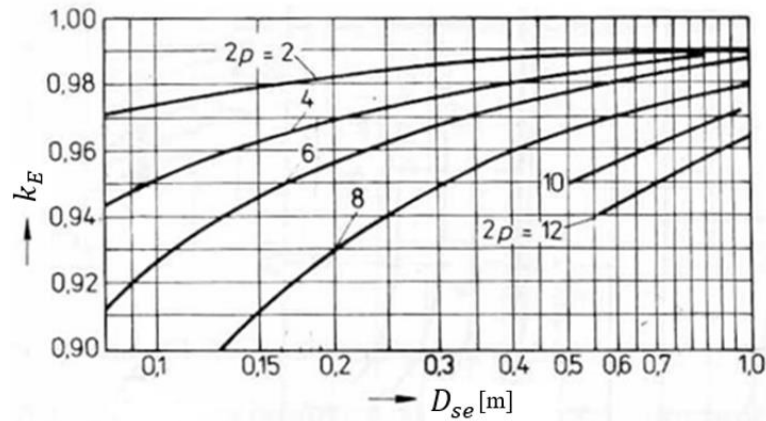


Figure 3.3: k_E coefficient values [1]

Based on the required shaft output power P_2 and the selected number of poles $2p$, as per Fig 3-4, selecting initial estimate values for Power Factor $\cos \varphi_1$ and electrical efficiency η :

- $\eta = 0.84$ [-]
- $\cos \varphi_1 = 0.84$ [-]

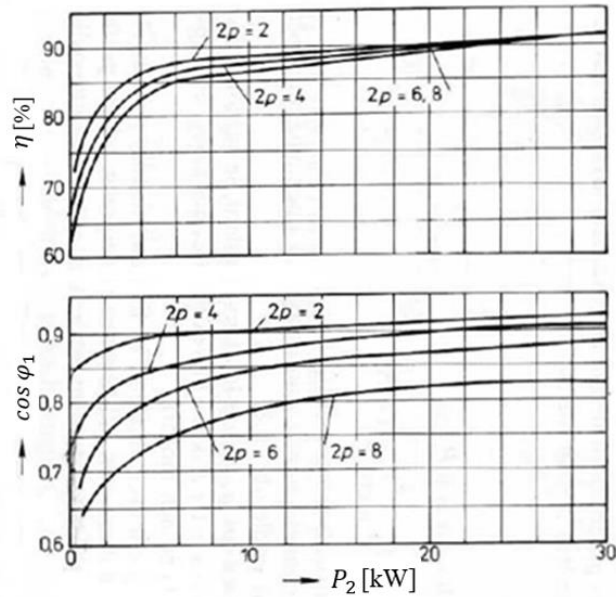


Figure 3.4: Efficiency and power factor [1]

Resulting electric input power P_1 estimate value:

$$P_1 = P_i = P_2 \frac{k_E}{\eta \cos \varphi_1} = 3,8 \cdot 10^3 \frac{0.96}{0.84 \cdot 0.84} = 5,171 \text{ [kW]} \quad (3.6)$$

The next step is the selection of the air gap magnetic flux density B_δ and the linear current density A_s . Selecting values based on Figure 3-5, however, the values were adjusted based on the analytical model testing during the solution selection: $B_\delta = 0,74$ [T] and $A_s = 25000$ [A/m].

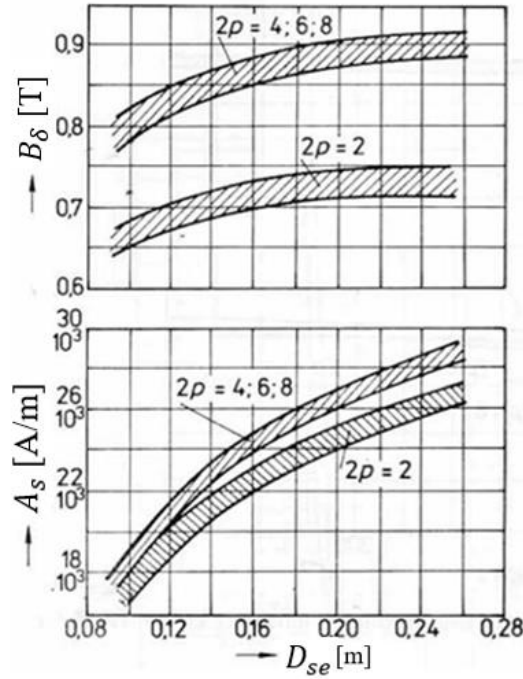


Figure 3.5: Induction flux and linear current density [1]

Additional coefficients defined are the average to peak flux density ratio α_i , and the factor k_B defining the deformation of the sinusoidal flux value:

$$\alpha_i = \frac{2}{\pi} = 0.64 \quad [-] \quad (3.7)$$

$$k_B = \frac{\pi}{2\sqrt{2}} = 1.11 \quad [-] \quad (3.8)$$

The stator winding factor for the fundamental k_{ws1} value selected based on the type of the stator winding and the number of poles. For a single layer winding stator $2p=4$ advised values are ranging from 0.95 to 0.96:

$$k_{ws1} = 0.96 \quad [-]$$

Estimating slip value, considering that machine is of a small power and, though, expecting a larger slip:

$$s = 0.06 \quad [-]$$

Generally, slip value s is defined as:

$$s = \frac{\omega_s - \omega}{\omega_s} \quad [-] \quad (3.9)$$

Given the required shaft angular speed ω , and estimating the slip value, the synchronous angular speed of the rotor shaft is:

$$\omega_s = \frac{\omega}{1-s} = \frac{167.55}{1-0.06} = 178.24 \quad [\text{rad/s}] \quad (3.10)$$

Load current frequency:

$$f_1 = \frac{\omega_s p}{2\pi} = \frac{178.24 \cdot 2}{2\pi} = 56.74 \quad [\text{Hz}] \quad (3.11)$$

Based on calculated values, and applying Arnold's constant formula, length of stator core is calculated as:

$$l_i = \frac{P_i}{D_s^2 \omega_s k_B k_{ws1} A_s B_\delta} = \frac{5171}{(103.7 \cdot 10^{-3})^2 \cdot 178.24 \cdot 1.11 \cdot 0.96 \cdot 24900 \cdot 0.740} = 138.3 \text{ [mm]} \quad (3.12)$$

Next step is controlling slot length to pole pitch ratio:

$$\lambda = \frac{l_i}{\tau_p} = \frac{138.3}{81.4} = 1.7 \text{ [-]} \quad (3.13)$$

As per Figure 3.6, the defined value is not in the range advised for a $2p = 4$ induction machine. Based on [1], as the found λ value is outside the advised range, the next step would be to select a bigger stack height/stator diameter and reiterating parameters calculation. As the design has a strict constraint for sizing of the stator outer diameter, accepting a deviation from advised value range of the λ ratio.

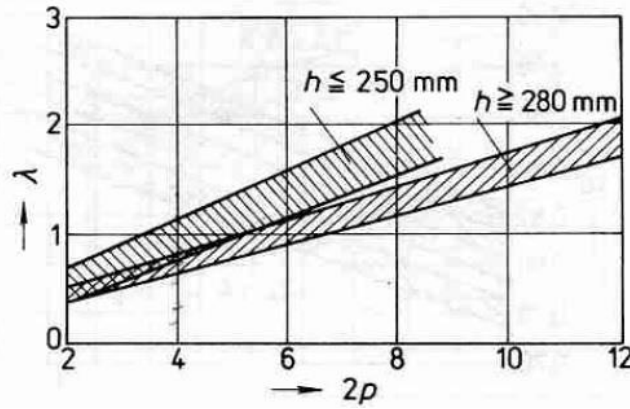


Figure 3.6: Slot length to pole pitch ratio [1]

Given the size and power, inductions machines with the stator slot length l_{FES} smaller than 250-300 mm, are not designed with radial ventilation channels for cooling [1]:

$$l_{FES} = l_i = 138.3 \text{ [mm]} \quad (3.14)$$

With this definition, the sizing of the induction machine main dimensions is completed.

3.4 Stator parameters

The next phase is calculating the stator slots number Q_s . This is done by selecting the stator slot $\tau_{s_min} = 8 \text{ [mm]}$ minimal width and a the $\tau_{s_max} = 11 \text{ [mm]}$ maximal width. The values are defined as per Figure 3-7 and, based on this, calculating the minimal and maximal slots number values.

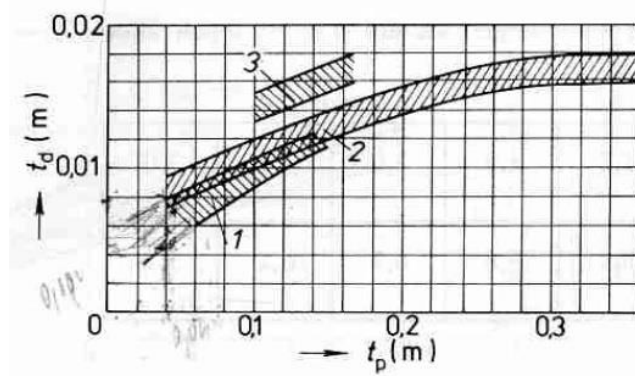


Figure 3.7: Stator slot width [1]

$$Q_{s_min} = \frac{\pi D_s}{\tau_{s_max}} = \frac{\pi \cdot 103.7}{11} = 29 [-] \quad (3.15)$$

$$Q_{s_max} = \frac{\pi D_s}{\tau_{s_min}} = \frac{\pi \cdot 103.7}{8} = 40 [-] \quad (3.16)$$

Observing induction machine stator slot definition rules, the stator slots number Q_s selected:

$$Q_s = 36 [-] \quad (3.17)$$

The selected stator slots number is dividable by the product of number of poles and the number of winding's electrical phases, result being the number of slots per phase and pole q_s :

$$q_s = \frac{Q_s}{2pm} = \frac{36}{4 \cdot 3} = 3 [-] \quad (3.18)$$

Based on the stator interior diameter, the number of poles and the number of phases, calculation of the stator slot width value τ_s is possible at this step:

$$\tau_s = \frac{\pi D_s}{2pmq_s} = \frac{\pi \cdot 103.7}{4 \cdot 3 \cdot 3} = 9 \text{ [mm]} \quad (3.19)$$

Given the size of the induction machine the design method advises a minimal value for τ_s of 6 to 7 mm. The calculated value meets the sizing requirement.

Based on the estimated input parameters, calculating the stator winding phase I_s current for 3 phase power:

$$I_s = \frac{P_2}{3U_{s,ph}\eta\cos\varphi} = \frac{3.8 \cdot 10^3}{3 \cdot 230 \cdot 0.84 \cdot 0.84} = 7.81 \text{ [A]} \quad (3.20)$$

Number of effective conductors in stator slot Z'_{Qs} :

$$Z'_{Qs} = \frac{\pi D_s A_s}{I_s Q_s} = \frac{\pi \cdot 103.7 \cdot 10^{-3} \cdot 25000}{7.81 \cdot 36} = 28.97 [-] \quad (3.21)$$

The found value can be rounded as it is very close to an integer value. If a large deviation from an integer value would be found, a direct round up would affect the resulting speed of the engine. If this would not be acceptable, selecting a corresponding number of wires per conductor that would create a value close to an integer number for the resulting number of conductors in slot. For the present case, by selecting $a = 1$ [1],

the resulting number of conductors in the stator slot is close enough to an integer. (note: the use of parallel winding wires has an impact on stator slot winding manufacturing process but also, using wires of smaller diameter, it may optimize the slot fill [1]).

The resulting number of stator winding conductors per slot Z_{QS} :

$$Z_{QS} = aZ'_{QS} = 1 \cdot 28.97 \cong 29 [-] \quad (3.22)$$

Stator winding number of turns N_s :

$$N_s = \frac{Z_{QS}Q_1}{2am} = \frac{29 \cdot 36}{2 \cdot 1 \cdot 3} = 174 [-] \quad (3.23)$$

Based on these values, the resulting stator linear current density A_s :

$$A_s = \frac{2I_s N_s m}{\pi D_s} = \frac{2 \cdot 7,81 \cdot 174 \cdot 3}{\pi \cdot 103,7 \cdot 10^{-3}} = 25028 [\text{Am}^{-2}] \quad (3.24)$$

The stator winding distribution factor k_{ds1} :

$$k_{ds1} = \frac{\sin \frac{\pi}{2m}}{q_s \sin \frac{\pi}{2mq}} = \frac{\sin \frac{\pi}{2 \cdot 3}}{3 \cdot \sin \frac{\pi}{2 \cdot 3 \cdot 3}} = 0.96 [-] \quad (3.25)$$

For a single layer winding, pitch factor $k_{ps} = 1 [-]$, resulting a winding factor fundamental k_{ws1} :

$$k_{ws1} = k_{ds1} k_{ps} = 0.96 [-]$$

Table 3-2: Coefficient k_{ws1} values [1]

ν	q	2	3	4	5	6	∞
1		0,966	0,960	0,958	0,957	0,957	0,955
5		0,259	0,217	0,205	0,200	0,197	0,191
7		-0,259	-0,177	-0,158	-0,149	-0,145	-0,136
11		-0,966	-0,177	-0,126	-0,110	-0,102	-0,087
13		-0,966	0,217	0,126	0,102	0,092	0,073
17		-0,259	0,960	0,158	0,102	0,084	0,056
19		0,259	0,960	-0,205	-0,110	-0,084	-0,050
23		0,966	0,217	-0,958	-0,149	-0,092	-0,041
25		0,966	-0,177	-0,958	0,200	0,102	0,038
29		0,259	-0,177	-0,205	0,957	0,145	0,033
31		-0,259	0,217	0,158	0,957	-0,197	0,031
35		-0,966	0,960	0,126	0,200	-0,957	-0,027
37		-0,966	0,960	-0,126	-0,149	-0,957	0,026
41		-0,259	0,217	-0,158	-0,110	-0,197	0,023
43		0,259	-0,177	0,205	0,102	0,145	0,022
47		0,966	-0,177	0,958	0,102	0,102	-0,021

The resulting airgap magnetic flux ϕ and magnetic flux density B_δ :

$$\phi = \frac{k_E U_{s,ph}}{4k_B N_s k_{ws1} f_1} = \frac{0,96 \cdot 230}{4 \cdot 1,11 \cdot 174 \cdot 0,96 \cdot 56,74} = 5.247 [\text{mWb}] \quad (3.26)$$

$$B_\delta = \frac{p\phi}{D_s l_i} = \frac{2 \cdot 5.247 \cdot 10^{-3}}{103,7 \cdot 10^{-3} \cdot 138,3 \cdot 10^{-3}} = 0.732 [\text{T}] \quad (3.27)$$

The next step is calculating the stator winding current density J_s and defining the required stator winding conductor effective crosscut area S_{ef} :

$$J_s = \frac{(AJ_s)}{A} = \frac{177 \cdot 10^9}{25028} = 7.192 \cdot 10^6 \text{ [A/m}^2\text{]} \quad (3.28)$$

For completing the step above, a stator thermal load AJ value is selected as per Figure 3-8, taking into consideration that engine cubature is smaller than the standard size for the same power output. For limiting the resulting stator winding current density, selecting a smaller AJ value, then the medium detailed in Figure 3-8:

$$AJ = 177 \cdot 10^9 \text{ [A}^2\text{/m}^3\text{]} \quad (3.29)$$

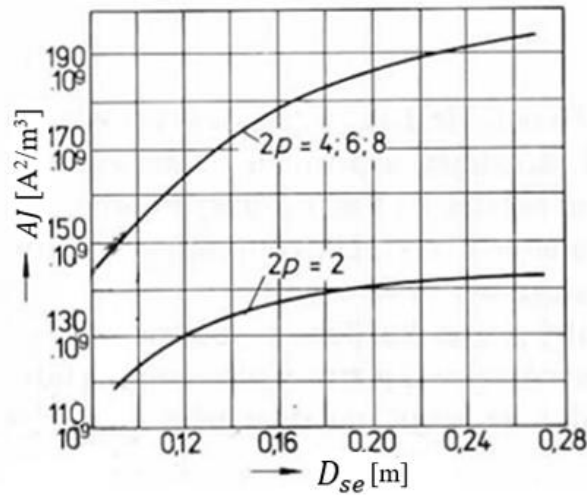


Figure 3.8: Thermal load parameter [1]

The required stator slot winding conductor crosscut S_{cs} :

$$S_{cs} = \frac{I_s}{az_p J_s} = \frac{7.81}{1 \cdot 2 \cdot 7.192 \cdot 10^6} = 0.543 \text{ [mm}^2\text{]} \quad (3.30)$$

This allows proceeding to selection of a standard wire gauge for the stator winding conductor cross section S_{cs} , based on the number of parallel branches $a = 1$ [-], and the number of wire strands $z_p = 2$ [-], where S_{cs} is the catalog selected conductor diameter, b_{oc} is the wire diameter, and δ_i is the wire insulation thickness and b_c is the total (conductor + insulation) stator winding wire diameter:

- $S_{cs} = 0.567 \text{ [mm}^2\text{]}$;
- $b_{oc} = 0.85 \text{ [mm]}$;
- $\delta_i = 0.07 \text{ [mm]}$.

Note: wire dimensions selected as per [1].

$$S_{ef} = az_p S_v = 1 \cdot 2 \cdot 0.567 = 1.134 \text{ [mm}^2\text{]} \quad (3.31)$$

$$b_c = b_{oc} + \delta_i = 0.85 + 0.07 = 0.97 \text{ [mm]} \quad (3.32)$$

The resulting stator winding conductor current density:

$$J_s = \frac{I_s}{an_p S_{cs}} = \frac{7.68}{1 \cdot 2 \cdot 0.636 \cdot 10^{-6}} = 6.887 \cdot 10^6 \text{ [A/m}^2\text{]} \quad (3.33)$$

3.5 Stator slot parameters

Selecting the stator slot type (Figure 3-9), with the following sizing parameters:

- the slot opening $b_0 = 3.5$ [mm];
- the tooth tip height $h_{0s} = 0.5$ [mm].

Stator slots used have constant tooth width at the base and the top. This setup allows a constant magnetic flux density in tooth's steel. b_0 dimension is normalized and, as the minimal size, should be bigger than the winding wire diameter $b_c + (1.5 \text{ to } 2\text{mm})$ [1]. Selection made, satisfies this requirement.

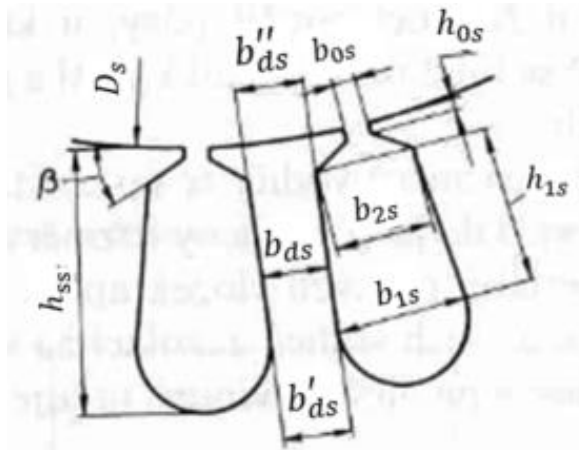


Figure 3.9: Stator slot dimensions [1]

The advised stator-teeth B_{ds} and the stator-yoke B_{ys} flux densities ranges are:

$$B_{ds} = 1.7 - 1.9 \text{ [T]}$$

$$B_{ys} = 1.4 - 1.6 \text{ [T]}$$

For initial calculation selecting minimum value for both parameters.

$$B_{ds} = 1.78 \text{ [T]}$$

$$B_{ys} = 1.4 \text{ [T]}$$

Estimating the stator stacking factor $k_{Fe} = 0.95$ [-].

Calculating the stator-teeth width b_{ds} :

$$b_{ds} = \frac{B_{\delta} \tau_s l_i}{B_{ds} l_{Fe} k_{Fe}} = \frac{0.732 \cdot 9 \cdot 10^{-3} \cdot 138.3}{1.78 \cdot 138.3 \cdot 0.95} = 4.1 \text{ [mm]} \quad (3.34)$$

The stator-yoke height h_{ys} :

$$h_{ys} = \frac{\phi}{2 B_{ys} l_{Fe} k_{Fe}} = \frac{5.247 \cdot 10^{-3}}{2 \cdot 1.4 \cdot 138.3 \cdot 0.95} = 14.26 \text{ [mm]} \quad (3.35)$$

The stator slot height h_{ss} :

$$h_{ss} = \frac{D_{se} - D_s}{2} - h_{ys} = \frac{156 - 103.7}{2} - 14.26 = 11.89 \text{ [mm]} \quad (3.36)$$

Calculating the slot width dimensions b_{1s} and b_{2s} , based on standard slot parameters [1] $b_{0s} = 3.5$ [mm] and $h_{0s} = 0.5$ [mm]:

$$b_{1s} = \frac{\pi(D_s + 2h_{ss})}{Q_s} - b_{ds} = \frac{\pi(103.7 + 2 \cdot 11.89)}{36} - 3.9 = 7.2 \text{ [mm]} \quad (3.37)$$

For b_{s2} and h_{s2} dimensions calculating based on stator slot top angle $\beta = 45^\circ$.

$$b_{2s} = \frac{\pi(D_s + 2h_{0s} - b_{0s}) - Q_s b_{ds}}{Q_s - \pi} = \frac{\pi(103.7 + 2 \cdot 0.5 - 3.5) - 36 \cdot 3.9}{36 - \pi} = 5.3 \text{ [mm]} \quad (3.38)$$

The stator tooth tip heights h_{2s} and h_{1s} :

$$h_{2s} = \frac{b_{2s} - b_{0s}}{2} = \frac{5.3 - 3.5}{2} = 0.9 \text{ [mm]} \quad (3.39)$$

$$h_{1s} = h_{ss} - (h_{0s} + h_{2s}) = 11.89 - (0.5 + 0.9) = 10.5 \text{ [mm]} \quad (3.40)$$

At this step, for completing sizing of the stator slot dimensions, taking in consideration the stacking alignment error of stator laminated steel sheets. For this approximation coefficient $\Delta b_{bs} = 0.2$ [mm] is estimated.

Modifying the b_{1s} , b_{2s} and h_{1s} parameters to adjusted values that are taking in consideration Δb_{bs} value:

$$b'_{1s} = b_{1s} - \Delta b_{bs} = 7.2 - 0.2 = 7 \text{ [mm]} \quad (3.41)$$

$$b'_{2s} = b_{2s} - \Delta b_{bs} = 5.3 - 0.2 = 5.1 \text{ [mm]} \quad (3.42)$$

$$h'_{1s} = h_{1s} - \Delta b_{bs} = 10.5 - 0.2 = 10.3 \text{ [mm]} \quad (3.43)$$

For calculating slot insulation liner crosscut area S_{is} , defining insulation thickness $b_{is} = 0.2$ [mm]:

$$S_{is} = b_{is}(2h_{ss} + b_{1s} + b_{2s}) = 0.2 \cdot (2 \cdot 11.89 + 7.2 + 5.3) = 12.1 \text{ [mm}^2\text{]} \quad (3.44)$$

Because no winding interlayer insulation is used, $S_{ls} = 0$ [mm], the resulting stator slot total active crosscut area S_{cus} :

$$\begin{aligned} S_{cus} &= \frac{(b'_{1s} + b'_{2s})h'_{1s}}{2} + \frac{\pi(b'_{1s})^2}{8} - S_{is} - S_{ls} = \\ &= \frac{(7 + 5.1) \cdot 10.3}{2} + \frac{\pi \cdot (7)^2}{8} - 11.1 - 0 = 69.5 \text{ [mm}^2\text{]} \end{aligned} \quad (3.45)$$

The stator slot fill factor k_T :

$$k_{Cu} = \frac{d_c^2 Z_{Qs} Z_p}{S_{cus}} = \frac{0.92^2 \cdot 29 \cdot 2}{69.5} = 0.706 \text{ [-]} \quad (3.46)$$

The calculated value is acceptable for stator machine winding manufacturing processes.

3.6 Air gap size

For induction machines with output power up to 20 kW and $2p \geq 4$, the air gap width δ is calculated based on:

$$\delta = (0.25 + D_s)10^{-3} = (0.25 + 103.7 \cdot 10^{-3}) \cdot 10^{-3} = 0.354 \text{ [mm]} \quad (3.47)$$

Selecting an air gap width value of $\delta = 0.4$ [mm], considering technical limitation associated with a small airgap value. Alternately, Figure 3.10 can be used for selecting the air gap width based on stator's interior diameter.

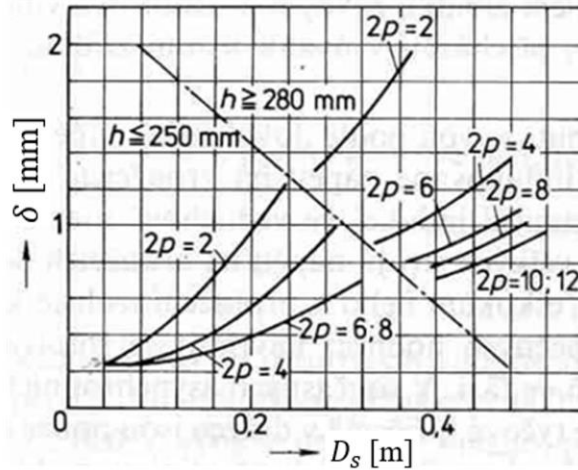


Figure 3.10: Air gap size [1]

3.7 Rotor parameters

A “squirrel cage” rotor type will be used for the design of this machine with aluminum rotor bars die-cast into rotor slots.

Selecting $Q_r = 26$ [-], which is a value permitted by Table 3-3 [2]. (Based on the number of pole pairs and corresponding stator slots number, “safe” combinations are the ones not marked in the table by a sign.)

Table 3-3: Permitted number of stator bars [2]

Q_s	Tens of the slot number of the rotor	Number of pole pairs $p = 1$ Ones of the rotor slot number Q_r										Number of pole pairs $p = 2$ Ones of the rotor slot number Q_r									
		0	1	2	3	4	5	6	7	8	9	0	1	2	3	4	5	6	7	8	9
24	1	-	x	○	x	+	x	-	x	○	x	-	x	○	x	+	x	+	x		x
	2	+	x	-	x	○	x	+	x	-	x	-	x	-	x	○	x	+	x	+	x
	3	○	x	+	x	-	x	○	x	+	x		x	-	x		x	○	x		x
36	1	-	x	○	x	+	x	-	x	○	x		x	○	x		x	±	x	○	x
	2	+	x	-	x	○	x	+	x	-	x	±	x		x	○	x		x	+	x
	3	○	x	+	x	-	x	○	x	+	x		x	-	x	-	x	○	x	+	x
	4	-	x	○	x	+	x	-	x	○	x	+	x		x	-	x		x	○	x
	5	+	x	-	x	○	x	+	x	-	x		x	+	x		x	-	x		x
48	1	-	x	○	x	+	x	-	x	○	x		x	○	x		x	+	x		x
	2	+	x	-	x	○	x	+	x	-	x	-	x	-	x	○	x	+	x	+	x
	3	○	x	+	x	-	x	○	x	+	x		x	-	x		x	○	x		x
	4	-	x	○	x	+	x	-	x	○	x	+	x		x	-	x	-	x	○	x
	5	+	x	-	x	○	x	+	x	-	x	+	x	+	x		x	-	x		x
	6	○	x	+	x	-	x	○	x	+	x	○	x		x	+	x		x	-	x

Source: Adapted from Richter (1954).

Value $Q_r = 22$ [-] is also in line with the rotor slot selection guidance detailed in [1], where it is stated that for $Q_r < Q_s$ appearance of higher harmonic moments is restricted more than in case $Q_r > Q_s$.

Calculating the rotor diameter D_s and the rotor stack length l_{Fer} :

$$D_r = D_s - 2\delta = 103.7 - 2 \cdot 0.4 = 102.9 \text{ [mm]} \quad (3.48)$$

$$l_{\text{Fer}} = l_i = 138.3 \text{ [mm]} \quad (3.49)$$

Based on the selected rotor slots number, the resulting rotor slot width τ_r :

$$\tau_r = \frac{\pi D_r}{Q_r} = \frac{\pi \cdot 102.9}{26} = 12.4 \text{ [mm]} \quad (3.50)$$

For calculating the induced current in rotor slot I_s , first, the rotor slot current transformation to stator slot ratio k_{rs} is defined:

$$k_{rs} = \frac{2mZ_{Qs}k_{ws1}}{Q_2} = \frac{2 \cdot 3 \cdot 174 \cdot 0.96}{26} = 38.55 \text{ [-]} \quad (3.51)$$

The resulting rotor bar current I_r is calculated:

$$I_r = k_{rs} I_s p_i = 38.55 \cdot 7.81 \cdot 0.87 = 262 \text{ [A]} \quad (3.52)$$

where, coefficient $k_i = 0.86 \text{ [-]}$ is defined based on the estimated coupling factor value as per Figure 3-11, below.

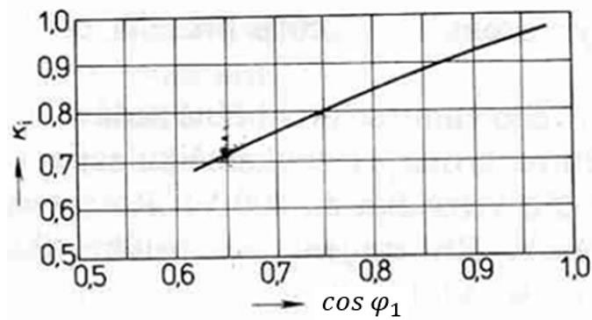


Figure 3.11: k_i coefficient [1]

3.8 Rotor slot parameters

Based on the selected rotor bar current density $J_r = 3.3 \cdot 10^6 \text{ [A/m}^2\text{]}$, calculating the required rotor bar cross section S_{cr} :

$$S_{cr} = \frac{I_r}{J_r} = \frac{262}{3.3 \cdot 10^6} = 79.4 \text{ [mm}^2\text{]} \quad (3.53)$$

The advised rotor-teeth flux density B_{dr} and the rotor-yoke flux density B_{yr} are:

- $B_{dr} = 1.75 - 1.85 \text{ [T]}$, selecting $B_{dr} = 1.75 \text{ [T]}$;
- $B_{yr} \leq 1.25 \text{ [T]}$, selecting $B_{yr} = 1 \text{ [T]}$.

The permitted rotor-teeth width b_{drmax} :

$$b_{drmax} = \frac{B_{\delta} \tau_r l_i}{B_{dr} l_{Fe2} k_{Fe}} = \frac{0.732 \cdot 12.4 \cdot 138.3}{1.65 \cdot 138.3 \cdot 0.95} = 5.5 \text{ [mm]} \quad (3.54)$$

Selecting bar type V, in an open slot setup (Figure 3-12, left) with the following sizing parameters:

- $b_{0r} = 1 \text{ [mm]}$;
- $h_{0r} = 0.7 \text{ [mm]}$;
- $h'_{0r} = 0.0 \text{ [mm]}$.

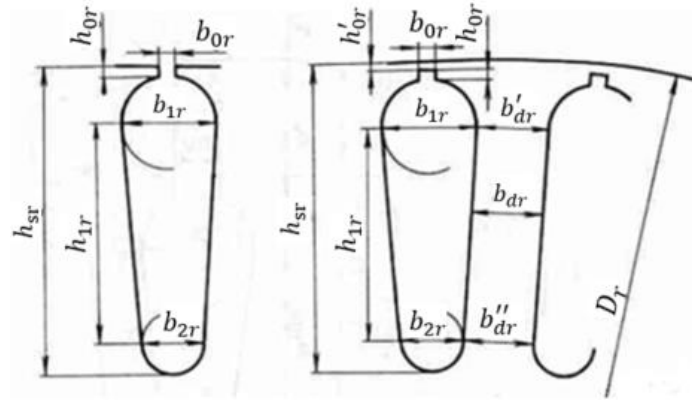


Figure 3.12: Rotor slot dimentios [1]

The resulting rotor slot width b_{1r} , b_{2r} and the h_{1r} dimension:

$$b_{1r} = \frac{\pi(D_r - 2h_{0r} - 2h'_{0r}) - Q_r b_{drmax}}{\pi + Q_r} = \frac{\pi(102.9 - 2 \cdot 0.7 - 2 \cdot 0.3) - 22 \cdot 5.5}{\pi + 26} = 6.0 \text{ [mm]} \quad (3.55)$$

$$b_{2r} = \sqrt{\frac{b_1^2 \left(\frac{Q_r + \pi}{2} \right) - 4S_{cr}}{\frac{Q_r - \pi}{2}}} = \sqrt{\frac{(6.0)^2 \left(\frac{26 + \pi}{2} \right) - 4 \cdot 79.5 \cdot 10^{-6}}{\frac{26 - \pi}{2}}} = 2.3 \text{ [mm]} \quad (3.56)$$

The found b_{2r} is above the minimal value, the advised value $b_{2r} > 1.5$ to 2 mm [1].

$$h_{1r} = (b_{1r} - b_{2r}) \frac{Q_r}{2\pi} = (6.0 - 2.3) \frac{26}{2\pi} = 15.3 \text{ [mm]} \quad (3.57)$$

The calculated rotor slot height h_{sr} :

$$\begin{aligned} h_{sr} &= h'_{0r} + h_{0r} + \frac{b_{1r}}{2} + h_{1r} + \frac{b_{2r}}{2} = \\ &= 0.7 + \frac{6.0}{2} + 15.3 + \frac{2.3}{2} = 20.2 \text{ [mm]} \end{aligned} \quad (3.58)$$

The resulting rotor bar cross section S_{dr} and the rotor bar current density J_{dr} :

$$\begin{aligned} S_{dr} &= \frac{\pi}{8} (b_{1r}^2 + b_{2r}^2) + \frac{1}{2} (b_{1r} + b_{2r}) h_{1r} = \\ &= \frac{\pi}{8} (6.0^2 + 2.3^2) + \frac{1}{2} (6.0 + 2.3) \cdot 15.3 = 79.7 \text{ [mm}^2\text{]} \end{aligned} \quad (3.59)$$

$$J_{dr} = \frac{I_r}{S_{cr}} = \frac{262}{79.7} = 3.287 \cdot 10^6 \text{ [A/m}^2\text{]} \quad (3.60)$$

The rotor end ring current transformation coefficient Δ and the calculated ring current I_{ring} and ring current density J_{ring} :

$$\Delta = 2 \sin \frac{2\pi}{Q_r} = 2 \sin \frac{2\pi}{26} = 0.479 \text{ [-]} \quad (3.61)$$

$$I_{ring} = \frac{I_r}{\Delta} = \frac{262}{0.479} = 547 \text{ [A]} \quad (3.62)$$

$$J_{ring} = 0.85 \cdot J_{dr} = 0.85 \cdot 3.287 \cdot 10^6 = 2.794 \cdot 10^6 \text{ [A/m}^2\text{]} \quad (3.63)$$

The required rotor end ring cross section area S'_{ring} :

$$S'_{ring} = \frac{I_{ring}}{J_{ring}} = \frac{547}{2.794 \cdot 10^6} = 195.8 \text{ [mm}^2\text{]} \quad (3.64)$$

The resulting rotor end ring width a_{ring} and the end ring height b_{ring} :

$$b_{\text{ring}} = 1.25h_{\text{dr}} = 1.25 \cdot 20.2 = 25.2 \text{ [mm]} \quad (3.65)$$

$$a_{\text{ring}} = \frac{S'_{\text{cring}}}{b_{\text{ring}}} = \frac{195.8}{25.2} = 7.8 \text{ [mm]} \quad (3.66)$$

The rotor end ring cross section area S_{cring} and the interior diameter D_{ring} :

$$S_{\text{cring}} = a_{\text{ring}}b_{\text{ring}} = 7.8 \cdot 25.2 = 196.6 \text{ [mm}^2\text{]} \quad (3.67)$$

$$D_{\text{ring}} = D_{\text{r}} - b_{\text{ring}} = 102.9 - 25.2 = 95.1 \text{ [mm]} \quad (3.68)$$

3.9 Magnetic circuit

Calculating magnetic flux densities in teeth and yokes (based on calculated air gap magnetic flux density and calculated teeth widths and yokes heights).

$$B_{\text{ds}} = \frac{B_{\delta}\tau_s l_i}{b_{\text{ds}} l_{\text{Fe}} k_{\text{Fe}}} = \frac{0.732 \cdot 9 \cdot 138.3}{4.1 \cdot 138.3 \cdot 0.95} = 1.69 \text{ [T]} \quad (3.69)$$

$$B_{\text{dr}} = \frac{B_{\delta}\tau_r l_i}{b_{\text{dr}} l_{\text{Fe}} k_{\text{Fe}}} = \frac{0.732 \cdot 14.7 \cdot 138.3}{7.2 \cdot 138.3 \cdot 0.95} = 1.72 \text{ [T]} \quad (3.70)$$

$$B_{\text{ys}} = \frac{\phi}{2h_{\text{ys}} l_{\text{Fe}} k_{\text{Fe}}} = \frac{5.247 \cdot 10^{-3}}{2 \cdot 14.3 \cdot 138.3 \cdot 0.95} = 1.4 \text{ [T]} \quad (3.71)$$

$$B_{\text{yr}} = \frac{\phi}{2h_{\text{yr}} l_{\text{Fe}} k_{\text{Fe}}} = \frac{5.247 \cdot 10^{-3}}{2 \cdot 13.5 \cdot 138.3 \cdot 0.95} = 1.48 \text{ [T]} \quad (3.72)$$

For the calculation in this of value h'_{yr} , which represents the apparent height off the rotor yoke, as the rotor shaft is considered non-magnetic, the apparent height of the stator yoke h'_{yr} equals actual height of the stator yoke h_{yr} :

$$h_{\text{yr}} = \frac{D_{\text{r}} - D_{\text{ri}}}{2} - h_{\text{sr}} = \frac{102.9 - 36}{4} - 20.2 = 13.5 \text{ [mm]} \quad (3.73)$$

$$h'_{\text{yr}} = h_{\text{yr}} = 13.5 \text{ [mm]} \quad (3.74)$$

The resulting magnetic tension in airgap $U_{m,\delta}$:

$$\begin{aligned} U_{m,\delta} &= 1.59 \cdot 10^6 B_{\delta} k_{\text{Cs}} \delta = \\ &= 1.59 \cdot 10^6 \cdot 0.732 \cdot 1.331 \cdot 0.4 \cdot 10^{-3} = 619.65 \text{ [A]} \end{aligned} \quad (3.75)$$

where the stator Carter factor for k_{Cs} is:

$$k_{\text{Cs}} = \frac{\tau_s}{\tau_s - k_s \delta} = \frac{9}{9 - 5.6 \cdot 0.4} = 1.331 \text{ [-]} \quad (3.76)$$

based on coupling factor k_s :

$$k_s = \frac{\left(\frac{b_{0s}}{\delta}\right)^2}{5 + \left(\frac{b_{0s}}{\delta}\right)} = \frac{\left(\frac{3.5}{0.4}\right)^2}{5 + \left(\frac{3.5}{0.4}\right)} = 5.6 \text{ [-]} \quad (3.77)$$

For calculating the magnetic tension in the stator's and the rotor's teeth calculating first the stator and the rotor tooth heights:

$$h_{ds} = h_{ss} = 11.9 \text{ [mm]} \quad (3.78)$$

$$h_{dr} = h_{sr} - 0.1b_{2r} = 20.2 - 0.1 \cdot 2.3 = 20 \text{ [mm]} \quad (3.79)$$

Magnetic tension is calculated for the entire flux line crossing teeth height twice for a closed loop crossing stator and rotor:

$$U_{m,ds} = 2h_{ds}H_{ds} = 2 \cdot 11.9 \cdot 10^{-3} \cdot 5932 = 141.06 \text{ [A]} \quad (3.80)$$

$$U_{m,dr} = 2h_{dr}H_{dr} = 2 \cdot 20 \cdot 10^{-3} \cdot 7236 = 289.44 \text{ [A]} \quad (3.81)$$

$H_{ds} = 5932 \text{ [A/m]}$ and $H_{dr} = 7236 \text{ [A/m]}$ coercivities values are corresponding to the B-H curve for 50 Hz frequency for SURA M350-50A magnetic steel [6].

The stator and the rotor teeth magnetic flux saturation k_{sat} :

$$k_{sat} = 1 + \frac{U_{m,ds} + U_{m,dr}}{U_{m,\delta}} = \frac{141.06 + 289.44}{619.65} = 1.69 \text{ [-]} \quad (3.82)$$

For calculating magnetic tension in the stator and the rotor yoke calculating first magnetic flux line medium lengths for the stator l_{ys} and the rotor l_{yr} :

$$l_{ys} = \frac{\pi(D_{se} - h_{ys})}{2p} = \frac{\pi(156 - 14.3)}{4} = 111.3 \text{ [mm]} \quad (3.83)$$

$$l_{yr} = \frac{\pi(D_{ri} + h_{yr})}{2p} = \frac{\pi(36 + 13.5)}{4} = 39 \text{ [mm]} \quad (3.84)$$

Magnetic tensions in the stator and the rotor yoke:

$$U_{m,ys} = l_{ys}H_{ys} = 111.3 \cdot 10^{-3} \cdot 517 = 57.5 \text{ [A]} \quad (3.85)$$

$$U_{m,yr} = l_{yr}H_{yr} = 13.5 \cdot 10^{-3} \cdot 124 = 43.53 \text{ [A]} \quad (3.86)$$

with $H_{ys} = 517 \text{ [A/m]}$ and $H_{yr} = 1116 \text{ [A/m]}$ as per [10].

The resulting magnetic tension for motor's magnetic circuit and magnetic circuit saturation coefficient are:

$$\begin{aligned} F_m &= U_{m,\delta} + U_{m,ds} + U_{m,dr} + U_{m,ys} + U_{m,yr} = \\ &= 619.7 + 141.1 + 289.4 + 57.5 + 43.53 = 1151.2 \text{ [A]} \end{aligned} \quad (3.87)$$

$$k_\mu = \frac{F_m}{U_\delta} = \frac{1151.2}{619.7} = 1.86 \text{ [-]} \quad (3.88)$$

Calculating magnetization current $I_{s,mag}$ and its relative value $i_{s,mag}$:

$$I_{s,mag} = \frac{pF_m}{0.9mN_s k_{ws1}} = \frac{2 \cdot 1151.2}{0.9 \cdot 3 \cdot 174 \cdot 0.96} = 5.11 \text{ [A]} \quad (3.89)$$

$$i_{s,mag} = \frac{I_{s,mag}}{I_s} = \frac{4.93}{8.57} = 0.65 \text{ [-]} \quad (3.90)$$

3.10 Electrical resistance and reactance

For completing the definition of induction machine's equivalent circuit, in this section, the stator's and the rotor's resistance and reactance, core loss resistance and magnetization branch reactance will be calculated. Equations apply for types of the stator and the rotor slots chosen for the design of this motor.

The stator and the rotor DC resistances are calculated for a nominal $\vartheta = 115$ [°C]. Copper and aluminum resistivity for this temperature: $\rho_{Cu115} = 10^{-6}/47$ [Ωm] and $\rho_{Al115} = 10^{-6}/21.5$ [Ωm] [1].

Total length of a coil turn l_{av} , considering the slot wire length $l_d = l_{Fes} = 0.138$ [m]:

$$l_{av} = 2(l_d + l_W) = 2 \cdot (0.138 + 0.138) = 0.552$$
 [m] (3.91)

The medium coil span l_W is calculated based on coefficient $K_W = 1.3$ [-] and additional length at exit from stator slot $B = 0.01$ [m] [1].

$$l_W = K_W b_c + 2B = 1.3 \cdot 0.091 + 2 \cdot 0.01 = 0.138$$
 [m] (3.92)

where medium pitch span b_c :

$$b_c = \frac{\pi(D_s + h_{ds})}{2p} \beta_1 = \frac{\pi(103.7 + 11.9) \cdot 10^{-3}}{4} \cdot 1 = 0.091$$
 [m] (3.93)

(span coefficient $\beta_1 = 1$, for full pitch winding)

The total conductor length in a stator coil:

$$l_c = l_{av} N_s = 0.552 \cdot 174 = 96.05$$
 [m] (3.94)

The resulting one phase stator resistance R_{DCs} and relative value of this resistance r_{DCs} :

$$R_{DCs} = \rho_{Cu115} \frac{l_c}{aS_{ef}} = \frac{10^{-6}}{47} \cdot \frac{96.05}{1.134 \cdot 10^{-6}} = 2.07$$
 [Ω] (3.95)

$$r_{DCs} = R_{DCs} \frac{I_s}{U_{s,ph}} = 2.07 \cdot \frac{7.81}{230} = 0.007$$
 [-] (3.96)

In case of “squirrel cage” rotor, one rotor winding turn is formed by one bar and associated end ring arcs connecting respective bar to the next one. As a result, resistivity of one rotor winding is calculated by summing resistivity of one bar plus resistivity of the two end ring connection sections.

The rotor bar resistivity R_{dr} :

$$R_{dr} = \rho_{Al115} \frac{l_{Fer}}{S_{cr}} = \frac{10^{-6}}{21.5} \cdot \frac{138.3 \cdot 10^{-3}}{79.7} = 8.465 \cdot 10^{-5}$$
 [Ω] (3.97)

The rotor end ring resistivity R_{dring} :

$$R_{dring} = \rho_{Al115} \frac{\pi D_{ring}}{Q_2 S_{cring}} = \frac{10^{-6}}{21.5} \cdot \frac{\pi \cdot 95.1 \cdot 10^{-3}}{26 \cdot 196.6 \cdot 10^{-6}} = 2.851 \cdot 10^{-6}$$
 [Ω] (3.98)

The resulting resistivity for one rotor winding R_{DCr} , the value of this resistivity referred to stator R'_{DCr} and its relative value r'_{DCr} :

$$R_{DCr} = R_{dr} + \frac{2R_{dring}}{A^2} = 8.465 \cdot 10^{-5} + \frac{2 \cdot 2.851 \cdot 10^{-6}}{0.0479^2} = 1.095 \cdot 10^{-4} [\Omega] \quad (3.99)$$

$$R'_{DCr} = R_{DCr} \frac{4m(N_s k_{ws1})^2}{Q_r} = 1.095 \cdot 10^{-4} \cdot \frac{4 \cdot 3(174 \cdot 0.96)^2}{26} = 1.41 [\Omega] \quad (3.100)$$

$$r'_{DCr} = R'_{DCr} \frac{I_s}{U_{s,ph}} = 1.41 \cdot \frac{7.81}{230} = 0.0479 [-] \quad (3.101)$$

The nominal slip s_N can be estimated based on the relative value of rotor resistivity referred to stator r'_{DCr} :

$$s_N \approx r'_{DCr} = 0.0479 [-] \quad (3.102)$$

Main flux linkage generates electro-mechanical energy transformation in an induction motor [2]. Other stator or rotor winding flux leakage linkages (for flux crossing airgap or other sections of the machine) are forming linkage reactance that need to be evaluated for defining analytical model of the induction machine.

For calculating rotor and stator winding reactance values [1] is analyzing slot, winding end-turns and differential reactance of stator and rotor.

The stator slot reactance $X_{s\sigma}$:

$$X_{s\sigma} = 15.8 \frac{f_1}{100} \left(\frac{N_1}{100} \right)^2 \frac{l'_i}{pq} (\lambda_{ds} + \lambda_{ws} + \lambda_{difs}) = 15.8 \frac{56.74}{100} \left(\frac{174}{100} \right)^2 \cdot \frac{138.3 \cdot 10^{-3}}{2 \cdot 3} \cdot (1.19 + 0.629 + 0.867) = 2.24 [\Omega] \quad (3.103)$$

Relative value of the stator reactance $x_{s\sigma}$:

$$x_{s\sigma} = X_{s\sigma} \frac{I_s}{U_{s,ph}} = 2.24 \cdot \frac{7.81}{230} = 0.076 [-] \quad (3.104)$$

The stator slot magnetic permeance coefficient λ_{ds} :

$$\lambda_{ds} = \frac{h_{3xs}}{3b_{2s}} k_\beta + \left(\frac{h_{2xs}}{b_{2s}} + \frac{3h_{1xs}}{b_{2s} + 2b_{0s}} + \frac{h_{0s}}{b_{0s}} \right) k'_\beta = \frac{9.78}{3 \cdot 5.3} \cdot 1 + \left(\frac{1.15}{5.3} + \frac{3 \cdot 0.9}{5.3 + 2 \cdot 3.5} + \frac{0.5}{3.5} \right) \cdot 1 = 1.19 [-] \quad (3.105)$$

with parameters:

$$h_{1xs} = h_{2s} = 0.9 [\text{mm}]; \quad (3.106)$$

$$h_{2xs} = 1.15 [\text{mm}] [1] \text{ Tab. D4.1c};$$

$$h_{3xs} = h_{1s} - 0.1b_{1s} = 10.5 - 0.1 \cdot 7.2 = 9.78 [\text{mm}]; \quad (3.107)$$

The slot sizing parameters are defined as per Figure 3-13.

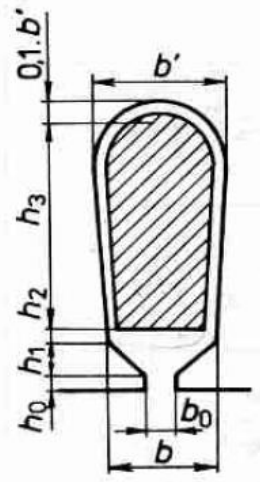


Figure 3.13: Stator slot parameters [1]

The stator winding end turn magnetic permeance coefficient λ_{ws} :

$$\begin{aligned}\lambda_{ws} &= 0.34 \frac{q}{l_i} (l_w - 0.64\beta\tau_p) = \\ &= 0.34 \cdot \frac{3}{138.3} (138 - 0.64 \cdot 1 \cdot 81.4) = 0.63 [-]\end{aligned}\quad (3.108)$$

The stator differential magnetic permeance coefficient λ_{difs} :

$$\lambda_{difs} = \frac{\tau_s}{12\delta k_{cs}} \xi_s = \frac{8.8}{12 \cdot 0.4 \cdot 1.331} \cdot 1.25 = 1.76 [-]\quad (3.109)$$

Where the coefficient ξ is:

$$\begin{aligned}\xi_s &= 2k'_\gamma k_\beta - k_{ws1}^2 \left(\frac{\tau_r}{\tau_s}\right)^2 (1 + \beta_\gamma^2) = \\ &= 2 \cdot 1.5 \cdot 1 - 0.96^2 \cdot \left(\frac{12.4}{9}\right)^2 \cdot (1 + 0^2) = 1.25 [-]\end{aligned}\quad (3.110)$$

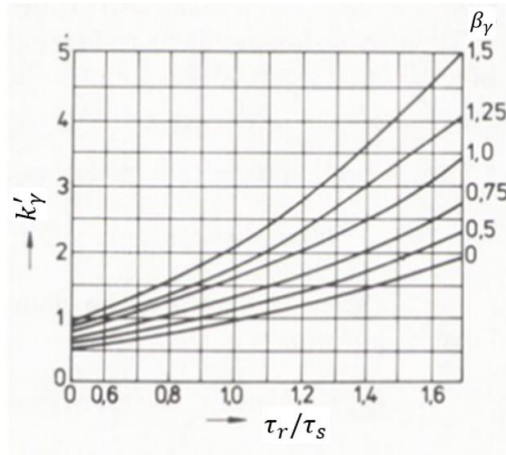


Figure 3.14: Coefficient k'_γ [1]

Selecting the coefficients $k_\beta = k'_\beta = 1 [-]$, $\beta_\gamma = 0 [-]$ for a full pitch stator winding and coefficient $k'_\gamma = 1.5 [-]$ value is defined as per Figure 3-14 for $\frac{\tau_r}{\tau_s} = \frac{12.4}{9} = 1.4 [-]$.

The leakage reactance of the rotor winding $X_{r\sigma}$:

$$\begin{aligned} X_{r\sigma} &= 7.9 f_1 l_i' (\lambda_{dr} + \lambda_{cr} + \lambda_{difr}) 10^{-6} = \\ &= 7.9 \cdot 56.74 \cdot 138.3 \cdot (1.61 + 0.235 + 2.5) \cdot 10^{-6} = \\ &= 2.694 \cdot 10^{-4} [\Omega] \end{aligned} \quad (3.111)$$

The rotor slot magnetic permeance coefficient λ_{dr} :

$$\begin{aligned} \lambda_{dr} &= \left[\frac{h_{3xr}}{3b_{1r}} \left(1 - \frac{\pi b_{1r}^2}{8S_{cr}} \right)^2 + 0.66 - \frac{b_{0r}}{2b_{1r}} \right] k_d + \frac{h_{0r}}{b_{0r}} = \\ &= \left[\frac{16.27}{3 \cdot 6.3} \left(1 - \frac{\pi \cdot 6^2}{8 \cdot 79.7} \right)^2 + 0.66 - \frac{0.7}{2 \cdot 6} \right] \cdot 1 + \frac{0.7}{1.5} = 1.61 [-] \end{aligned} \quad (3.112)$$

The parameter $k_d = 1 [-]$ for nominal run [1].

$$\begin{aligned} h_{3xs} &= h_{sr} - h_{0r} - 0.5b_{1r} - 0.1b_{2r} = \\ &= 20.2 - 0.7 - 0.5 \cdot 6 - 0.1 \cdot 2.3 = 16.27 [\text{mm}]; \end{aligned} \quad (3.113)$$

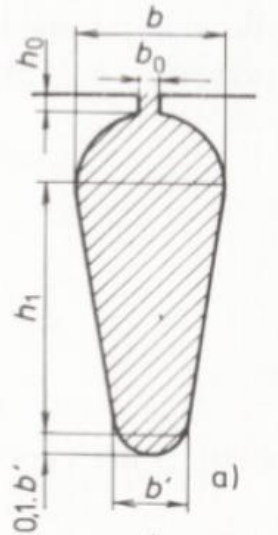


Figure 3.15: Rotor slot parameters [1]

The rotor end winding magnetic permeance coefficient λ_{wr} :

$$\lambda_{wr} = \frac{2.3 D_{ring}}{Q_r l_i' \Delta^2} \log \frac{4.7 D_{ring}}{2(a_{ring} + b_{ring})} = \frac{2.3 \cdot 95.1}{26 \cdot 138.3 \cdot 0.479^2} \log \frac{4.7 \cdot 95.1}{2 \cdot (25.2 + 7.8)} = 0.235 [-] \quad (3.114)$$

The rotor differential magnetic permeance coefficient λ_{difr} :

$$\lambda_{difr} = \frac{\tau_r}{12 \delta k_{Cr}} \xi_r = \frac{12.4}{12 \cdot 0.4 \cdot 1.054} \cdot 1 = 2.5 [-] \quad (3.115)$$

$$\xi_r = 1 + \frac{1}{5} \left(\frac{\pi p}{Q_r} \right)^2 - \frac{\Delta_z}{1 - \left(\frac{p}{Q_r} \right)^2} = 1 + \frac{1}{5} \left(\frac{\pi \cdot 2}{26} \right)^2 - \frac{0.3}{1 - \left(\frac{2}{26} \right)^2} = 1 [-] \quad (3.116)$$

The coefficient $\Delta_z = 0.03 [-]$ value is defined as per Figure 3-16 for $\frac{b_{0r}}{\tau_r} = \frac{1.5}{9} = 0.1 [-]$ and $\frac{b_{0r}}{\delta} = \frac{1.5}{0.4} = 4 [-]$.

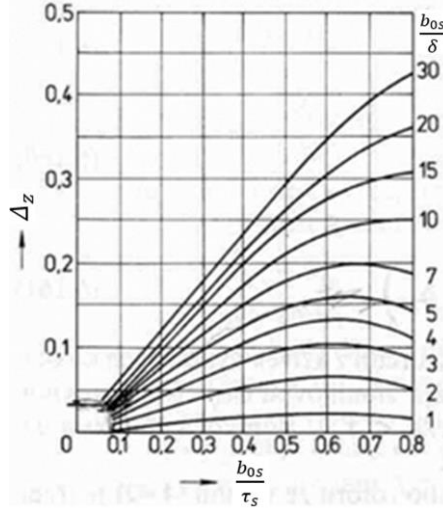


Figure 3.16: Coefficient Δ_z [1]

The rotor leakage reactance, and per unit value referred to stator:

$$X'_{r\sigma} = X_{r\sigma} \frac{4m(N_s k_{ws1})^2}{Q_r} = 2.694 \cdot 10^{-4} \cdot \frac{4 \cdot 3 \cdot (174 \cdot 0.96)^2}{26} = 3.47 [\Omega] \quad (3.117)$$

$$x'_{r\sigma} = X'_{r\sigma} \frac{I_s}{U_{s,ph}} = 3.47 \cdot \frac{7.81}{230} = 0.118 [-] \quad (3.118)$$

3.11 Energy losses

As per [3], losses affecting operation of an induction machine can be categorized as iron losses (magnetic hysteresis and eddy current losses), resistive (stator and rotor windings Joule losses), additional losses (stray losses) and mechanical losses (bearing and windage losses).

Estimate of the losses occurring through machine operation is important for qualifying power output efficiency level of the machine and, also, used as an input for calculating heat transfer in between different components of the motor and heat removal required for ensuring optimal motor components temperature and, together with this a long lifetime of the induction machine. The analytical method detailed in [1], and used in this thesis, is analyzing iron losses grouping them in two categories: primary (calculated under nominal machine load) and additional (calculated under no-load).

As in nominal mode, the magnetization current frequency and so, magnetic flux frequency in rotor core has a very small value ($f_r = sf_s$), iron core losses are calculated only for the stator core.

For calculating primary iron core losses, an estimate of stator teeth and stator yoke mass is done. The stator teeth mass m_{ds} :

$$m_{ds} = Q_s h_{ds} b_{dsav} l_{Fe1} k_{Fe1} \gamma_{Fe} = 36 \cdot 11.89 \cdot 10^{-3} \cdot 4.1 \cdot 10^{-3} \cdot 138.3 \cdot 10^{-3} \cdot 0.95 \cdot 7800 = 1.8 [\text{kg}] \quad (3.119)$$

The stator yoke mass m_{ys} :

$$\begin{aligned} m_{ys} &= \pi(D_{se} - h_{ys})h_{ys}l_{Fes}k_{Fes}\gamma_{Fe} = \\ &= \pi(156 \cdot 10^{-3} - 14.3 \cdot 10^{-3}) \cdot 14.3 \cdot 10^{-3} \cdot 138.3 \cdot 10^{-3} \cdot 0.95 \cdot 7800 = \\ &= 6.52 \text{ [kg]} \end{aligned} \quad (3.120)$$

In this step calculating, as well, the rotor teeth total mass m_{dr} :

$$\begin{aligned} m_{dr} &= Q_r h_{dr} b_{drav} l_{Fer} k_{Fer} \gamma_{Fe} = 26 \cdot 20 \cdot 10^{-3} \cdot 5.54 \cdot 10^{-3} \cdot 138.3 \cdot 10^{-3} \cdot \\ &\cdot 0.95 \cdot 7800 = 2.95 \text{ [kg]} \end{aligned} \quad (3.121)$$

The primary iron core hysteresis losses estimate ΔP_{Feh} :

$$\begin{aligned} \Delta P_{Feh} &= \Delta p_{1,0} \left(\frac{f_1}{50} \right)^\beta (k_{dy} B_{ys}^2 m_{ys} + k_{dd} B_{ds}^2 m_{ds}) = \\ &= 1.39 \cdot \left(\frac{56.74}{50} \right)^{1.4} \cdot (1.6 \cdot 1.4^2 \cdot 6.52 + 1.8 \cdot 1.69^2 \cdot 1.8) = 49.3 \text{ [W]} \end{aligned} \quad (3.122)$$

Estimating Sura M350-50A steel core mass density value $\gamma_{Fe} = 7800 \text{ [kg/m}^3\text{]}$, medium loss at 1T (50Hz) $\Delta p_{1,0} = 1.39 \text{ [W/kg]}$ [9] and coefficients $\beta = 1.4 \text{ [-]}$, $k_{dy} = 1.6 \text{ [-]}$ and $k_{dd} = 1.8 \text{ [-]}$ [1].

As per [1], additional iron core losses are of two types: the stator and the rotor teeth surface losses generated by variable magnetic flux density over tooth surface and pulse losses generated by variable magnetic flux density in stator and rotor tooth mass.

Through variability of the air gap size above the rotor and the stator teeth, the rotor movement creates a variable magnetic flux density, with the estimated amplitude:

- for stator slot openings:

$$B_{0s} = \beta_{0s} k_{Cs} B_\delta = 0.38 \cdot 1.331 \cdot 0.732 = 0.37 \text{ [T]}; \quad (3.123)$$

- for rotor slot opening:

$$B_{0r} = \beta_{0r} k_{Cr} B_\delta = 0.25 \cdot 1.054 \cdot 0.732 = 0.19 \text{ [T]}. \quad (3.124)$$

The coefficients $\beta_{0s} = 0.38 \text{ [-]}$ for $\frac{b_{0s}}{\delta} = 8.75 \text{ [-]}$ and $\beta_{0r} = 0.25 \text{ [-]}$ for $\frac{b_{0r}}{\delta} = 3.75 \text{ [-]}$ are estimated as per Figure 3-17.

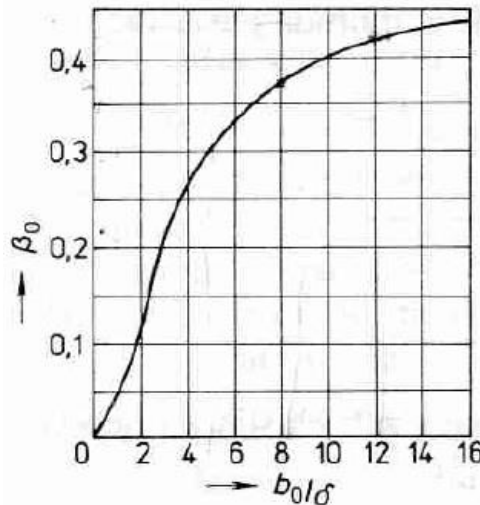


Figure 3.17: β_0 coefficient [1]

The stator surface losses density $p_{\delta ps}$:

$$p_{\delta ps} = 0.5k_{0s} \left(\frac{Q_r n}{10000} \right)^{1.5} (B_{0s} \tau_r 10^3)^2 = 0.5 \cdot 1.04 \cdot \left(\frac{26 \cdot 1600}{10000} \right)^{1.5} \cdot (0.37 \cdot 12.4)^2 = 125.2 \text{ [W/m}^2\text{]} \quad (3.125)$$

The rotor surface losses density $p_{\delta pr}$:

$$p_{\delta pr} = 0.5k_{0r} \left(\frac{Q_s n}{10000} \right)^{1.5} (B_{0r} \tau_s 10^3)^2 = 0.5 \cdot 1.04 \cdot \left(\frac{36 \cdot 1600}{10000} \right)^{1.5} \cdot (0.19 \cdot 9)^2 = 29.2 \text{ [W/m}^2\text{]} \quad (3.126)$$

The coefficient $k_{0s} = k_{0r} = 1.4$ [-] for machines smaller than 160 kW [1].

The resulting total stator teeth surface losses $\Delta P_{\delta ps}$ and rotor teeth surface losses $\Delta P_{\delta pr}$:

$$\Delta P_{\delta ps} = p_{\delta ps}(\tau_s - b_{0s})Q_s l_{Fes} = 125.2 \cdot (9 - 3.5) \cdot 10^3 \cdot 36 \cdot 138.3 \cdot 10^3 = 3.43 \text{ [W]} \quad (3.127)$$

$$\Delta P_{\delta pr} = p_{\delta pr}(\tau_r - b_{0r})Q_s l_{Fer} = 29.2 \cdot (12.4 - 1.5) \cdot 10^3 \cdot 36 \cdot 138.3 \cdot 10^3 = 1.14 \text{ [W]} \quad (3.128)$$

Teeth pulse losses are calculated based on amplitude of magnetic field densities pulsation in the middle of the stator and the rotor tooth B_{ps} and B_{pr} , respectively:

$$B_{ps} = \frac{\gamma'_s \delta}{2\tau_s} B_{dsav} = \frac{0.399 \cdot 0.4 \cdot 10^{-3}}{2 \cdot 9 \cdot 10^{-3}} \cdot 1.69 = 0.015 \text{ [T]} \quad (3.129)$$

$$B_{pr} = \frac{\gamma'_r \delta}{2\tau_r} B_{drav} = \frac{1.312 \cdot 0.4 \cdot 10^{-3}}{2 \cdot 12.4 \cdot 10^{-3}} \cdot 1.72 = 0.036 \text{ [T]} \quad (3.130)$$

As the stator and the rotor teeth are constant width, $B_{dsav} = B_{ds}$ and $B_{drav} = B_{dr}$. The parameters γ_s and γ_r are the coupling factors from the stator and the rotor slots Carter coefficients, calculated for apparent slot opening κ_δ as per Figure 3-18:

$$\gamma'_s = \frac{\left(\frac{b'_{0s}}{\delta} \right)^2}{5 + \left(\frac{b'_{0s}}{\delta} \right)} = \frac{\left(\frac{1.32}{0.4} \right)^2}{5 + \left(\frac{1.32}{0.4} \right)} = 1.312 \text{ [-]} \quad (3.131)$$

$$\text{with } b'_{0s} = \frac{b_{0s}}{3} \left(1 + \frac{0.5\tau_s}{\tau_s b_{0s} + \kappa_{\delta s}} \right) = \frac{3.5}{3} \cdot \left(1 + \frac{0.5 \cdot 9}{9 \cdot 3.5 + 2.8} \right) = 1.32 \text{ [mm]} \quad (3.132)$$

and $\kappa_{\delta s} = 2.8 \text{ [mm}^2\text{]} for $\frac{b_{0s}}{\delta} = 8.75$ as per Figure 3-18.$

$$\gamma'_r = \frac{\left(\frac{b'_{0r}}{\delta} \right)^2}{5 + \left(\frac{b'_{0r}}{\delta} \right)} = \frac{\left(\frac{0.65}{0.4} \right)^2}{5 + \left(\frac{0.65}{0.4} \right)} = 0.399 \text{ [-]} \quad (3.133)$$

$$\text{with } b'_{0r} = \frac{b_{0r}}{3} \left(1 + \frac{0.5\tau_r}{\tau_r b_{0r} + \kappa_{\delta r}} \right) = \frac{1.5}{3} \cdot \left(1 + \frac{0.5 \cdot 12.4}{12.4 \cdot 1.5 + 2} \right) = 0.65 \text{ [mm]} \quad (3.134)$$

and $\kappa_{\delta s} = 2 \text{ [mm}^2\text{]} for $\frac{b_{0r}}{\delta} = 3.75$ [-] as per Figure 3-18.$

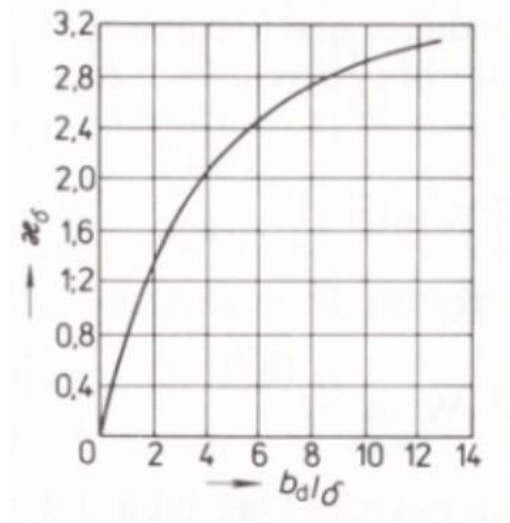


Figure 3.18: κ_δ coefficient [1]

The stator teeth pulse loss ΔP_{ps} :

$$\Delta P_{ps} \approx 0.11 \left(\frac{Q_r n}{1000} B_{ps} \right)^2 m_{ds} = 0.11 \left(\frac{26 \cdot 1600}{1000} \cdot 0.015 \right)^2 \cdot 1.8 = 0.077 \text{ [W]} \quad (3.135)$$

The rotor teeth pulse loss ΔP_{pr} :

$$\Delta P_{pr} \approx 0.11 \left(\frac{Q_r n}{1000} B_{ps} \right)^2 m_{ds} = 0.11 \left(\frac{36 \cdot 1600}{1000} \cdot 0.036 \right)^2 \cdot 2.95 = 0.242 \text{ [W]} \quad (3.136)$$

The total additional iron core loss ΔP_{Fed} :

$$\Delta P_{Fed} = \Delta P_{ps} + \Delta P_{pr} + \Delta P_{\delta pr} + \Delta P_{\delta ps} = 0.077 + 0.242 + 3.43 + 1.14 = 4.9 \text{ [W]} \quad (3.137)$$

The resulting total iron core loss ΔP_{Fe} :

$$\Delta P_{Fe} = \Delta P_{Feh} + \Delta P_{Fed} = 49.3 + 4.9 = 54.2 \text{ [W]} \quad (3.138)$$

The mechanical losses ΔP_{mech} :

$$\Delta P_{mech} = K_T \left(\frac{n}{10} \right)^2 D_{se}^4 = 5 \cdot \left(\frac{1600}{10} \right)^2 \cdot (156 \cdot 10^{-3})^4 = 75.8 \text{ [W]} \quad (3.139)$$

As per [1], coefficient $K_T = 5$ [-] for motor with $D_e \leq 0.25$ [m] and $2p = 2$.

The total additional losses ΔP_d

$$\Delta P_d = 0.005 P_{1N} = 0.005 \frac{P_{2N}}{\eta} = 0.005 \cdot \frac{3800}{0.84} = 22.6 \text{ [W]} \quad (3.140)$$

Based on the iron core, mechanical and no-load current losses, approximate value of the no-load stator current I_{s0} is calculated:

$$I_{s0} \approx \sqrt{I_{s0,Cu}^2 + I_{s,mag}^2} = \sqrt{0.42^2 + 5.11^2} = 5.13 \text{ [A]} \quad (3.141)$$

where the no-load current $I_{s0,Cu}$:

$$I_{s0,Cu} = \frac{\Delta P_{Fe} + \Delta P_{mech} + \Delta P_{j10}}{m U_{s,ph}} = \frac{54.2 + 75.8 + 161.8}{3 \cdot 230} = 0.42 \text{ [A]} \quad (3.142)$$

And the no-load iron core losses $\Delta P_{s0,Cu}$:

$$\Delta P_{s0,Cu} \approx 3 R_{DCs} I_{s,mag}^2 = 3 \cdot 2.066 \cdot 5.11^2 = 161.8 \text{ [W]} \quad (3.143)$$

The resulting zero-load power factor $\cos \varphi_0$:

$$\cos \varphi_0 = \frac{I_{s0,Cu}}{I_{s0}} = \frac{0.41}{4.95} = 0.08 [-] \quad (3.144)$$

To complete the calculation of the induction machine equivalent scheme parameters, calculating the absolute value of the resistive R_{12} and X_{12} reactive components of the impedance Z_{12} , the fictive resistance corresponding to the iron core losses R_{Fe} and the iron core magnetization reactance X_m .

$$R_{12} \approx \frac{\Delta P_{Feh}}{m I_{s,mag}^2} = \frac{49.3}{3 \cdot 5.13^2} = 0.63 [\Omega] \quad (3.145)$$

$$R_{Fe} \approx \frac{m X_m^2 I_{s,mag}^2}{\Delta P_{Fe}} = \frac{3 \cdot 44.41^2 \cdot 5.11^2}{54.2} = 2643.9 [\Omega] \quad (3.146)$$

$$X_m \approx X_{12} \approx \frac{U_{s,ph}}{I_{s,mag}} - X_{s\sigma} = \frac{230}{5.11} - 2.24 = 42.77 [\Omega] \quad (3.147)$$

3.12 Load characteristic of the induction machine

As per [1] calculating the induction machine load and starting characteristics requires calculating the reduced equivalent parameters model of the machine. Based on this, the machine's parameters are calculated for slip values ranging from a value close to zero to the nominal slip, for calculating the load characteristic and from a slip equal to 1 to a slip value close to 0, for calculating the starting characteristic of the machine.

For the calculated output power $P_2 = 3.8$ [KW], load characteristic calculation allows identification of precise nominal slip s_N value.

The reduced equivalent model of the induction motor is calculated based on the vector

$$\overline{c_1} = \frac{\overline{Z_s} + \overline{Z_m}}{\overline{Z_m}} \text{ which has as components :}$$

$$c_{1r} = \frac{R_{12}(R_{DCs} + R_{12}) + X_m(X_{s\sigma} + X_{12})}{R_{12}^2 + X_{12}^2} = \frac{0.63 \cdot (2.07 + 0.68) + 42.77 \cdot (2.24 + 44.41)}{0.63^2 + 42.77^2} = 1.05 [-] \quad (3.148)$$

$$c_{1i} = \frac{X_{s\sigma} R_{12} - R_{DCs} X_{12}}{R_{12}^2 + X_{12}^2} = \frac{2.24 \cdot 0.63 - 2.07 \cdot 42.77}{0.63^2 + 42.77^2} = -0.0475 [-] \quad (3.149)$$

Resulting $\overline{c_1}$ vector absolute value:

$$|\overline{c_1}| = c_1 = \sqrt{c_{1r}^2 + c_{1i}^2} = \sqrt{1.05^2 + (0.0475)^2} = 1.054 [-] \quad (3.150)$$

and parameters:

$$a' = c_{1r}^2 - c_{1i}^2 = 1.05^2 - (-0.0475)^2 = 1.107 [-] \quad (3.151)$$

$$b' = 2c_{1r}c_{1i} = 2 \cdot 1.05 \cdot (-0.0475) = -0.1 [-] \quad (3.152)$$

$$a = c_{1r}R_{DCs} - c_{1i}X_{s\sigma} - b'X'_{r\sigma} = 1.05 \cdot 2.066 - (-0.0475 \cdot 2.24) - (-0.1 \cdot 3.469) = 2.629 [\Omega] \quad (3.153)$$

$$b = c_{1r}X_{s\sigma} + c_{1i}R_{DCs} + a'X'_{r\sigma} = 1.05 \cdot 2.24 + (-0.0475 \cdot 2.066) + 1.107 \cdot 3.469 = 5.918 [\Omega] \quad (3.154)$$

As an example, performing the calculation for the found nominal slip $s_N = 0.047$ [-]. As the slip is nominal, the calculated parameters below represent nominal values, as well.

Equivalent model parameters under given load:

$$\frac{a'R'_{DCr}}{s} = \frac{1.107 \cdot 1.41}{0.047} = 33.21 \text{ } [\Omega] \quad (3.155)$$

$$\frac{b'R'_{DCr}}{s} = \frac{(0.1) \cdot 1.41}{0.047} = 3 \text{ } [\Omega] \quad (3.156)$$

$$R = a + \frac{a'R'_{DCr}}{s} = 2.629 + \frac{1.107 \cdot 1.41}{0.047} = 35.84 \text{ } [\Omega] \quad (3.157)$$

$$X = b + \frac{b'R'_{DCr}}{s} = 5.918 + \frac{(-0.1) \cdot 1.41}{0.047} = 2.92 \text{ } [\Omega] \quad (3.158)$$

$$Z = \sqrt{R^2 + X^2} = \sqrt{35.84^2 + 2.92^2} = 35.96 \text{ } [\Omega] \quad (3.159)$$

The rotor current vector absolute value and arguments:

$$I_r'' = 3U_{s,ph}/Z = 3 \cdot 230/35.96 = 6.4 \text{ } [A] \quad (3.160)$$

$$\cos \varphi_r' = R/Z = 35.84/35.96 = 0.997 \text{ } [-] \quad (3.161)$$

$$\sin \varphi_r' = X/Z = 2.92/35.96 = 0.081 \text{ } [-] \quad (3.162)$$

The stator current vector components $I_{s,Cu}$ and $I_{s,mag}$ and the absolute value I_s :

$$I_{s,Cu} = I_{s0,Cu} + I_r'' \cos \varphi_r' = 0.42 + 6.4 \cdot 0.997 = 6.69 \text{ } [A] \quad (3.163)$$

$$I_{s,mag} = I_{s0,mag} + I_r'' \sin \varphi_r' = 5.11 + 6.4 \cdot 0.081 = 5.63 \text{ } [A] \quad (3.164)$$

$$I_s = \sqrt{I_{s,Cu}^2 + I_{s,mag}^2} = \sqrt{6.69^2 + 5.63^2} = 8.74 \text{ } [A] \quad (3.165)$$

The rotor bar current value referred to stator I_r' :

$$I_r' = c_1 I_r'' = 1.054 \cdot 6.4 = 6.75 \text{ } [A] \quad (3.166)$$

Input power for the given load P_1 :

$$P_1 = P_P = 3U_{s,ph} I_s^2 \cdot 10^{-3} = 3 \cdot 230 \cdot 8.74^2 \cdot 10^{-3} = 4.62 \text{ } [kW] \quad (3.167)$$

The stator $\Delta P_{s,Cu}$ and rotor $\Delta P_{r,Cu}$ Joule losses:

$$\Delta P_{s,Cu} = 3R_{DCs} I_s^2 \cdot 10^{-3} = 3 \cdot 2.07 \cdot 8.74^2 \cdot 10^{-3} = 0.473 \text{ } [kW] \quad (3.168)$$

$$\Delta P_{r,Cu} = 3R'_{DCr} I_r'^2 \cdot 10^{-3} = 3 \cdot 1.41 \cdot 6.75^2 \cdot 10^{-3} = 0.193 \text{ } [kW] \quad (3.169)$$

Additional losses calculated for the given load ΔP_d :

$$\Delta P_d = \Delta P_{dN} (I_s/I_{sN})^2 = 0.0226 \cdot (8.74/7.81)^2 = 0.028 \text{ } [kW] \quad (3.170)$$

Total losses ΔP :

$$\begin{aligned} \Delta P &= \Delta P_{Fe} + \Delta P_{mech} + \Delta P_{s,Cu} + \Delta P_{r,Cu} + \Delta P_d = \\ &= 0.054 + 0.076 + 0.473 + 0.193 + 0.028 = 0.82 \text{ } [kW] \end{aligned} \quad (3.171)$$

Output power, efficiency and power factor values:

$$P_2 = P_1 - \Delta P = 4.62 - 0.82 = 3.8 \text{ } [kW] \quad (3.172)$$

$$\eta = 1 - \frac{\Delta P}{P_1} = 1 - \frac{0.82}{4.62} = 0.822 \text{ } [-] \quad (3.173)$$

$$\cos \varphi = \frac{I_{s,Cu}}{I_s} = \frac{6.69}{8.74} = 0.765 \text{ } [-] \quad (3.174)$$

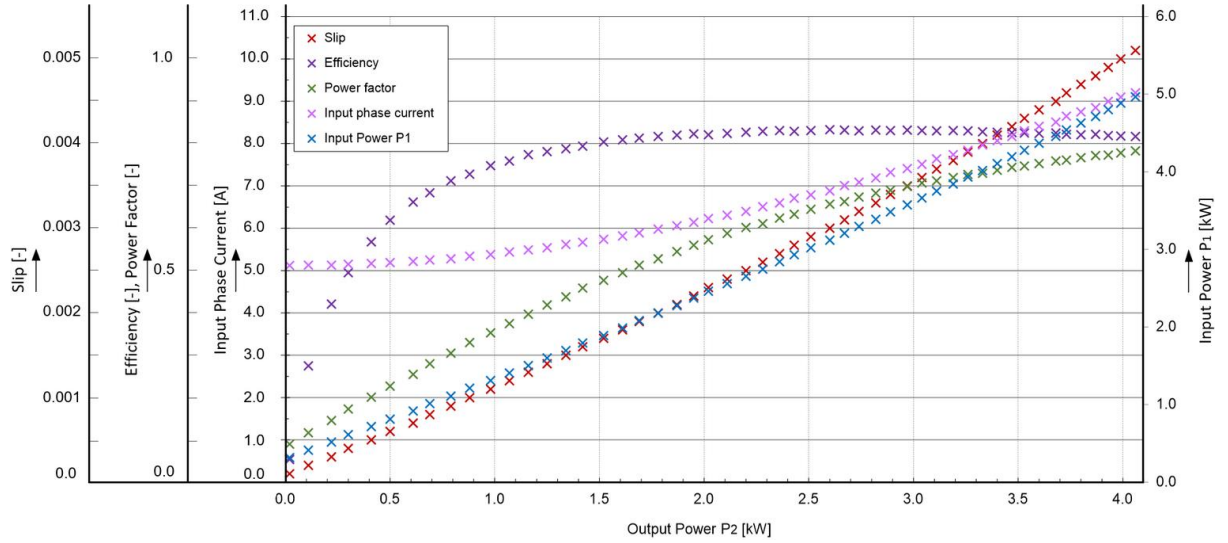


Figure 3.19: Load characteristics of the machine (based on [1])

3.13 Starting characteristic of the induction machine

Calculating starting characteristics of the induction machine allows analysis of the motor under different load values and, together with this, an evaluation of the locked rotor torque, the locked rotor stator current and the brake down torque and slip.

The locked rotor torque value is important as at start the motor should generate enough torque to overcome the static mechanical moment of the rotor and of the connected physical load [7].

Also, calculating the locked rotor current allows an evaluation of the requirements for the power supply system of the motor, as, at start (slip $s = 1$ [-]), the starting current is several times higher than the nominal one as, at start, the stator current is magnetizing magnetic circuit of the stator and of the rotor [17]. Due to the high value of slip, the hysteresis and eddy current losses of the rotor steel stack have at start-up values much higher than the ones at a nominal run; this is increasing the value of the start current as well. The power supply system of the motor should be sized to be able to deliver required start current with no impact on power supply system or other consumers.

A positive phenomenon is generated during the start by the so-called skin effect produced by the high rotor current frequency in the rotor bars. This makes that current density to be different in the lower part and the higher part of the rotor bar causing the total bar resistance to become higher than the one at the nominal speed and its reactance to be lower [1]. This has an overall positive effect as increasing rotor resistance generates a higher moment and a decreased reactance. This is decreasing starting current requirements, as well.

Because of this effect, calculating starting characteristics is requiring calculating reactance parameters taking in consideration the skin effect affecting rotor bars.

As an example, detailing below starting characteristics calculation for slip $s = 1$ [-] and for nominal temperature $\vartheta = 115$ [°C].

The skin effect depth parameter for rotor aluminum bars at this temperature ξ :

$$\xi = 63.61 h_{\text{bar}} \sqrt{s} = 63.61 \cdot 19.3 \cdot 10^{-3} \cdot \sqrt{1} = 1.23 \text{ [-]} \quad (3.175)$$

for height of the rotor bar being h_{bar} :

$$h_{\text{bar}} = h_{\text{dr}} - h_{0r} = 20 - 0.7 = 19.3 \text{ [mm]} \quad (3.176)$$

The skin effect reduced rotor bar height h_R :

$$h_R = \frac{h_{\text{bar}}}{1 + \varphi(\xi)} = \frac{19.3}{1 + 0.17} = 16.5 \text{ [mm]} \quad (3.177)$$

with function $\varphi(\xi) = 0.17$ [-] defined as per Figure 3.20.

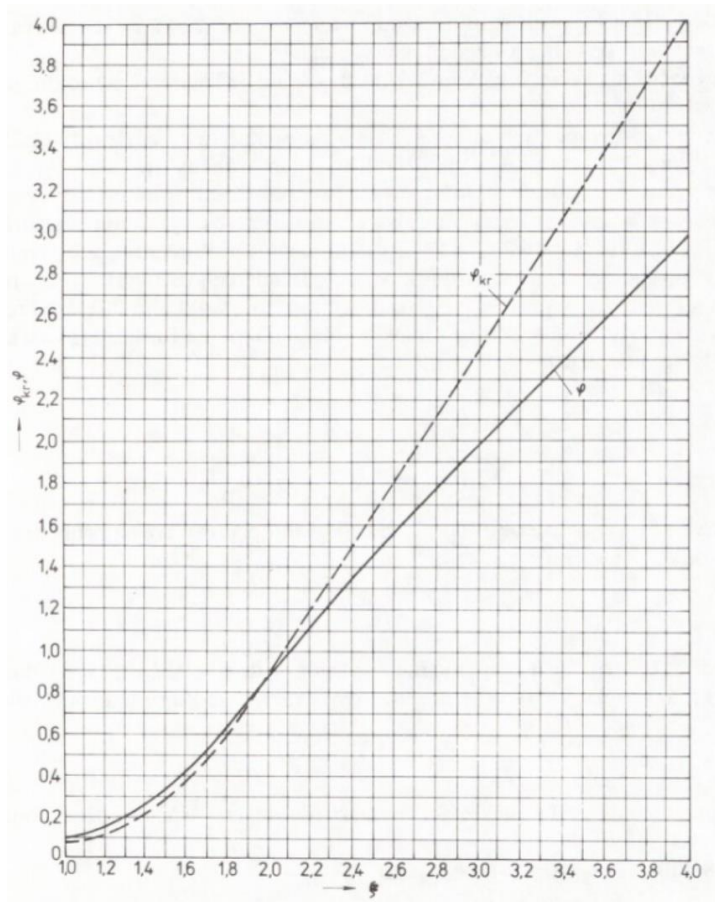


Figure 3.20: $\varphi(\xi)$ function [1]

The reduced rotor bar cross section area S_R :

$$\begin{aligned} S_R &= \frac{\pi b_{1r}^2}{8} + \frac{b_{1r} + b_R}{2} \left(h_R - \frac{b_{1r}}{2} \right) = \\ &= \frac{\pi \cdot 6^2}{8} + \frac{6 + 2.7}{2} \left(16.5 - \frac{6}{2} \right) = 72.9 \text{ [mm}^2\text{]} \end{aligned} \quad (3.178)$$

with the bar width b_R , being:

$$\begin{aligned} b_R &= b_{1r} - \frac{b_{1r} - b_{2r}}{h_{1r}} \left(h_R - \frac{b_{1r}}{2} \right) = \\ &= 6 - \frac{6 - 2.3}{15.3} \left(16.5 - \frac{6}{2} \right) = 2.7 \text{ [mm]} \end{aligned} \quad (3.179)$$

The resulting resistance factor K_R :

$$K_R = 1 + \frac{R_{dr}}{R_{DCr}} (k_R - 1) = 1 + \frac{8.465 \cdot 10^{-5}}{1.095 \cdot 10^{-4}} \cdot (1.09 - 1) = 1.07 \text{ [-]} \quad (3.180)$$

with the coefficient k_R defined as:

$$k_R = \frac{s_{cr}}{s_R} = \frac{79.7}{72.9} = 1.09 \text{ [-]} \quad (3.181)$$

The skin effect rotor resistance calculated to stator $R'_{DCr\xi}$:

$$R'_{DCr\xi} = K_R R'_{DCr} = 1.07 \cdot 1.41 = 1.509 \text{ } [\Omega] \quad (3.182)$$

The rotor slot magnetic permeance coefficient $\lambda_{dr\xi}$, calculated taking in consideration the skin effect influence:

$$\begin{aligned} \lambda_{dr\xi} &= \left[\frac{h_{3xr}}{3b_{1r}} \left(1 - \frac{\pi b_{1r}^2}{8S_{cr}} \right)^2 + 0.66 - \frac{b_{0r}}{2b_{1r}} \right] k_d + \frac{h_{0r}}{b_{0r}} = \\ &= \left[\frac{16.27}{3 \cdot 6.3} \left(1 - \frac{\pi \cdot 6^2}{8 \cdot 79.7} \right)^2 + 0.66 - \frac{0.7}{2 \cdot 6} \right] \cdot 0.93 + \frac{0.7}{1.5} = 1.53 \text{ [-]} \end{aligned} \quad (3.183)$$

with parameter $k_d = \varphi'(\xi) = 0.93 \text{ [-]}$ defined as per Figure 3-21.

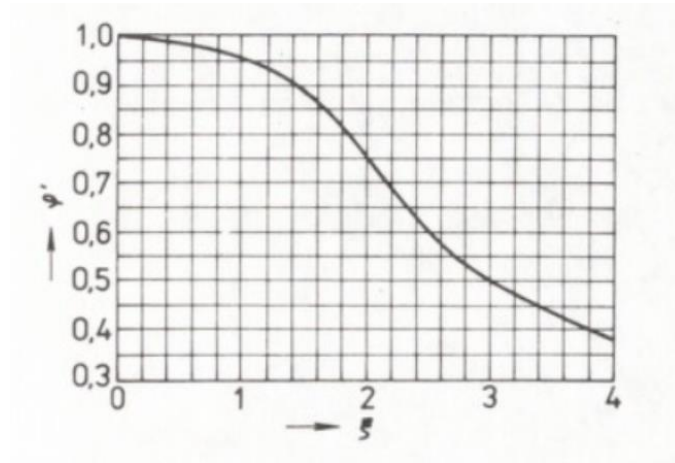


Figure 3.21: $\varphi'(\xi)$ function [1]

The given skin effect influence, reactance factor K_X is:

$$K_X = \frac{\lambda_{dr\xi} + \lambda_{wr} + \lambda_{difr}}{\lambda_{dr} + \lambda_{wr} + \lambda_{difr}} = \frac{1.53 + 0.235 + 2.5}{1.61 + 0.235 + 2.5} = 0.982 \text{ [-]} \quad (3.184)$$

Resulting rotor reactance referred to stator $X'_{r\sigma\xi}$:

$$X'_{r\sigma\xi} = K_X X'_{r\sigma} = 0.982 \cdot 3.47 = 3.41 \text{ } [\Omega] \quad (3.185)$$

Due to high values of the stator at the rotor currents in between the start when $s = 1 \text{ [-]}$ and until the critical slip s_{max} value is reached, for calculating starting characteristics parameters, magnetic circuits saturation affecting induction motor should be taken in consideration.

Saturation is affecting primarily the stator and the rotor teeth (sections above the stator and the rotor slots openings), the effect being an apparent increase of dimension of slots

openings, consequently reducing magnetic conductivity of affected regions, and, as a result, a decrease of the rotor and the stator reactance.

The rotor current calculated without taking magnetic saturation I'_r in consideration:

$$I'_r \approx \frac{U_{s,ph}}{\sqrt{\left(R_{DCS} + \frac{R'_{DCr\xi}}{s}\right)^2 + (X_{s\sigma} + X'_{r\sigma\xi})^2}} = \frac{230}{\sqrt{\left(2.066 + \frac{1.509}{1}\right)^2 + (2.24 + 3.407)^2}} = 34.4 \text{ [A]} \quad (3.186)$$

Magnetic tension in a stator slot F_{dav} :

$$F_{dav} = 0.7 \frac{k_n I'_r Z_{Qs}}{a} \left(k'_\beta + k_{ps} k_{ws1} \frac{Q_s}{Q_r} \right) = \\ = 0.7 \frac{1.35 \cdot 34.4 \cdot 29}{1} \cdot \left(1 + 1 \cdot 0.96 \cdot \frac{36}{26} \right) = 2196 \text{ [A]} \quad (3.187)$$

Where the coefficient $k_n \in (1.25; 1.4)$ [1] is defining the increase of winding current and the coefficient $k'_\beta = k_\beta = 1$ [-] for one layer, full pitch winding.

The apparent airgap magnetic flux density $B_{f\delta}$:

$$B_{f\delta} = \frac{F_{dav}}{1.6\delta C_n} 10^{-6} = \frac{2196}{1.6 \cdot 0.4 \cdot 10^{-3} \cdot 0.982} \cdot 10^{-6} = 3.49 \text{ [T]} \quad (3.188)$$

with the parameter C_n , being defined as:

$$C_n = 0.64 + 2.5 \sqrt{\frac{\delta}{\tau_s + \tau_r}} = 0.64 + 2.5 \sqrt{\frac{0.4}{9 + 12.4}} = 0.982 \text{ [-]} \quad (3.189)$$

For the calculated apparent magnetic flux density $B_{f\delta}$, as per the function detailed in Figure 3-22, coefficient $\kappa_\delta = 0.6$ [-] is defined.

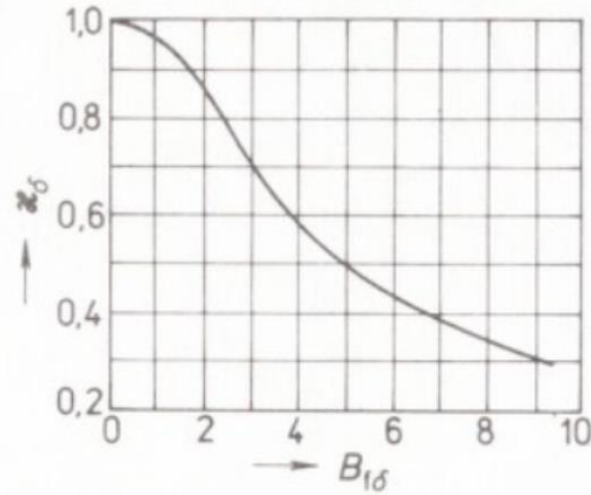


Figure 3.22: $\kappa_\delta(B_{f\delta})$ function [1]

The stator and the rotor slot openings, taking magnetic saturation in consideration, Δb_{0s} and Δb_{0r} :

$$\Delta b_{0s} = (\tau_s - b_{0s})(1 - \kappa_\delta) = (9 - 3.5)(1 - 0.6) = 2.2 \text{ [mm]} \quad (3.190)$$

$$\Delta b_{0r} = (\tau_r - b_{0r})(1 - \kappa_\delta) = (12.4 - 1.5)(1 - 0.6) = 4.4 \text{ [mm]} \quad (3.191)$$

The stator and the rotor slots magnetic permeance coefficients, under saturation influence, $\Delta\lambda_{dssat}$ and $\Delta\lambda_{drsat}$:

$$\Delta\lambda_{dssat} = \frac{h_{0s}+0.58h_{2s}}{b_{0s}} \cdot \frac{\Delta b_{0s}}{\Delta b_{0s}+1.5b_{0s}} = \frac{0.5+0.58 \cdot 0.9}{3.5} \cdot \frac{2.2}{2.2+1.5 \cdot 3.5} = 0.086 [-] \quad (3.192)$$

$$\Delta\lambda_{drsat} = \frac{h_{0r}}{b_{0r}} \cdot \frac{\Delta b_{0r}}{\Delta b_{0r}+b_{0r}} = \frac{0.7}{1.5} \cdot \frac{4.4}{4.4+1.5} = 0.35 [-] \quad (3.193)$$

Stator slot magnetic permeance λ_{dssat} and magnetic differential permeance $\lambda_{difssat}$ coefficients:

$$\lambda_{dssat} = \lambda_{ds} - \Delta\lambda_{dssat} = 1.19 - 0.086 = 1.104 [-] \quad (3.194)$$

$$\lambda_{difssat} = \lambda_{difs}\kappa_{\delta} = 1.76 \cdot 0.6 = 1.056 [-] \quad (3.195)$$

The rotor slot magnetic permeance $\lambda_{dr\xi sat}$ and the magnetic differential permeance $\lambda_{difrsat}$ coefficients:

$$\lambda_{dr\xi sat} = \lambda_{dr\xi} - \Delta\lambda_{dssat} = 1.53 - 0.35 = 1.18 [-] \quad (3.196)$$

$$\lambda_{difrsat} = \lambda_{difr}\kappa_{\delta} = 2.5 \cdot 0.6 = 1.5 [-] \quad (3.197)$$

Taking in consideration the skin effect and magnetic circuit saturation, resulting stator slot reactance $X_{s\sigma sat}$, rotor slot reactance $X'_{r\sigma\xi sat}$ and iron core magnetization reactance X_{msat} are:

$$X_{s\sigma sat} = X_{s\sigma} \frac{\lambda_{dssat}+\lambda_{ws}+\lambda_{difs}}{\lambda_{ds}+\lambda_{ws}+\lambda_{difs}} = 2.24 \cdot \frac{0.086+0.63+1.056}{1.19+0.63+1.76} = 1.746 [\Omega] \quad (3.198)$$

$$X'_{r\sigma\xi sat} = X'_{r\sigma} \frac{\lambda_{dr\xi sat}+\lambda_{wr}+\lambda_{difrsat}}{\lambda_{dr}+\lambda_{wr}+\lambda_{difr}} = 3.47 \cdot \frac{1.18+0.235+1.5}{1.61+0.235+2.5} = 2.327 [\Omega] \quad (3.199)$$

$$X_{msat} = X_m \frac{F_m}{U_{m\delta}} = 44.41 \cdot \frac{1112.5}{619.65} = 79.7 [\Omega] \quad (3.200)$$

Reduced equivalent model parameters:

$$c_{1psat} = 1 + \frac{X_{s\sigma sat}}{X_{msat}} = 1 + \frac{1.746}{79.7} = 1.022 [-] \quad (3.201)$$

$$a_p = R_{DCs} + c_{1psat} \frac{R'_{DCr\xi}}{s} = 2.066 + 1.022 \cdot \frac{1.509}{1} = 3.608 [\Omega] \quad (3.202)$$

$$b_p = X_{s\sigma sat} + c_{1psat} X'_{r\sigma\xi sat} = 1.746 + 1.022 \cdot 2.327 = 4.124 [\Omega] \quad (3.203)$$

For calculated motor starting parameters, the rotor bar relative to stator I'_r and stator the winding I_s current values are:

$$I'_r = \frac{U_{s,ph}}{\sqrt{a_p^2 + b_p^2}} = \frac{230}{\sqrt{3.608^2 + 4.124^2}} = 42 [A] \quad (3.204)$$

$$\begin{aligned} I_s &= I'_r \sqrt{a_p^2 + (b_p + X_{msat})^2} = \\ &= 42 \cdot \sqrt{3.608^2 + 4.124 + 79.7)^2} = 43.3 [A] \end{aligned} \quad (3.205)$$

The relative value of the locked rotor current i_0 :

$$i_0 = \frac{I_s}{I_{sN}} = \frac{43.3}{7.81} = 5.54 [-] \quad (3.206)$$

The relative value of the locked rotor torque t_0 :

$$t_0 = \left(\frac{I'_r}{I'_{rN}}\right)^2 K_R \frac{s_N}{s} = \left(\frac{I'_r}{I'_{rN}}\right)^2 K_R \frac{s_N}{s} = 1.96 [-] \quad (3.207)$$

The critical slip s_{max} is calculated based on the medium stator and the rotor reactance values $X_{s\sigma sat}$ and $X'_{r\sigma\xi sat}$, based on the values corresponding to the slip values in between 0.4 and 0.3.

$$s_{max} = \frac{R'_{DCr\xi}}{\frac{X_{s\sigma sat}}{c_{1psat}} + X'_{r\sigma\xi sat}} = \frac{1.41}{\frac{1.746}{1.022} + 2.379} = 0.34 [-] \quad (3.208)$$

The critical torque t_{max} is calculated based on value of the critical slip s_{max} :

$$t_{max} = \left(\frac{I'_r}{I'_rN}\right)^2 K_R \frac{s_N}{s_{max}} = \left(\frac{30.4}{6.75}\right)^2 \cdot 1 \cdot \frac{0.047}{0.34} = 2.8 [-] \quad (3.209)$$

3.12 Thermal characteristic and cooling

Thermal characteristic of the machine is estimated based on calculated energy losses, temperature rise, heat transfer and heat removal in between different components of the machine and machine and exterior environment.

The method used [1] is assuming nominal run parameters for losses generation. The exception are the losses generated in the stator and the rotor windings, for which, energy loss is estimated for a higher temperature rise than the one of the other components of the machine. During nominal run, winding maximum temperature rise is limited by the wire insulation class used.

Stator winding surface temperature rise is calculated separately for winding section hosted in the stator slot and for the winding end-turn section.

For a totally enclosed machine, as the stator winding section in the stator slot is in the proximity of the stator magnetic steel core, heat transfer from the winding to the stator core surface is better than the one for the stator winding end-turn. As result, the temperature increase will be higher in the end-turn section of the winding, this requiring a separate analysis for the winding section in the stator slot and for the end-turn section.

Energy loss in stator winding (stator slot section) $\Delta P'_{sd,Cu}$:

$$\Delta P'_{sd,Cu} = k_p \Delta P_{s,Cu} \frac{2l_{Fes}}{l_{av}} = 1.07 \cdot 0.473 \cdot \frac{2 \cdot 0.1383}{0.552} = 253.6 [W] \quad (3.210)$$

The correction factor k_p is defined based on wire the insulation type: for the insulation class F $k_p = \rho_{140}/\rho_{115} = 1.07 [1]$.

The stator slot winding temperature rise $\Delta\vartheta_{us}$:

$$\Delta\vartheta_{us} = K \frac{\Delta P'_{sd,Cu} + \Delta P_{Feh}}{\pi D_s l_{Fes} \alpha_1} = 0.2 \cdot \frac{253.6 + 49.3}{\pi \cdot 103.7 \cdot 10^{-3} \cdot 138.3 \cdot 10^{-3} \cdot 95} = 14.35 [^{\circ}C] \quad (3.211)$$

Temperature drop in the stator slot insulation $\Delta\vartheta_{ids}$:

$$\begin{aligned} \Delta\vartheta_{ids} &= \frac{\Delta P'_{sd,Cu}}{Q_s O_{ds} l_1} \left(\frac{b_{1s}}{\lambda_{ekv}} + \frac{b_{1s} + b_{2s}}{16\lambda'_{ekv}} \right) = \\ &= \frac{253.6}{36 \cdot 0.4 \cdot l} \left(\frac{7.5 \cdot 10^{-3}}{0.16} + \frac{7.5 \cdot 10^{-3} + 5.4 \cdot 10^{-3}}{16 \cdot 0.93} \right) = 3.66 [^{\circ}C] \end{aligned} \quad (3.212)$$

Where O_{ds} is circumference of the stator slot winding:

$$\begin{aligned} O_{ds} &= 2h_{ds} + b_{1s} + b_{2s} = \\ &= 2 \cdot 11.9 \cdot 10^{-3} + 7.2 \cdot 10^{-3} + 5.3 \cdot 10^{-3} = 0.036 \text{ [m]} \end{aligned} \quad (3.213)$$

The slot insulation equivalent heat transfer $\lambda_{ekv} = 0.16 \text{ [Wm}^{-2}\text{K}^{-1}]$ [1] and the winding conductor insulation medium heat transfer $\lambda'_{ekv} = 1.1 \text{ [Wm}^{-2}\text{K}^{-1}]$ as per Figure 3-23 for $d/d_{vi} = 0.85/0.92 = 0.92[-]$.

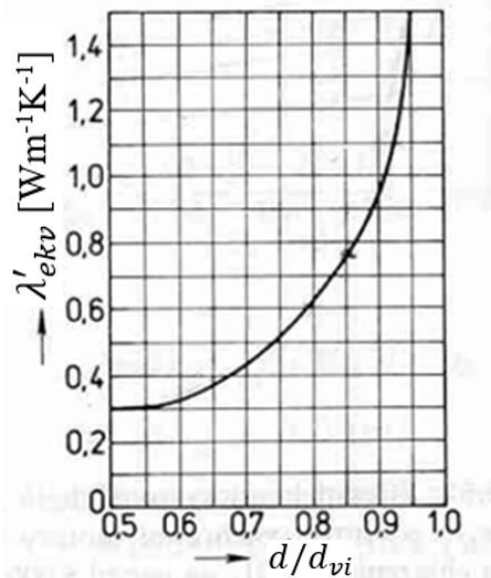


Figure 3.23: Equivalent heat transfer coefficient [1]

Energy loss in the stator winding end-turn:

$$\Delta P'_{sw,Cu} = k_p \Delta P_{s,Cu} \frac{2l_w}{l_{av}} = 1.07 \cdot 473 \cdot \frac{2 \cdot 0.138}{0.552} = 253.1 \text{ [W]} \quad (3.214)$$

Temperature drop in the winding end-turn insulation $\Delta\vartheta_{iws}$:

$$\begin{aligned} \Delta\vartheta_{iws} &= \frac{\Delta P'_{sw,Cu}}{2Q_s Q_{ws} l_w} \left(\frac{b_{ws}}{\lambda_{ekv}} + \frac{h_{ds}}{12\lambda'_{ekv}} \right) = \\ &= \frac{253.1}{2 \cdot 36 \cdot 0.036 \cdot 0.138} \left(\frac{0}{0.16} + \frac{11.9 \cdot 10^{-3}}{12 \cdot 0.93} \right) = 0.64 \text{ [}^\circ\text{C]} \end{aligned} \quad (3.215)$$

Circumference of the winding end-turn is equal to circumference of the stator winding in the stator slot ($O_{ws} = O_{ds} = 0.036 \text{ [m]}$) and no additional insulation for the stator winding end-turn section ($b_{ws} = 0 \text{ [m]}$).

Stator winding end-turn temperature rise above air temperature inside engine $\Delta\vartheta_{ws}$:

$$\Delta\vartheta_{ws} = \frac{K \Delta P'_{sw,Cu}}{2\pi D_s l_{av} \alpha_1} = \frac{0.2 \cdot 253.1}{2\pi \cdot 103.7 \cdot 10^{-3} \cdot 0.552 \cdot 95} = 17.62 \text{ [}^\circ\text{C]} \quad (3.216)$$

The heat transfer coefficient $\alpha_1 = 95 \text{ [Wm}^{-2}\text{K}^{-1}]$ for $D_{se} = 156 \text{ [mm]}$ as per Figure 3-24.

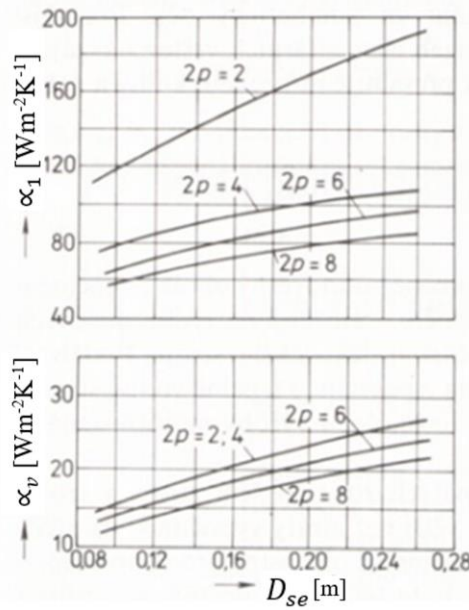


Figure 3.24: Heat transfer coefficients [1]

The medium stator winding temperature rise above air temperature inside motor $\Delta\vartheta'_s$:

$$\begin{aligned}\Delta\vartheta'_s &= \frac{(\Delta\vartheta_{us} + \Delta\vartheta_{ids})2l_c}{l_{av}} + \frac{(\Delta\vartheta_{iws} + \Delta\vartheta_{ws})2l_c}{l_{av}} = \\ &= \frac{(14.35 + 3.66) \cdot 2 \cdot 0.1356}{0.552} + \frac{(0.64 + 17.62) \cdot 2 \cdot 0.1356}{0.552} = 18.15 [^\circ\text{C}]\end{aligned}\quad (3.217)$$

The sum of all losses will have as effect temperature rise of air inside the motor $\Sigma\Delta P'_{air}$:

$$\begin{aligned}\Sigma\Delta P'_{air} &= \Sigma\Delta P' - (1 - K)(\Delta P'_{sw,Cu} + \Delta P_{Feh}) - 0.9\Delta P_{Mech} = \\ &= 870 - (1 - 0.2) \cdot (253.1 + 49.3) - 0.9 \cdot 75.8 = 559 [\text{W}]\end{aligned}\quad (3.218)$$

where $\Sigma\Delta P'$ represents the sum of induction machine energy losses including additional Joules losses caused by temperature rise in the stator and the rotor winding:

$$\begin{aligned}\Sigma\Delta P' &= \Sigma\Delta P + (k_\vartheta - 1)(\Delta P_{s,Cu} + \Delta P_{r,Cu}) = \\ &= 820 + (1.07 - 1)(473 + 193) = 870 [\text{W}]\end{aligned}\quad (3.219)$$

The equivalent heat transfer surface area S_{IM} of the induction machine:

$$S_{IM} = (\pi D_{se} + 8O_{fins})(l_1 + 2l_{v1}) = 0.446 [\text{m}^2]\quad (3.220)$$

The stator cooling fins height $O_{fins} = 0.18 [\text{m}]$ for $h = 100 [\text{mm}]$ as per Figure 3-25.

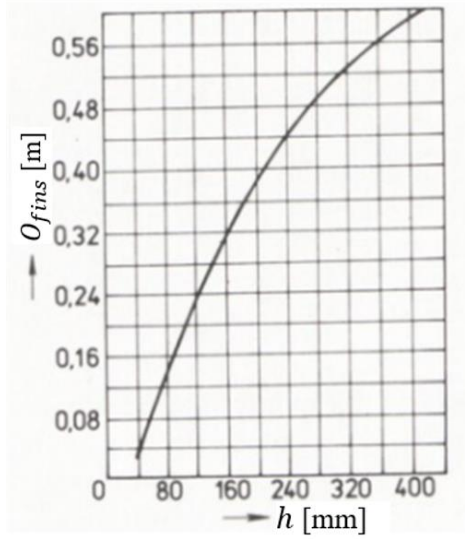


Figure 3.25: Cooling fins height [1]

Temperature rise of air inside the motor (above outside air temperature) $\Delta\vartheta_{air}$:

$$\Delta\vartheta_{air} = \frac{\Sigma\Delta P'_{air}}{S_{IM}\alpha_v} = \frac{559}{0.446 \cdot 20.4} = 61.49 [^{\circ}C] \quad (3.221)$$

The heat transfer coefficient $\alpha_v = 20.4 [Wm^{-2}K^{-1}]$ for $D_{se} = 156 [mm]$ as per Figure 3-25.

Stator winding medium temperature rise (above outside air temperature) $\Delta\vartheta_{ws}$:

$$\Delta\vartheta_{ws} = \Delta\vartheta'_s + \Delta\vartheta_{air} = 18.15 + 61.49 = 79.64 [^{\circ}C] \quad (3.222)$$

Airflow required for cooling the induction motor Q_{air} :

$$Q_{air} = \frac{k_m \Sigma\Delta P'_{air}}{1100\Delta\vartheta_{air}} = \frac{2.8 \cdot 559}{1100 \cdot 61.49} = 0.023 [m^3s^{-1}] \quad (3.223)$$

with coefficient k_m , which as per [1] is defining change of cooling conditions on the length of stator case cooled by exterior fan, being:

$$k_m = m_v \sqrt{\frac{n}{100} D_{se}} = 1.8 \cdot \sqrt{\frac{1600}{100} 0.156} = 2.94 [-] \quad (3.224)$$

and coefficient $m_v = 1.8 [-]$, for $2p = 4 [-]$ and $h \leq 132 [mm]$.

Quantity of air provided by an exterior fan connected to engine shaft Q'_{air} :

$$Q'_{air} = 0.6 D_e^3 \frac{n}{100} = 0.6 \cdot 0.156^3 \cdot \frac{1600}{100} = 0.036 [m^3s^{-1}] \quad (3.225)$$

The calculation above shows that, if motor would be air-cooled by an external fan connected to the engine shaft, the cooling required for the calculated induction machine correspond to requirements.

The induction machine will be attached to a water pump hosted inside a pipe, cooling being realized through the water being pumped. If no additional thermal flow barrier is created in between the motor and the cooling agent, this creates better cooling conditions than the ones calculated for the air.

The engine should not run in absence of cooling water and a temperature sensor and overheat protection should be fit to power system of the machine.

4. RMXprt SIMULATION

Designed motor parameters calculated in the previous section have been set up and tested with the help of ANSYS Electronics Desktop – RMXprt design and simulator program.

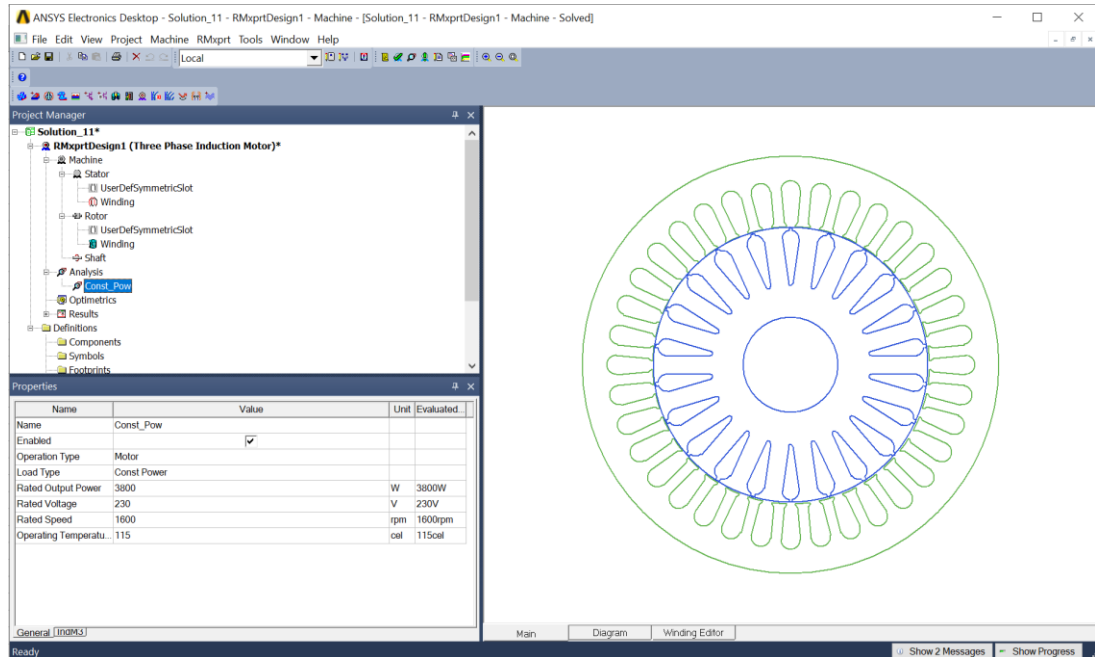


Figure 4.1: ANSYS RMXprt model

The induction motor stator, rotor, slot and winding parameters have been configured accordingly to the values calculated through the analytical method used in the thesis.

For the stator and the rotor core, the vendor-provided magnetic steel properties were defined in the materials section of RMXprt for Sura M350-50A magnetic steel properties.

Model analysis has been defined for 3.8 kW constant power, 1600 revolutions per minute speed and operating temperature of 110 °C, Delta winding connection configuration and 230V phase voltage. The load current frequency was adjusted to the value of synchronous frequency for the slip of the simulated machine.

The winding and the wire type were set up in line with the analytical model settings and the resistivity of copper and aluminum materials were adjusted to 110 °C references detailed in [1].

The result of induction machine calculation is compatible with ANSYS RMXprt simulation. Summary of the simulation output results are detailed in Table 4-1, next to the parameters calculated in section 3 of this thesis.

Table 4-1: Modeled machine parameters

Parameters	Kopylov model	RMxpert model
Input power P_1 [kW]	4.595	4.49
Output power P_2 [W]	3.8	3.8
Efficiency η [-] (at 110 [°C])	0.822	0.846
Slip s_N [-]	0.047	0.046
Power factor $\cos \varphi_1$ [-]	0.77	0.79
Stator phase current I_s [A]	8.7	8.2
Slot fill factor k_{Cu} [%]	70.6	67.2
Total loss ΔP [kW]	0.8	0.69
Stator winding loss $\Delta P_{s,Cu}$ [kW]	0.473	0.415
Rotor cage loss $\Delta P_{r,Cu}$ [kW]	0.193	0.183
Iron core loss ΔP_{Fe} [kW]	54.2	73.6
Stator resistance R_{DCS} [Ω]	2.066	2.073
Stator leakage reactance $X_{s\sigma}$ [Ω]	2.24	1.82
Rotor resistance R'_{DCr} [Ω]	1.41	1.48
Rotor leakage reactance $X'_{r\sigma}$ [Ω]	3.47	2.52
Iron core loss resistance R_{Fe} [Ω]	2563	1754
Magnetizing reactance X_m [Ω]	44.4	46.9
Stator-teeth flux density B_{ds} [T]	1.69	1.6
Rotor-teeth flux density B_{ys} [T]	1.72	1.58
Stator-yoke flux density B_{dr} [T]	1.4	1.64
Rotor-yoke flux density B_{yr} [T]	1.48	1.42
Air-gap flux density B_δ [T]	0.732	0.666
Specific electric loading A_s [A/m]	25735	26185
Stator thermal load AJ_s [A ² /m ³]	180·10 ⁹	189·10 ⁹
Stator current density J_s [A/mm ²]	6.89	7.2
Rotor bar current density J_r [A/mm ²]	3.29	3.1
Rotor ring current density J_{ring} [A/mm ²]	2.79	2.63

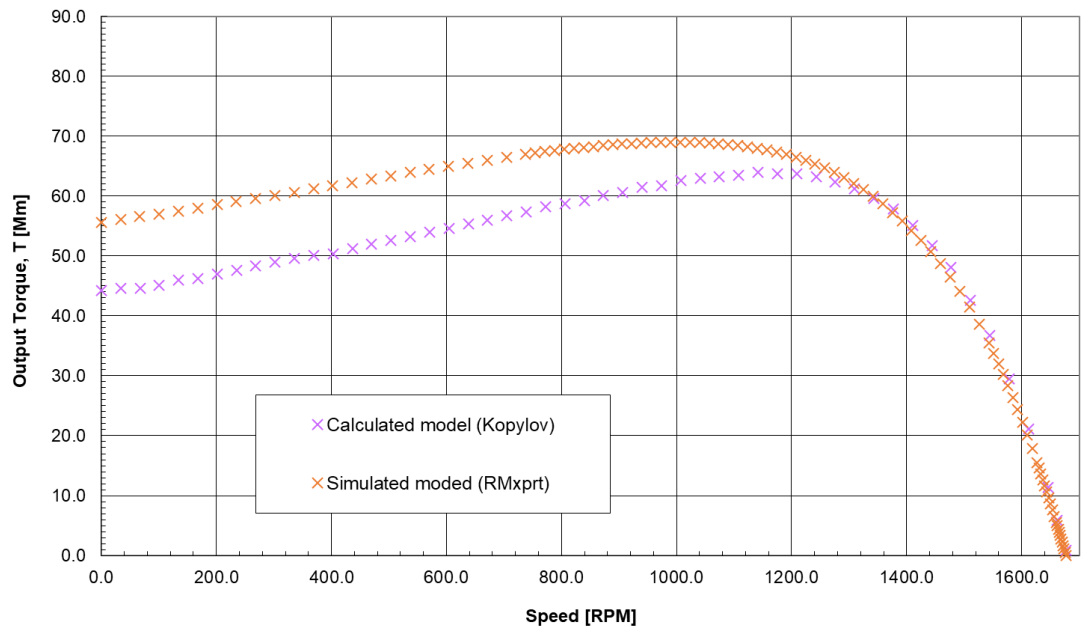


Figure 4.2: Output torque characteristics

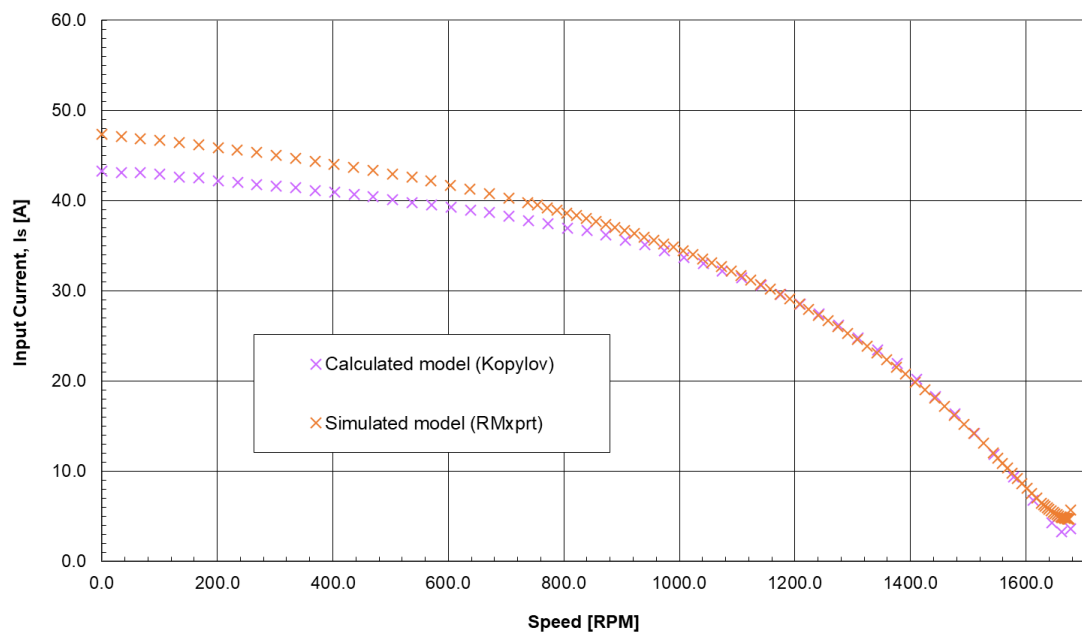


Figure 4.3: Input current characteristics

5. STATOR STACK LENGTH REDUCTION

5.1 General considerations

As per [9], performing design optimization can be categorized as “theoretical optimization” and “technical optimization”, with better results being achieved through the first method, as design incorporates only “positive parameters” to respond to objectives for the designed induction machine. “Theoretical optimization” achieves better results than “Technical optimization” because the latter must respond to and incorporates technical constraints set by design input parameters.

In case of current design, as per categorization provided by [9] we can assess that we speak about a technical optimization, with constraint imposed by outer diameter of the stator stack.

As one of the objectives of this thesis, using RMxpert, an analysis of options available for reducing stator stack length of the engine is done in the next sections.

Starting with the machine’s constant C_A equation, proportionality relationship in between different parameters of this equation can be analyzed.

$$C_A = \frac{D_s^2 l_i \omega_s}{P_i} = \frac{2}{\pi \alpha_\delta k_B k_{V1} A B_\delta} \quad (5.1)$$

As the optimization objective is reducing the iron core stack length l_i , following options can be outlined:

- Decreasing the internal power P_i . As the output shaft power P_2 is fixed, a decrease of the internal power can be achieved through increasing electrical efficiency of the induction machine.
- Increasing stator inner diameter D_s .
- Increasing synchronous speed of the machine ω_s .
- Increasing linear current density of the air gap A .
- Increasing air-gap magnetic flux density B_δ .
- Skewing the stator or the rotor slots, which maintains constant iron core stack length l_i , but reduces length of the stator pack.

Electrical, magnetic, mechanical and thermal parameters of the induction machine form a complex system. Update of each parameter could influence or change directly or indirectly other parameters of the machine.

This means that options listed above are subject to technical constraints generated not only through direct update of the respective parameter, but also through changes produced also to other parameters defining the machine (ex: increasing current density will reduce length of the steel core pack, but increased electrical load will produce additional Joule losses, which on their turn could require higher temperature grade wire insulation or improved machine cooling methods).

Out of methods listed above, increase of the stator inner diameter D_s and machine synchronous speed ω_s will be removed from analysis, as constraints are imposed on the stator outer diameter D_{se} and on machine nominal speed. The other options are analyzed in the next sections.

For reaching optimization objectives, reducing stator length can be done only with respecting electric, magnetic, mechanic and thermal requirements of the engine.

5.2 Decreasing losses

Decreasing the internal power P_i , while maintaining the shaft output power P_2 , can be achieved through decrease of energy losses of the machine.

As a summary these resistive losses in the stator and the rotor conductors, iron losses in magnetic circuit, mechanical losses and additional losses [2]. Given available information and type of the engine under design, options will be studied only for reducing resistive and iron losses.

RMxpert simulation shows that (before optimization) stator and rotor resistive (Joule) losses represent 81.8% of total energy loss at nominal speed and temperature. As these losses are increasing quadratically with the value of the current density crossing electrical circuit, a decrease of the current density is desired.

This can be achieved, directly, through an increase of the effective winding cross-cut area in the slots, through an increase of the winding wire diameter (method can be used primarily for the stator) or through the use of a different material with lower resistivity coefficient (method used for the rotor).

Iron losses can be reduced through the use of magnetic steel with improved hysteresis and eddy current loss parameters.

5.2.1 Copper rotor bars

In practical terms, decrease of rotor's resistivity is achieved through replacement of rotor's aluminum bars with copper. Better conductivity is achieved. As copper has a higher melting temperature than aluminum (1083 °C versus 660 °C) technical difficulties had to be removed before manufacturing could become an adopted industrial process. [7]

Even if it requires more copper mass than an aluminum squirrel cage rotor, use of copper rotor will improve volume and mass of the motor [9]. As per [1] current density in rotor copper bars could have values in between 4 and 8 A/m², smaller size engines reaching higher current density values.

For the scenario analyzed in RMxpert copper will be set up for rotor bars, maintaining first stator stack length unchanged, and, in the next test steps, stator length was decreased progressively. Stop of the test scenario was reaching the limits for machine's electric and magnetic parameters as detailed by [3].

Results of the tests are detailed in Table 5-1.

Table 5-1: Copper rotor bars simulation

Parameters	Start model	Copper rotor	Reduced length 1	Reduced length 2	Reduced length 3
Length of stator [mm]	138.3	138.3	135	131	130
Wire diameter [mm]	0.85	0.85	0.85	0.85	0.85
Slot fill factor [%]	67.2	67.2	67.2	67.2	67.2
Efficiency [%] (at 110 [°C])	84.62	86.07	85.36	84.48	84.26
Nominal slip [-]	0.0459	0.0241	0.0238	0.0236	0.0235
Power factor [-]	0.79	0.77	0.74	0.72	0.71
Stator phase current [A]	8.17	8.29	8.64	9.06	9.16
Iron-core loss current [A]	0.118	0.12	0.122	0.126	0.126
Magnetizing current [A]	4.43	4.84	5.36	5.94	6.08
Rotor phase current [A]	6.42	6.27	6.3	6.34	6.35
Total loss [W]	690.7	615.1	652	698.1	710.2
Stator winding loss [W]	415.3	427.7	464.5	510.3	522.2
Rotor cage loss [W]	182.7	93.7	92.8	91.7	91.5
Iron core loss [W]	73.6	74.7	75.7	77.1	77.5
Saturation factor for teeth [-]	1.26	1.3	1.36	1.42	1.43
Teeth & yoke saturation factor [-]	1.52	1.62	1.76	1.91	1.94
Stator Current Density [A/mm ²]	7.2	7.3	7.61	7.98	8.07
Rotor Current Density [A/mm ²]	3.1	3.03	3.05	3.07	3.07
Rotor Ring Current Density [A/mm ²]	2.63	2.57	2.58	2.6	2.6

Analysis Results:

- A decrease of the stator stack length to 131 [mm] can be achieved, though use of copper for the rotor cage.
- Reducing further the stack size increases the stator's current above the advised current density limit of 8 A/mm² [3].

5.2.2 Stator slot fill increase

For stator slots, as winding is made of copper wires, the method is limited by the amount of space available in the slot (defined through the slot fill factor k_{Cu} coefficient) and maximum technological value this coefficient can have for allowing efficient installation of the winding in the slot.

For machine winding forming and installation the maximum allowed value is $k_{Cu} = 70-75$ [%]. In the case of the designed machine, the slot utilization factor is $k_{Cu} = 67.2$ [%]. This gives very little room for performing an increase of the slot fill.

Analysis Results:

- By increasing the winding conductor diameter to 0.9 mm a slot utilization factor $k_{Cu} = 74.67$ [%] is obtained, with a decrease of 10 % of the stator winding loss.

- Given power budget saving, stator stack length can be decreased to 134 mm (reduced length 4, Tab.5-2).
- A further decrease brings the efficiency level at the same level as the original model.

Table 5-2: Stator slot fill increase simulation

Parameters	Start model	Slot utilization increase	Reduced length 1	Reduced length 2	Reduced length 3	Reduced length4	Reduced length 5
Length of stator [mm]	138.3	138.3	137	136	135	134	133
Wire diameter [mm]	0.85	0.9	0.9	0.9	0.9	0.9	0.9
Slot fill factor [%]	67.2	74.7	74.7	74.7	74.7	74.7	74.7
Efficiency [%] (at 110 [°C])	84.62	85.46	85.31	85.17	85	84.74	84.56
Nominal slip [-]	0.0459	0.0452	0.045	0.0449	0.0448	0.0446	0.0445
Power factor [-]	0.79	0.78	0.78	0.77	0.76	0.75	0.74
Stator phase current [A]	8.17	8.2	8.29	8.37	8.46	8.62	8.72
Iron-core loss current [A]	0.118	0.119	0.12	0.121	0.121	0.122	0.123
Magnetizing current [A]	4.43	4.55	4.69	4.82	4.96	5.19	5.33
Rotor phase current [A]	6.42	6.37	6.38	6.38	6.4	6.4	6.41
Total loss [W]	690.7	646.4	654.6	661.7	670.9	684.5	694
Stator winding loss [W]	415.3	372.8	381.4	388.9	397.9	412	421.6
Rotor cage loss [W]	182.7	178	179.1	178.4	178.3	177.5	177
Iron core loss [W]	73.6	74.6	75.1	75.4	75.8	76	76.4
Saturation factor for teeth [-]	1.26	1.27	1.29	1.3	1.31	1.34	1.35
Teeth & yoke saturation factor [-]	1.52	1.55	1.58	1.62	1.65	1.72	1.76
Stator Current Density [A/mm ²]	7.2	6.4	6.5	6.6	6.7	6.8	6.9
Rotor Current Density [A/mm ²]	3.1	3.08	3.08	3.09	3.09	3.1	3.10
Rotor Ring Current Density [A/mm ²]	2.63	2.61	2.61	2.61	2.62	2.62	2.63

5.3 Reducing iron core losses

Reducing iron core loss can be done using different of magnetic steel type, with better hysteresis and eddy current loss properties. The method is limited by the fact that steels with lower hysteresis loss could show higher eddy current loss.

Figure 5.1 details the specific iron core losses for magnetic steel materials used in simulations performed. As hysteresis and eddy current losses are proportional to the steel mass, higher losses (that could be optimized) are associated with higher power output, volume and mass machines. Due to this relationship, for model discussed in this thesis, when materials with lower specific iron core loss are used, the impact (losses “saving”) is minimal.

Because rotor’s current frequency is very small, limiting rotor generated hysteresis and eddy current losses has minimal effects on overall loss budget of the machine. As per table Tab. 5-3, minimal differences can be observed for using better properties steels for rotor stack.

Analyzing RMxprt simulations, it can be concluded that, through the use of different steel types, biggest impact on optimizing losses is generated by the use of steels with better magnetic properties (higher magnetic flux density saturation), which allow lower magnetization current values with positive effect on stator and rotor copper losses.

Table 5-3: Magnetic steel tests

Stator magnetic steel type	Sura M350 50A	Sura M300 35A	Sura M300 35A	Sura M700 50A	Sura M700 50A	Sura NO10	Sura NO10	VACOFLUX 48	VACOFLUX 48
Rotor magnetic steel type	Sura M350 50A	Sura M300 35A	Sura M350 50A	Sura M700 50A	Sura M350 50A	Sura NO10	Sura M350 50A	VACOFLUX 48	Sura M350 50A
Stator stack [mm]	138.3	138.3	138.3	138.3	138.3	138.3	138.3	138.3	138.3
Wire diameter [mm]	0.85	0.85	0.85	0.85	0.85	0.85	0.85	0.85	0.85
Slot fill factor [%]	67.2	67.17	67.17	67.17	67.17	67.17	67.17	67.17	67.17
Efficiency [%] at 110 [°C]	84.62	84.29	84.38	84.3	84.15	84.89	84.93	87.2	86.65
Slip [%]	4.59	4.6	4.6	4.56	4.57	4.59	4.58	4.5	4.53
Power factor [%]	78.4	78.7	82	81.3	79.1	79.3	86.2	83.4	78.4
Stator phase current [A]	8.23	8.3	8.25	7.93	8.01	8.17	8.15	7.3	7.59
Iron-core loss current [A]	0.118	0.124	0.124	0.185	0.185	0.096	0.096	0.045	0.045
Magnetizing current [A]	4.43	4.62	4.55	3.92	4.07	4.45	4.42	2.98	3.54
Rotor phase current [A]	6.42	6.43	6.42	6.4	6.41	6.42	6.41	6.35	6.37
Total loss [W]	690.7	708.1	703.2	707.3	715.9	676.5	674.2	557.7	585.5
Stator winding loss [W]	415.3	428.4	423.7	390.9	399.3	414.9	412.8	331.4	358.1
Rotor cage loss [W]	182.7	183.3	183.1	181.7	182.1	182.7	182.6	178.9	180.1
Iron core loss [W]	73.6	77.28	77.4	115.8	115.5	59.88	59.92	28.4	28.27
Stator-Teeth Flux Density [T]	1.6	1.59	1.59	1.62	1.61	1.6	1.6	1.69	1.63
Rotor-Teeth Flux Density [T]	1.58	1.57	1.57	1.6	1.59	1.58	1.59	1.67	1.61
Stator-Yoke Flux Density [T]	1.64	1.64	1.64	1.64	1.64	1.64	1.64	1.62	1.65
Rotor-Yoke Flux Density [T]	1.42	1.42	1.42	1.41	1.42	1.42	1.42	1.4	1.42
Air-Gap Flux Density [T]	0.666	0.66	0.663	0.676	0.67	0.664	0.665	0.704	0.679
Teeth saturation factor [-]	1.26	1.29	1.27	1.19	1.23	1.27	1.26	1.01	1.19
Teeth & yoke sat. factor [-]	1.52	1.59	1.56	1.34	1.39	1.53	1.51	1.01	1.21

Analysis Results:

- The decrease of the power losses is minimal for Sura M300 35A, Sura M700 50A and Sura NO10.
- No stack length optimization simulation was performed for these magnetic steels, as no meaningful length reduction (based on the criteria's used in the previous two sections) would be obtained.
- Length optimization is possible using VACOFLUX 48 as magnetic steel.

The B-H characteristics for tested steels are detailed in Figure 5-2.

Length optimization for VACOFLUX 48 is done in the next section, taking advantage of improved core loss and magnetic saturation of this magnetic steel.

As VACOFLUX 48 has high magnetic saturation (saturation magnetization at 2.35 [T] [14]), the stator slot size can be increased through reduction of the stator tooth width, together with an increase of the stator slot height, so that the stator copper fill could be further increased for reducing Joule losses in the stator's winding.

For maintaining optimum magnetic properties, VACOFLUX 48 requires annealing as a final heat process. The required annealing temperature, holding time and cooling rate are being defined based on the manufacturer's recommended process values [14].

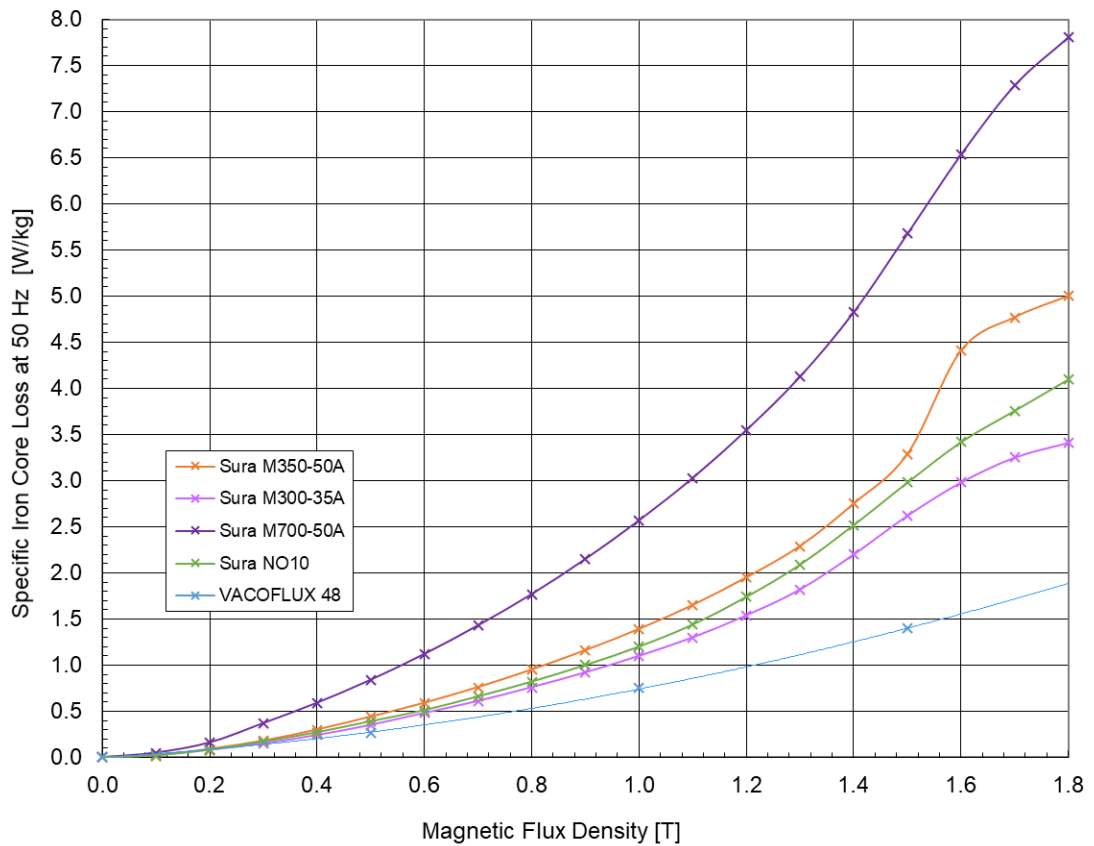


Figure 5.1: Specific iron core losses at 50 Hz [6][11][12][13][14]

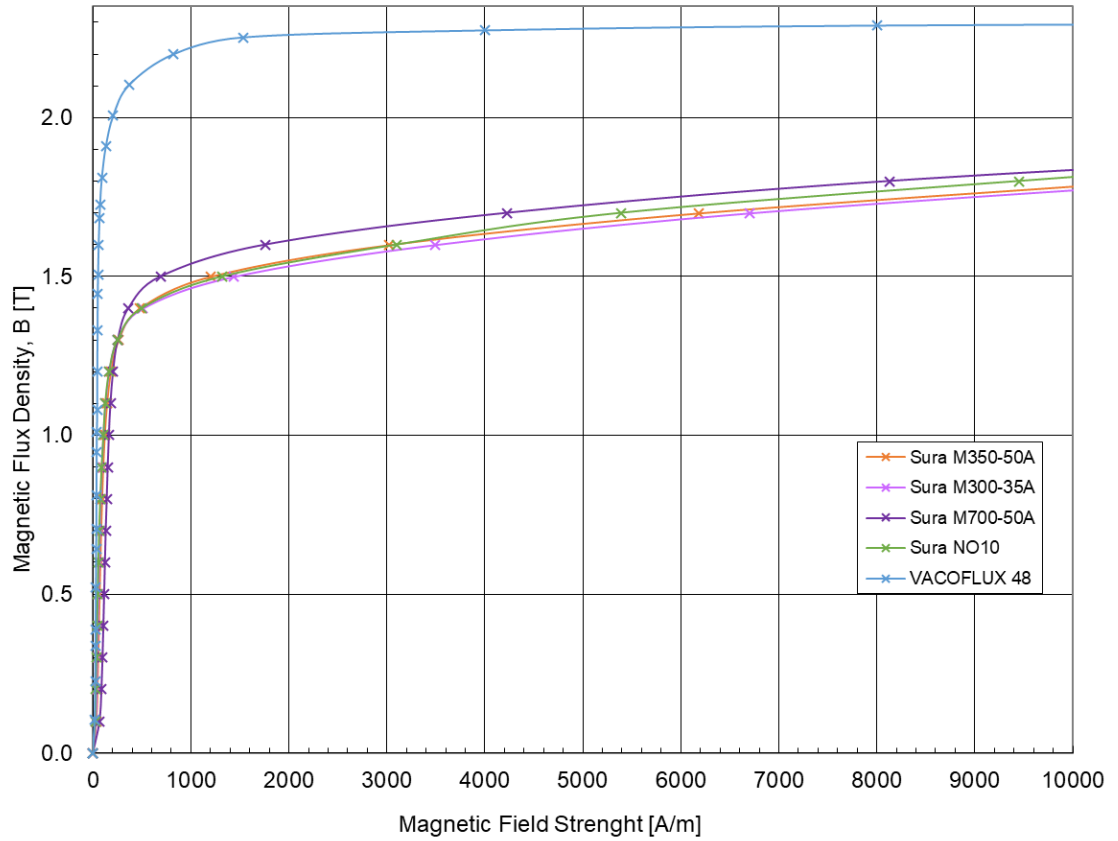


Figure 5.2: B-H characteristics for tested magnetic steels [6][11][12][13][14]

5.6 Design output

Based on insights gained in sections above, initial design of the induction motor can be updated.

As design adjustments the following setup is applied:

- Stator magnetic steel: VACOFLUX 48.
- Rotor magnetic steel: Sura M700 50A.
- Selected stator tooth maximum flux density $B_{ds} = 2.2$ [T].
- Reducing stator tooth width size $b_{ds} = 3.3$ [mm]. Resulting airgap flux density $B_{\delta} = 0.8$ [T].
- Adding 2 more stator winding turns for decreasing airgap flux density to $B_{\delta} = 0.76$ [T]. The resulting stator winding turns $Z_{Qs} = 31$ [-].
- Increasing stator slot height to from initial $h_{ds} = 10.5$ [mm], to $h_{ds} = 11.3$ [mm] (resulting an intermediate stator fill density $k_{Cu} = 0.583$ [-]).
- Increasing stator winding conductor diameter to $b_{oc} = 0.95$ [mm]. The resulting stator fill density is $k_{Cu} = 0.716$ [-].
- Replacing aluminum rotor bars with copper bars.
- Reducing magnetic steel stack length to $l_{Fes} = l_{Fer} = 115$ [mm].

Through use of VACOFLUX 48 high magnetic saturation steel, magnetic flux density in magnetic circuit can be increased without a further need of increasing magnetizing current value [14].

Better magnetic circuit characteristics allows an increase of the stator slot area through the decrease of the stator tooth width and of the stator yoke height, allowing as well use of stator winding copper conductors of higher diameter, and through this reducing the stator winding resistance which has as result a decrease of the stator slot copper losses, as well.

Use of copper for the rotor's cage allows a decrease of the rotor Joule losses, through decrease of resistance of rotor bar and rotor ring electrical circuits. Specific for induction machines, decrease of the rotor's winding resistance has as side effect a decrease of the locked rotor moment and of the one associated with maximum moment of the motor [8]. From a motor drive functional perspective, critical value is the one of the locked rotor moment, value based on the new design being acceptable, given purpose of the motor.

Sura M700 50A was selected for rotor's magnetic steel as it has good magnetic properties for magnetic flux densities present in rotor teeth and yoke. Even if M700 50A has a bigger specific core loss characteristic, the rotor's eddy currents and magnetic hysteresis losses small at rotor level as the rotor's current frequency is very small.

Adding 2 winding turns to the stator's winding, allows a decrease of magnetic flux density in the air gap, which otherwise would raise beyond a 0.8 value when stack length is decreased.

All design change actions allow a decrease of the stator core length from initial value of 138.3 [mm] to 115 [mm], a further decrease being limited by consequent increase of the stator teeth magnetic flux density above an acceptable level. Technical parameters of engine's updated design are detailed in Table 5-4.

Table 5-4: Designed model characteristics

Parameters	Optimized (proposed) model
Input power P_1 [kW]	4.29
Total loss ΔP [W]	490.7
Stator winding loss $\Delta P_{s,Cu}$ [kW]	339.2
Rotor cage loss $\Delta P_{r,Cu}$ [kW]	80.9
Iron core loss ΔP_{Fe} [kW]	34.7
Output power P_2 [W]	3.8
Rated voltage U_{1N} [V]	230/400
Pole pairs $2p$ [-]	4
Efficiency η [%] (at 110 [°C])	88.6
Power factor [%]	77.6
Stator phase current I_s [A]	7.89
Stator winding turns Z_{0s} [-]	31
Winding conductor diameter b_{0c} [mm]	0.95
Slot fill factor k_{Cu} [%]	71.63
Locked rotor torque [N·m]	39.8
Brake-down torque ratio [-]	3.2
Brake-down slip [%]	19
Nominal slip s_N [%]	2.08
Stack length $l_{FeS} = l_{Fer}$ [mm]	115
Stator exterior diameter D_{se} [mm]	156
Stator interior diameter D_s [mm]	103.7
Air gap length δ [mm]	0.4
Magnetic steel type stator	VACOFLUX 48
Magnetic steel type rotor	Sura M700 50A
Stator resistance R_{DCs} [Ω]	1.77
Stator leakage reactance $X_{s\sigma}$ [Ω]	2.2
Rotor resistance R'_{DCr} [Ω]	0.69
Rotor leakage reactance $X'_{r\sigma}$ [Ω]	2.36
Iron core loss resistance R_{Fe} [Ω]	3737
Magnetizing reactance X_m [Ω]	46.44
Stator-Teeth Flux Density B_{ds} [T]	2.2
Rotor-Teeth Flux Density B_{ys} [T]	1.74
Stator-Yoke Flux Density B_{dr} [T]	2.09
Rotor-Yoke Flux Density B_{yr} [T]	1.65
Air-Gap Flux Density B_δ [T]	0.761
Specific Electric Loading A_s [A/m]	27347
Stator Thermal Load AJ_s [A ² /m ³]	154·10 ⁹
Stator Current Density J_s [A/mm ²]	5.63
Rotor Bar Current Density J_r [A/mm ²]	3.24
Rotor Ring Current Density J_{ring} [A/mm ²]	2.74

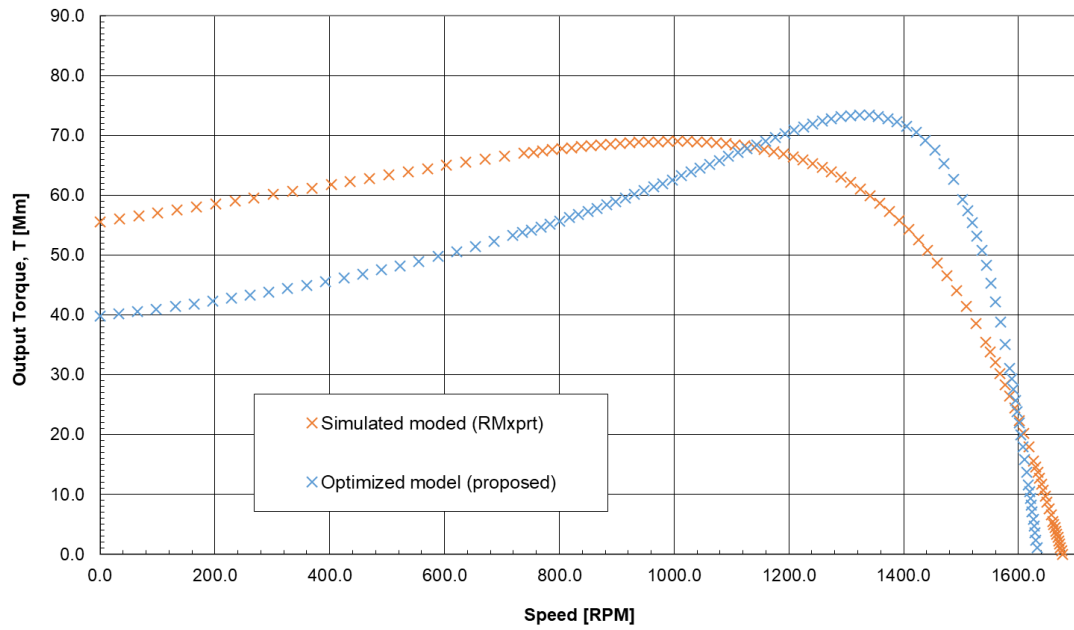


Figure 5.3: Output torque characteristics

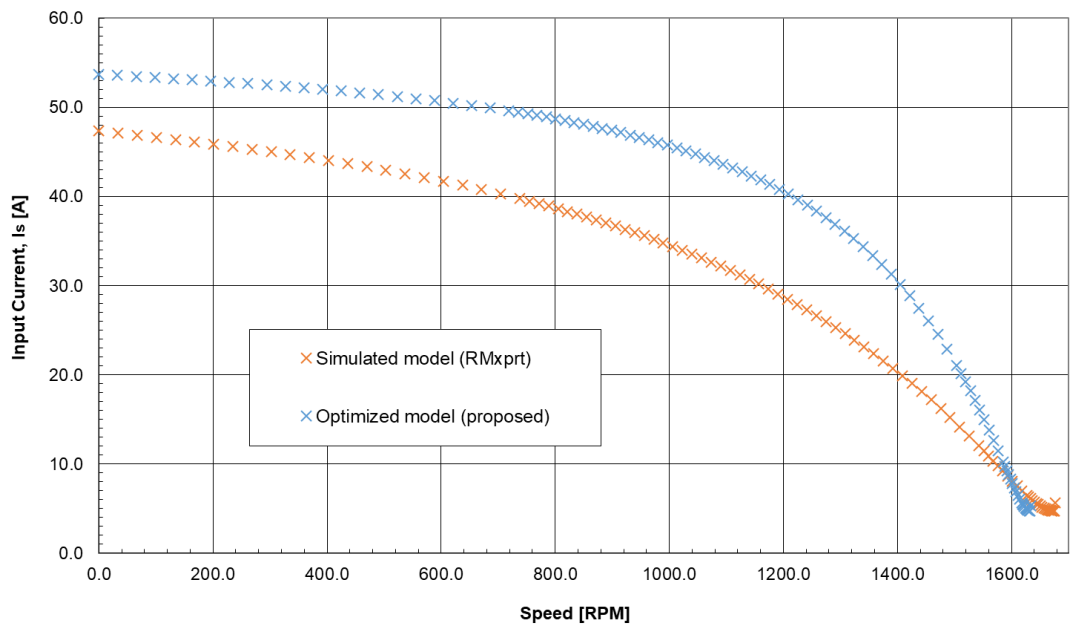


Figure 5.4: Input current characteristics

6. CONCLUSION

The main goal of this thesis was the design of an induction machine providing an output power of 3.8 kW at nominal speed 1600 RPM. The engine should drive a pump and it is intended to be mounted inside a pipe system, an additional design requirement being a fixed exterior diameter of the stator stack of 156 mm.

For performing engine's calculation, a computer program was built. This program is written in Python 3, based on Anaconda open source code distribution platform. As user interface a Jupyter notebook client running on top of the Anaconda platform is being used. Advantage of this platform, for fulfilling the purpose for this thesis, is the fact that the programming code and the code calculation outputs are flexibly presented in sequenced sections, presented in a regular web browser interface. The presentation interface is responding very well to iterative nature of the engine calculation process, this being the main advantage, over other programming platforms, for developing the computer program for performing the engine's calculation.

Availability free of a license acquisition cost together with availability of add-on libraries for extending data manipulation, analysis and presentation capabilities of the programming platform are also advantages for using Python 3, Anaconda and Jupyter notebooks for performing the tasks required in the induction machine design process.

Calculation of engine's dimensions and electrical, magnetic, mechanical and thermal parameters was done using method detailed in source [1]. First step of the calculation requires the definition of the engine's main design parameters and of the stator and the rotor stacks and slots parameters. The requirement for a fixed engine stator stack exterior diameter represents the main constraint at this step. This is imposing the need for selection of design parameters at the limit or very close to the limit of advised value ranges for respective parameters.

Calculation required multiple iterations for finding exit values corresponding to design needs. Engine's stator and rotor (including slots) parameters have been defined, and together with this also magnetic and electric circuits parameters. Given the required nominal speed and based on the selection of the stator's winding characteristics, the engine is designed to be connected to the power grid through a power electronic convertor. Based on the selected number of poles, in a star winding connection configuration, the engine can be attached directly to the 3 phase, 400V, 50Hz power grid, running at speed close to natural synchronous speed of 1500 RPM, for the given power grid electrical current frequency.

The next step was the engine's electrical parameters and losses calculation. This was done taking in consideration the effects induced at locked rotor/engine start and zero and nominal load engine running configurations. As result, the engine's equivalent model parameters were calculated, together with the load and the starting characteristics of the motor.

As the last step in the engine's parameters calculation, thermal characteristic and cooling parameters have been evaluated.

Even if relatively simple in construction, modeling the induction's machine mechanical, electrical and magnetic parameters (static and dynamic) requires a complex analytical system. Calculation method used in this thesis (based on [1]) requires a very

good understanding of the method itself, this being mandatory for performing an accurate the calculation that it is based on selection of various slot and materials types and based on various parameter's sizing as defined and available for selection in the method.

For completing second goal of this thesis, the induction machine's calculated parameters have been analyzed with the help of ANSYS Electronics Desktop – RMxpert design and simulator program. For this, a three-phase induction motor model has been setup in RMxpert. The design results have been assessed through use of a constant power analysis. The outputs show that motor's parameters calculated in first part of this thesis are compatible with the ones calculated with the help of RMxpert.

A third goal of this thesis was the analysis of ways on how to reduce the size of designed induction machine via RMxpert software. For performing this task, several options for reducing the size of the machine have been outlined, starting from the relationship in between coefficients defining the machine's constant C_A equation. Given constraints imposed on the design of the motor, options that have been analyzed in RMxpert were: decreasing power losses through use of copper rotor bars, through increasing stator slot fill (increase winding conductor cross-section area) and through use of different stator and rotor stack magnetic steel. In testing different magnetic steel options, testing option for use of high magnetic saturation steel has been included. Based on the analysis, it can be concluded that the most significant impact for achieving a better power density and implicitly, as the output power remains unchanged, reducing size of the machine is given by use of rotor copper bars and use of high magnetic saturation steel.

Based on these finding, in the last section of this thesis design of the motor has been updated to incorporate the optimization options analyzed in the previous section. For the stator, the stator's magnetic steel was replaced with high magnetic saturation steel, this allowing the increase of the stator slot size, followed by the increase of the stator's winding conductor diameter and by an increase of the stator winding turns. For the rotor's cage material, aluminum was replaced with copper. Incorporated design changes allowed decrease of losses and consequently permitted an increase the power density of the machine, through the reduction of the stator slack length.

In conclusion, the work in this thesis shows the complexity and a number of requirements regarding the design process of an induction machine, and together with this, also performing the optimization of selected technical parameters. Modeling computer programs, as the one developed for calculating technical parameters of the machine, or as ANSYS RMxpert, are greatly reducing the workload and the amount of time required for testing various scenarios associated with the design. As long as the initial design it is, to a fair extent, optimized, the use of better properties materials yields the most potential for a further properties' optimization. As the induction machine is a complex technical system, the foundation for successfully performing its design and optimization is the accumulated experience and understanding, as deeply as possible, the theoretical basis defining the induction machine parameters and properties.

Literatura

- [1] KOPYLOV, Igor Petrovič. *Stavba elektrických strojů: celostátní vysokoškolská učebnice pro elektrotechnické fakulty vysokých škol technických*. Praha: Státní nakladatelství technické literatury, 1988.
- [2] PYRHONEN, Juha, Tapani JOKINEN a Valeria HRABOVCOVÁ. *Design of rotating electrical machines*. Second edition. Chichester, West Sussex, United Kingdom: Wiley, 2014. ISBN 9781118581575.
- [3] ONDRŮŠEK, Čestmír. *Elektrické stroje: Skripta předmětu*. FAKULTA ELEKTROTECHNIKY A KOMUNIKAČNÍCH TECHNOLOGIÍ VYSOKÉ UČENÍ TECHNICKÉ V BRNĚ. BRNO: FEKT VUT v Brně.
- [4] JAMES, Henry. *Three phase induction motors – Operating principle*. *Electrical Engineering Portal* [online]. Serbia: Electrical Engineering Portal PR, 2012, February, 3rd 2012 [cit. 2019-01-06]. Dostupné z: <https://electrical-engineering-portal.com/three-phase-induction-motors-operating-principle>
- [5] HUGHES, Austin a Bill DRURY. *Electric motors and drives: fundamentals, types and applications*. 4th ed. Amsterdam: Elsevier, 2013. ISBN 978-0-08-098332-5.
- [6] Cogent Power Non-oriented Electrical Steel Datasheet M350-50A. Cogent Power [online]. Online [cit. 2019-05-22]. Dostupné z: <https://cogent-power.com/cms-data/downloads/m350-50a.pdf>
- [7] BOLDEA, I. a NASAR, S. A. *The induction machine handbook*. Boca Raton: CRC Press, 2002. ISBN 08-49--0004-5.
- [8] *Pohony s asynchronními motory - Elektrické pohony: Skripta předmětu*. BRNO: FAKULTA ELEKTROTECHNIKY A KOMUNIKAČNÍCH TECHNOLOGIÍ VYSOKÉ UČENÍ TECHNICKÉ V BRNĚ.
- [9] J. Appelbaum, E. F. Fuchs and J. C. White, "Optimization of Three-Phase Induction Motor Design Part I: Formulation of the Optimization Technique," in *IEEE Transactions on Energy Conversion*, vol. EC-2, no. 3, pp. 407-414, Sept. 1987.
- [10] J. Appelbaum, I. A. Khan, E. F. Fuchs and J. C. White, "Optimization of Three-Phase Induction Motor Design Part II: The Efficiency and Cost of an Optimal Design," in *IEEE Transactions on Energy Conversion*, vol. EC-2, no. 3, pp. 415-422, Sept. 1987.
- [11] Cogent Power Non-oriented Electrical Steel Datasheet NO 10. Cogent Power [online]. Online [cit. 2019-05-22]. Dostupné z: https://cogent-power.com/cms-data/downloads/Hi-Lite_NO10.pdf
- [12] Cogent Power Non-oriented Electrical Steel Datasheet M300-35A. Cogent Power [online]. Online [cit. 2019-05-22]. Dostupné z: <https://cogent-power.com/cms-data/downloads/M300-35A.pdf>

- [13] Cogent Power Non-oriented Electrical Steel Datasheet M700-50A. Cogent Power [online]. Online [cit. 2019-05-22]. Dostupné z: <https://cogent-power.com/cms-data/downloads/m700-50a.pdf>
- [14] VACUUMSCHMELZE Soft magnetic cobalt-iron alloys VACOFLUX and VACODUR. VACUUMSCHMELZE [online]. Online [cit. 2020-04-14]. Dostupné z: <https://vacuumschmelze.com/Assets/Cobalt-Iron%20Alloys.pdf>
- [15] Induction Versus DC Brushless Motors, 2007. *www.tesla.com* [online]. 45500 Fremont Boulevard, Fremont, CA 94538: Tesla, January 9, 2007 [cit. 2020-05-30]. Dostupné z: <https://www.tesla.com/blog/induction-versus-dc-brushless-motors>
- [16] Motor guide – basic technical information about low voltage standard motors, 2014. *www.abb.com/motors&generators* [online]. Affolternstrasse 44, 8050 Zurich, Switzerland: ABB Asea Brown Boveri [cit. 2020-03-30]. Dostupné z: <https://new.abb.com/docs/librariesprovider53/about-downloads/low-voltage-motor-guide.pdf>
- [17] Electric machines design course: J.R. Hendershot course lectures, 2020. *University of Minnesota - Consortium of Universities for Sustainable Power* [online]. CUSP UMN: University of Minnesota [cit. 2020-05-30]. Dostupné z: <https://cusp.umn.edu/electric-machines-drives/electric-machines-design>
- [18] ZAVADIL, Robert, Vadim ZHEGLOV, Yuriy KAZACHKOV, Bo GONG, Juan SANCHEZ a Jun LI. *Documentation, User Support, and Verification of Wind Turbine and Plant Models* [online]. United States: EnerNex, 2012-09-18, s. 25-44 [cit. 2020-04-12]. DOI: 10.2172/1051403. Dostupné z: <https://www.osti.gov/servlets/purl/1051403>

List of symbols and abbreviations

Abbreviations:

FEKT	Fakulta elektrotechniky a komunikačních technologií
VUT	Vysoké učení technické v Brně
MMF	Magnetomotive Force
PWM	Pulse-Width Modulation
IGBT	Insulated Gate Bipolar Transistor
MOSFET	Metal Oxide Semiconductor Field Effect Transistor
GTO	Gate Turn-Off thyristor

Symbols:

$2p$	number of poles	[-]
a	winding number of parallel branches	[-]
a	reduced equivalent model parameter	[Ω]
a'	reduced equivalent model parameter	[-]
a_{ring}	rotor end ring width	[m]
A_s	linear current density	[A/m]
AJ	stator thermal load	[A ² /m ³]
b	reduced equivalent model parameter	[Ω]
b'	reduced equivalent model parameter	[-]
b_{0c}	conductor diameter	[m]
b_{0c}	winding wire diameter	[m]
b_{0r}	rotor slot opening	[m]
b_{0s}	stator slot opening	[m]
b_{1r}	rotor slot width	[m]
b_{1s}	stator slot width	[m]
b'_{1s}	stator slot adjusted width	[m]
b_{2r}	rotor slot width	[m]
b_{2s}	stator slot width	[m]
b'_{2s}	stator slot adjusted width	[m]
b_{2s}	stator slot width	[m]
b_c	stator coil medium pitch span	[m]
b_{ds}	stator teeth width	[m]

b_{drmax}	maximum rotor teeth width	[m]
b_{is}	insulation liner thickness	[m]
b_{ring}	rotor end ring height	[m]
b_R	rotor bar width	[m]
b_{ws}	stator winding end-turn insulation thickness	[m]
B	stator slot exit additional length	[m]
B_{0r}	rotor slot opening mag. flux density amplitude	[T]
B_{0s}	stator slot opening mag. flux density amplitude	[T]
B_{dr}	rotor tooth air gap magnetic flux density	[T]
B_{ds}	stator tooth air gap magnetic flux density	[T]
B_{drav}	medium rotor tooth air gap magnetic flux density	[T]
B_{dsav}	medium stator tooth air gap magnetic flux density	[T]
$B_{f\delta}$	apparent air gap magnetic flux density	[T]
B_{pr}	rotor pulsation amplitude magnetic flux density	[T]
B_{ps}	stator pulsation amplitude magnetic flux density	[T]
B_{yr}	rotor yoke air gap magnetic flux density	[T]
B_{ys}	stator yoke air gap magnetic flux density	[T]
B_{δ}	air gap magnetic flux density	[T]
$\overline{c_1}$	reduced equivalent model vector	[-]
c_{1i}	reduced equivalent model vector component	[-]
c_{1psat}	reduced equivalent model vector component under skin effect	[-]
c_{1r}	reduced equivalent model vector component	[-]
$\cos \varphi_0$	no load power factor	[-]
$\cos \varphi_1$	power factor (PF)	[-]
$\cos \varphi'_r$	rotor current vector argument	[-]
C_n	parameter	[-]
D_r	diameter of the rotor	[m]
D_{ring}	rotor end ring interior diameter	[m]
D_s	interior diameter of the stator	[m]
D_{se}	exterior diameter of the stator	[m]
f_1	load current frequency	[Hz]
f_r	rotor magnetization current frequency	[Hz]
f_s	stator magnetization current frequency	[Hz]
F_{dav}	stator slot magnetic tension	[A]

F_m	magnetic tension	[A]
h_{0r}	rotor tooth tip height	[m]
h'_{0r}	closed rotor overcover width	[m]
h_{0s}	stator tooth tip height	[m]
h_{1r}	rotor tooth height	[m]
h_{1s}	stator tooth height	[m]
h_{1xs}	stator tooth height segment 1	[m]
h_{2xs}	stator tooth height segment 2	[m]
h_{3xr}	rotor tooth height segment 3	[m]
h_{3xs}	stator tooth height segment 3	[m]
h'_{1s}	stator tooth tip height	[m]
h_{2s}	stator tooth tip height	[m]
h_{bar}	rotor bar height	[m]
h_{dr}	rotor tooth height	[m]
h_{ds}	stator tooth height	[m]
h_R	reduced rotor bar height	[m]
h_{sr}	rotor slot height	[m]
h_{ss}	stator slot height	[m]
h'_{yr}	rotor yoke apparent height	[m]
h_{ys}	stator yoke height	[m]
h_{yr}	rotor yoke height	[m]
H_{dr}	rotor tooth coercivity	[A/m]
H_{ds}	stator tooth coercivity	[A/m]
H_{yr}	rotor yoke coercivity	[A/m]
H_{ys}	stator yoke coercivity	[A/m]
i_μ	magnetizing current relative value	[-]
I_{s0}	no load stator current	[A]
$I_{s0,Cu}$	no load Joule losses current	[A]
$i_{s,mag}$	magnetization current relative value	[-]
$I_{s,mag}$	magnetization current	[A]
I_s	stator winding phase current	[A]
$I_{s,Cu}$	stator current copper loss component	[A]
I_r	rotor bar current	[A]
I'_r	rotor bar current value referred to stator	[A]

I_r''	rotor bar current (vector absolute value)	[A]
I_{ring}	rotor ring current	[A]
J	current density	[A/m ²]
J_{dr}	rotor bar current density	[A/m ²]
J_s	stator winding current density	[A/m ²]
J_r	estimated rotor bar current density	[A/m ²]
k_{0r}	coefficient	[-]
k_{0s}	coefficient	[-]
k_B	shape deformation coefficient	[-]
k_c	Carter factor	[-]
k_{Cr}	rotor Carter factor	[-]
k_{Cs}	stator Carter factor	[-]
k_{Cu}	stator slot fill factor	[-]
k_d	coefficient	[-]
k_{dd}	coefficient iron core losses stator tooth	[-]
k_{dy}	coefficient iron core losses stator yoke	[-]
k_{ds1}	stator winding distribution factor	[-]
k_E	induced electromagnetic tension coefficient	[-]
k_{Fe}	stacking factor	[-]
k_h	shaft size coefficient	[-]
k_i	coupling factor	[-]
k_m	coefficient	[-]
k_n	coefficient	[-]
k_{ps}	stator winding pitch factor	[-]
k_{rs}	rotor current transformation to stator ratio	[-]
k_R	resistance coefficient	[-]
k_s	coupling factor	[-]
k_{sat}	saturation factor	[-]
k_{ws1}	stator winding coefficient (first harmonic)	[-]
k_W	coil span coefficient	[-]
k_z	tooth saturation coefficient	[-]
k_β	coefficient	[-]
k'_β	coefficient	[-]
k'_γ	coefficient	[-]

k_μ	magnetic circuit saturation coefficient	[-]
k_ϑ	coefficient	[-]
K	coefficient	[-]
K_D	stack height to length ratio	[-]
K_R	skin effect resistance factor	[-]
K_X	skin effect reactance factor	[-]
l	length	[m]
l_c	stator winding length	[m]
l_{av}	stator coil turn length	[m]
l_d	stator slot coil length	[m]
l_{Fes}	stator stack length	[m]
l_{Fer}	rotor stack length	[m]
l_i	ideal stack length	[m]
l_w	stator slot coil span	[m]
l_{yr}	rotor flux line medium length	[m]
l_{ys}	stator flux line medium length	[m]
m	number of electrical phases	[-]
m_z	critical torque relative value	[-]
m_{dr}	rotor teeth mass	[kg]
m_{ds}	stator teeth mass	[kg]
m_v	coefficient	[kg]
m_{yr}	rotor teeth mass	[kg]
m_{ys}	stator yoke mass	[kg]
n	rotation speed	[RPM]
n_s	synchronous rotation speed	[RPM]
N_s	stator winding number of turns	[-]
O_{ds}	stator slot winding circumference	[m]
O_{fins}	stator cooling fins height	[m]
O_{iws}	stator slot winding end-turn circumference	[m]
p	number of pole pairs	[-]
$p_{\delta pr}$	rotor surface losses density	[W/m ²]
$p_{\delta ps}$	stator surface losses density	[W/m ²]
P_i	internal electromagnetic power	[kW]
P_{in}	input power	[kW]

P_1	input power	[kW]
P_2	output power	[kW]
q_s	number of slots per pol and phase	[-]
Q_{air}	airflow required	[m ³ s ⁻¹]
Q'_{air}	airflow provided	[m ³ s ⁻¹]
Q_{s_min}	minimum number of stator slots	[-]
Q_{s_max}	maximum number of stator slots	[-]
Q_s	stator slots number	[-]
Q_r	rotor slots number	[-]
r_{DCs}	stator resistance relative value	[-]
r'_{DCr}	rotor resistance referred to stator relative value	[-]
R	equivalent model resistance	[Ω]
R_{dr}	rotor bar resistance	[Ω]
R_{dring}	rotor bar resistance	[Ω]
R_{DCr}	rotor resistance	[Ω]
R_{DCs}	stator resistance	[Ω]
R'_{DCr}	rotor resistance referred to stator	[Ω]
$R'_{DCr\xi}$	skin effect rotor resistance referred to stator	[Ω]
R_{Fe}	fictive resistance corresponding to iron core losses	[Ω]
s	slip	[-]
s_{max}	critical slip	[-]
s_N	nominal slip	[-]
$\sin \phi'_r$	rotor current vector argument	[-]
S	surface area	[m ²]
S_{cs}	stator winding conductor effective crosscut area	[m ²]
S_{dr}	rotor bar crosscut area	[m ²]
S_{cr}	rotor bar effective crosscut area	[m ²]
S_{cus}	stator slot total active crosscut area	[m ²]
S_{is}	stator slot insulation liner crosscut area	[m ²]
S_{IM}	equivalent heat transfer surface area	[m ²]
S_{ls}	stator slot interlayer insulation crosscut area	[m ²]
S_{ef}	stator winding conductor crosscut area	[m ²]
S_{ring}	rotor end ring crosscut area	[m ²]
S'_{ring}	estimated rotor end ring crosscut area	[m ²]

S_R	skin effect reduced rotor bar cross section area	[m ²]
t_{max}	maximum rotor torque relative value	[-]
T	mechanical torque	[Nm]
T_1	locked rotor torque	[Nm]
T_{max}	maximum rotor torque	[Nm]
T_n	nominal rotor torque	[Nm]
u	voltage, instant value	[V]
$U_{m,dr}$	rotor tooth magnetic tension	[A]
$U_{m,ds}$	stator tooth magnetic tension	[A]
$U_{m,yr}$	rotor yoke magnetic tension	[A]
$U_{m,ys}$	stator yoke magnetic tension	[A]
$U_{m,\delta}$	airgap magnetic tension	[A]
$U_{s,ph}$	stator winding phase voltage	[V]
$x_{s\sigma}$	stator reactance relative value	[Ω]
$x_{r\sigma}$	rotor reactance relative value	[Ω]
$x'_{r\sigma}$	rotor reactance relative value referred to stator	[Ω]
x_{12}	iron core reactance	[Ω]
x_μ	iron core reactance	[Ω]
X	equivalent model reactance	[Ω]
X_m	magnetization reactance	[Ω]
X_{msat}	magnetization reactance under saturation	[Ω]
$X_{r\sigma}$	rotor reactance	[Ω]
$X'_{r\sigma}$	rotor reactance referred to stator	[Ω]
$X'_{r\sigma\xi}$	rotor reactance referred to stator under skin effect	[Ω]
$X'_{r\sigma\xi sat}$	rotor reactance referred to stator under skin effect and saturation	[Ω]
$X_{s\sigma}$	stator reactance	[Ω]
$X_{s\sigma sat}$	stator reactance under saturation	[Ω]
z_p	number of wire strands	[-]
Z_{Qs}	stator winding conductors	[-]
Z'_{Qs}	effective number of stator winding conductors	[-]
α_1	heat transfer coefficient	[-]
α_v	thermal conductivity	[-]
α_δ	pole cover coefficient	[-]
α_i	average to peak flux density ratio	[-]

β	coefficient	[-]
β_{0r}	flux density coefficient	[-]
β_{0s}	flux density coefficient	[-]
β_γ	coefficient	[-]
γ_{Fe}	magnetic steel mass density	[kg/m ³]
γ'_r	rotor coupling factor	[-]
γ'_s	stator coupling factor	[-]
δ	air gap size	[m]
δ_i	insulation thickness	[m]
Δ	end ring current transformation coefficient	[-]
Δb_{0r}	rotor slot opening variation	[m]
Δb_{0s}	stator slot opening variation	[m]
Δb_{bs}	stacking alignment variation	[m]
$\Delta p_{1,0}$	iron steel medium losses at 1T	[W/kg]
ΔP	total losses	[W]
ΔP_d	total additional losses	[W]
ΔP_{Fe}	total iron core losses	[W]
ΔP_{Fed}	additional iron core losses	[W]
ΔP_{mech}	mechanical losses	[W]
ΔP_{pr}	rotor teeth pulse losses	[W]
ΔP_{ps}	stator teeth pulse losses	[W]
$\Delta P_{r,Cu}$	rotor Joule losses	[W]
$\Delta P_{s0,Cu}$	no-load stator Joule losses	[W]
$\Delta P_{s,Cu}$	stator Joule losses	[W]
$\Delta P'_{sd,Cu}$	energy loss in stator winding	[W]
$\Delta P'_{sw,Cu}$	energy loss in stator winding end turn	[W]
Δ_z	coefficient	[-]
$\Delta P_{\delta ps}$	stator teeth surface losses	[W]
$\Delta P_{\delta pr}$	rotor teeth surface losses	[W]
$\Delta \vartheta_{air}$	air temperature rise	[°C]
$\Delta \vartheta_{ids}$	stator slot insulation temperature drop	[°C]
$\Delta \vartheta'_s$	medium stator winding temperature rise	[°C]
$\Delta \vartheta_{us}$	stator slot winding temperature rise	[°C]
$\Delta \vartheta_{iws}$	temperature drop in winding end-turn insulation	[°C]

$\Delta\vartheta_{ws}$	stator winding end-turn temperature rise	[°C]
$\Delta\lambda_{drs\text{sat}}$	rotor slot magnetic permeance coefficient variation	[-]
$\Delta\lambda_{dss\text{sat}}$	stator slot magnetic permeance coefficient variation	[-]
$\Sigma\Delta P'_v$	energy loss sum	[W]
η	electrical efficiency	[-]
ϑ	temperature	[°C]
λ	slot length to pole pitch ratio	[-]
λ_{difr}	rotor differential permeance coefficient	[-]
λ_{difs}	stator differential permeance coefficient	[-]
λ_{dr}	rotor slot permeance coefficient	[-]
$\lambda_{dr\xi}$	skin effect rotor slot permeance coefficient	[-]
λ_{ds}	stator slot permeance coefficient	[-]
$\lambda_{dr\xi\text{sat}}$	rotorslot permeance coefficient under saturation	[-]
$\lambda_{dss\text{sat}}$	stator slot permeance coefficient under saturation	[-]
$\lambda_{difrs\text{sat}}$	rotor differential permeance coefficient under saturation	[-]
$\lambda_{difss\text{sat}}$	stator differential permeance coefficient under saturation	[-]
λ_{ekv}	slot insulation equivalent thermal conductivity	[Wm ⁻² K ⁻¹]
λ'_{ekv}	stator winding conductor insulation thermal conductivity	[Wm ⁻² K ⁻¹]
λ_{wr}	rotor winding turn permeance coefficient	[-]
λ_{ws}	stator winding turn permeance coefficient	[-]
ξ	skin effect depth parameter	[-]
ξ_r	coefficient	[-]
ρ	electrical resistivity	[Ωm]
τ_p	pole pitch	[m]
τ_s	stator slot width	[m]
τ_r	rotor slot width	[m]
ϕ	magnetic flux	[Wb]
κ_δ	apparent airgap magnetic flux density coefficient	[-]
$\kappa_{\delta r}$	rotor slot apparent slot opening	[m]
$\kappa_{\delta s}$	stator slot apparent slot opening	[m]
ω	angular velocity, angular frequency	[rad/s]
ω_0	phase current angular velocity	[rad/s]
ω_s	synchronous angular velocity	[rad/s]

Attachment files:

1. BP_Motor_Calculation.IPYNB - Motor calculation program (Jupyter notebook file);
2. BP_Motor_Calculation.html – HTML Export of Jupyter notebook web interface for the motor calculation program.